BSP PREDICTION USING GEOMETRIC MODELLING AND DPX

THE PREDICTION OF BODY SEGMENT PARAMETERS USING GEOMETRIC MODELLING AND DUAL PHOTON ABSORPTIOMETRY

By

JENNIFER DURKIN, B.Sc.

A Thesis

Submitted to the School of Graduate Studies

in Partial Fulfilment of the Requirements

for the Degree

Master of Science

McMaster University

MASTER OF SCIENCE (1998) McMaster University
(Human Biodynamics) Hamilton, Ontario

TITLE: The Prediction of Body Segment Parameters Using Geometric Modelling and Dual Photon Absorptiometry

AUTHOR: Jennifer Durkin, B.Sc. (McMaster University)

SUPERVISOR: Dr. James J. Dowling

NUMBER OF PAGES: xi, 136

ABSTRACT

Understanding human movement requires that biomechanists have knowledge of the kinematics and kinetics of the motion. Calculating the internal kinetics of a movement requires the input of segment inertial characteristics. Errors in the estimations of these body segment parameters (BSPs) may have detrimental effects on segmental kinetic calculations.

The purposes of this study were to use i) investigate a new technique for measuring BSPs using dual photon absorptiometry (DPX) and ii) to investigate population differences in BSP values, develop geometric models to predict BSPs and compare geometric predictions with other prediction methods.

In study 1, DPX measured whole body mass of humans with a group mean percent difference of -1.05% from criterion measurements. DPX also measured mass, centre of mass along a transverse axis (CM) and moment of inertia about the centre of mass (I_{CG}) of a homogeneous object and a human cadaver leg with percent errors less than 4% from criterion measurements.

In Study 2, 100 subjects were selected from four subpopulation groups according to gender (males/females) and age (19-30/ 55^{+} years). Using DPX, six body segments were measured for mass (forearm, hand, thigh, leg, foot, head) and

four were measured for CM and radius of gyration (forearm, thigh, leg, head). Linear regression equations were developed and compared with geometric predictions and prediction equations from a popular literature source (Winter, 1990).

Population differences were statistically significant for all body segments and all segment parameters except hand mass. Large segmental differences between individuals of similar size were also observed. The results showed the linear regression equations to provide the best estimations of BSPs. The geometric models and the predictions from Winter (1990) were poor for most segments.

This study provided the foundation for a new method of BSP prediction. The population specific linear regression equations developed in this study should be used to predict BSPs for individuals similar to those examined in this experiment. While geometric models provided poor predictions, future improvements may increase their performance.

I dedicate this thesis to my parents whose constant love and support have helped me to pursue my dreams and realize my potential. Thank you for everything.

ACKNOWLEDGEMENTS

Thanks to my supervisor Dr. Jim Dowling for your guidance and friendship and for making the past two years enjoyable and challenging. Thanks for always having the time. Thanks to Dr. David Andrews for being there in the final stretch. Your support and advice were greatly appreciated. Thanks to my committee members Dr. David Andrews, Dr. Digby Elliott, Dr. Michael Pierrynowski and Dr. David Pearsall for your input and assistance. Thanks to my fellow grad students and friends for making the past two years ones that I will never forget: Kevin, Gianni, Rod, Kristen, Dave D., Tim, Sandy and Ted.

TABLE OF CONTENTS

CHAPTER II

LIST OF TABLES

LIST OF FIGURES

CHAPTER I

STUDY 1:
A NEW TECHNIQUE FOR MEASURING BODY SEGMENT PARAMETERS USING DUAL PHOTON ABSORPTIOMETRY

1.0 INTRODUCTION

Understanding human movement requires that biomechanists have knowledge of the characteristics and causes of a movement. As such, the complete biomechanical analysis of a human movement requires that the kinematics and kinetics of the motion be calculated. The kinematics of a movement may be measured directly by digitally tracking the linear and angular displacements of body segment joint centres and differentiating to obtain velocities and accelerations. The external kinetics of a movement, that is, the external forces and moments acting on the body, may also be measured directly using a force transducer. The internal kinetics of a movement must be measured indirectly, however, requiring the input of segmental kinematics, external kinetics and specific body segment parameters (BSPs).

The internal kinetics of a movement are often measured using either an inverse dynamics approach or a forward solutions approach. Each method treats the body as a chain of rigid links (body segments) connected together by frictionless hinge joints (Winter, 1990). The required kinematics may be obtained using video or optoelectronic devices that track the movement of reflective markers, light-emitting diodes or infra-red diodes. Electrogoniometers and accelerometers may also contribute information regarding joint angular displacement and segment acceleration, respectively. The external kinetics are often obtained using a force plate to measure ground reaction forces. The necessary body segment parameters

are difficult to obtain directly, however and must be estimated using predictive methods available in the literature.

For the past few decades, there has been an increase in attempts to develop methods for accurately measuring or predicting human BSPs. Some researchers have used cadavers to help provide reasonable estimates (Dempster, 1955; Clauser, McConville and Young, 1969; Chandler et al., 1975) while others have attempted to measure them directly on living humans (Drillis and Contini, 1966; Young, Chandler and Snow, 1983). Some have tested the use of medical imaging equipment (Zatsiorsky and Seluyanov, 1983; Martin et al., 1989) and others have explored the application of mathematical models or regression equations for BSP prediction (Hanavan, 1964; Morlock and Yeadon, 1986). These attempts have been limited in many respects, however, particularly in their application across gender, age, race and activity level.

The importance of segment parameter errors on the accuracy of segmental joint force and moment calculations has been somewhat neglected in the past. While attempts to investigate this issue have been limited, current research indicates that segment parameter error may have rather detrimental effects on segmental force and moment calculations. For instance, Capozzo and Berme (1990) found that the magnitude of segment parameter errors could be up to 48, 25 and 80% for segment mass, centre of mass location and frontal axis moment of inertia, respectively. Furthermore, Krabbe, Farkas and Baumann (1997) investigated the effect of segment parameter errors on elite distance runners. Using

an inverse dynamics method with a 3D model of the lower extremity they concluded that "the calculation of the moment of inertia force is necessary for the calculation of the intersegment moments of the hip and - if the touch down phase is of special interest - for the knee in opposition to the ankle" (pp. 519).

Pearsall and Costigan (1998) investigated the variation between BSP estimates with six different prediction methods. These methods were applied to young male volunteers and BSP estimations were compared, resulting in segment parameter variations of up to 40%. Pearsall and Costigan (1998) also investigated how segment parameter errors affected kinetic calculations. Using an inverse dynamics approach on walking, results showed that changes in the BSP predictor influenced kinetic output significantly, although the absolute changes were not that considerable. They added, however, that the ground reaction force in stance phase is significantly larger than the mass-acceleration component of the lower limb. Segment parameter importance would be much greater in situations with high segmental accelerations or for movements that do not have high external loads as in throwing (Pearsall and Costigan, 1998).

The research available therefore suggests that segment parameter errors have a significant effect on the accuracy of segmental force and moment calculations for movements involving high segmental accelerations or low external loads. Additionally, the effect of these errors may be even more detrimental in forward solutions approaches (Pearsall and Costigan, 1998). Given that the methods currently available for predicting segment inertial parameters are flawed, there

exists a need for a method that can predict these parameters for different populations with a high level of accuracy. The purpose of this study is to investigate a new method for measuring mass, centres of mass and moments of inertia of human body segments using dual photon x-ray absorptiometry (DPX). It is hypothesized that DPX will prove to be a useful and accurate tool for measuring human BSP's, providing a new technique for obtaining personalized BSP information and developing predictive equations for several different populations.

2.0 REVIEW OF LITERATURE

Several techniques for measuring or predicting human BSPs have been developed. These techniques may be categorized according to the methods used including cadaver studies, living subjects studies, medical imaging technology and mathematical modeling.

2.1 Cadaver Studies

The investigation into the physical characteristics of the human body began centuries ago where researchers would perform measurements on cadaver specimens that had been sectioned in some particular manner. One of the earliest reported studies involving the segmentation of cadavers was performed by Harless in 1860. Harless attempted to define absolute and relative lengths of human limb segments and proceeded to define segment volumes on five male and three female cadavers (Drillis and Contini, 1966). In a following study, Harless investigated the static moments of inertia of limb segments using two cadavers (Drillis and Contini, 1966). In 1889, Braune and Fischer conducted a study using three male cadavers to determine the lengths and masses of human limb segments. Regression equations were later developed from these measurements by Drillis and Contini (1966) for the prediction of BSPs (Drillis and Contini, 1966).

In 1955, Dempster conducted, what has been to date, the most extensive

analysis of human body segment parameters (Drillis and Contini, 1966). Dempster (1955) examined eight male cadavers (1 embalmed, 7 fresh) , aged 52 to 83 years of age and between 113 and 159.5 lbs. Segment masses were obtained through weighing and centres of mass were measured using a knife-edge balance technique. Moments of inertia were measured using a pendulum technique combined with parallel axis theorem. From the data, regression equations were developed for the prediction of these BSPs.

In 1959, Mori and Yamamoto measured segment masses on three male and three female Japanese cadavers. The techniques of their measurements were not reported, however (Clauser, McConville and Young, 1969). Fujikawa (1963) continued this research on six more cadavers and again, the techniques were not reported (Clauser, McConville and Young, 1969).

In 1969, Clauser, McConville and Young measured segment volumes, masses and centres of mass on thirteen embalmed male cadavers. The mean age and standard deviation of the specimens was 49 years (±13) with a mean mass and standard deviation of 66.5 kg (±8.7). Volumes were measured by calculating the difference between segment weight in air and water as well as by water immersion. Centres of mass were measured using balance tables. In a following study, Chandler et al. (1975) measured segment masses, centres of mass and moments of inertia on six embalmed male cadavers. Both studies developed regression equations for the prediction of these BSPs.

Clarys and Marfell-Jones (1986) sectioned three male and three female

embalmed cadavers, developing regression equations to predict segment masses. Masses were measured by weighing both in air and water. In 1994, six more cadavers were used to measure segment masses as well as component tissue masses. Regression equations were then developed to predict these masses from anthropometric variables.

Despite numerous attempts to measure and predict human BSPs using cadavers, several problems persisted with these methods. Of the studies listed above, only 64 subjects in total were examined. This problem was a result of specimen availability as well as very large time commitments and expense involved with the methods. Furthermore, among the specimens chosen for study, the majority were elderly white males, limiting the applicability of the results to other age groups or to individuals of a different gender, activity level or race.

Another problem with the cadaver studies was the inability to reliably compare results between the various studies. Segmentation methods differed between most studies, sometimes drastically, limiting the ability to compare data and predictive equations. Furthermore, fluid and tissue lost during the segmentation process may have caused losses in mass and thus inertia calculations.

2.1.1 Segmentation Methods

An influential factor in the results of cadaver studies was how the cadavers were segmented. Harless (1860) sectioned his cadavers by sawing through the tissue at the pivotal axis of primary joints. He then disarticulated the joints and

folded remaining skin around the ends of segments to prevent tissue and fluid losses (Clauser, McConville and Young, 1969). Braune and Fischer (1889), in an attempt to prevent fluid and tissue losses, froze their specimens. The segmentation methods were similar to those of Harless, however the freezing procedure prevented the disarticulation of joints and therefore required segmentation right through the joints (Clauser, McConville and Young, 1969).

In an effort to distribute soft tissue between adjacent segments, Dempster (1955) froze the joints of his cadavers in a mid-flexed position, bissecting the joints through joint centres. Furthermore, Dempster's segmentation methods differed significantly from other studies in that the shoulder girdle was removed from the trunk and the head and neck were kept together as one segment, sectioned at the C7-T1 level.

Clauser, McConville and Young. (1969) used x-rays of living subjects in different joint positions to define joint centre locations. The cadaver specimens were then frozen at the joints and segmentation lines were marked with a lead strip. Fluoroscopy was used to ensure the segmentation line matched the desired location and the frozen joints were sectioned. The method of sectioning joints in a mid-flexed position as Dempster (1955) had done was attempted but not successful. As a result, joints were bissected in the extended position. Furthermore, the method of Dempster (1955) in which the shoulder girdle was removed from the torso was eliminated. The torso remained intact at the shoulder and the upper arm was removed by a straight cut through the head of the humerus. Chandler, et al. (1975)

used segmentation procedures that were similar to Clauser, McConville and Young (1969).

Clarys and Marfell-Jones (1986; 1994) used segmentation methods that were adapted from Clauser, McConville and Young (1969). The difference was in the sectioning of bony parts. While both Clauser, McConville and Young (1969) and Chandler, et al. (1975) cut directly through both soft tissue and bone at joint centres, Clarys and Marfell-Jones (1986;1994) sectioned through soft tissue, circumventing the bony parts in an effort to keep the bone of a segment with that segment.

2.2 Living Subject Studies

In addition to cadaver research, several studies have examined methods for measuring BSPs using living subjects. Drillis and Contini (1966) measured various body segment parameters on twenty living males aged 20 to 40 years old. Segment volume and density were measured using both water immersion and reaction change methods and segmental moments of inertia were measured using a compound pendulum method and quick release. In 1983, Young, Chandler and Snow measured forty-six living females for segment volumes, masses, centres of mass and moments of inertia using anthropometric and stereophotometric methods. From photographs, surface areas were reconstructed and anthropometric values were applied to arrive at these segment parameters.

Plagenhoef (1983) conducted a study which compared the values from

Dempster (1955) to 135 living subjects (35 males, 100 females). Segment masses and centres of mass were calculated using water immersion and lead models were developed to measure radii of gyration. The lead models involved constructing plaster models of the limbs of subjects. Plagenhoef (1983) also used one male cadaver to determine the inertial parameters of the trunk segment. By using a cadaver for trunk inertia calculations, it was assumed that the properties of the tissue sampled approximated those of living tissue.

Other techniques for measuring BSPs on living subjects have been investigated. Peyton (1986) used an oscillation technique to measure the moment of inertia of a forearm segment. This method was found to produce results comparable to Dempster (1955) but accuracy was compromised by shoulder muscle contraction. Furthermore, the apparatus was useful for measuring the inertia of the forearm but its applicability to other body segments was limited. Jensen (1978; 1989) and Jensen and Fletcher (1994) used photogrammetry to measure BSPs of humans at various ages.This method was used to develop geometric models of body segments using elliptical zones. Segment masses needed for this method were estimated using regression equations from cadaver studies.

While many methods have been used to measure BSPs on living humans, several assumptions were necessary. For instance, the water immersion methods used by Drillis and Contini (1966) and Plagenhoef (1983), the stereophotometric methods used by Young, Chandler and Snow (1983) and the photogrammetry method used by Jensen (1978; 1989) and Jensen and Fletcher (1994) all assumed

that the densities of body segments were known and constant throughout. Furthermore, these density values were often obtained from cadaver studies, assuming that cadaveric tissue retained similar physical properties as living tissue. The reaction change method used by Drillis and Contini (1966) assumed that the centres of mass of the segments were known, as were the relative masses of the segments which were determined through water immersion methods. Also, the pendulum method used by Drillis and Contini (1966) assumed that the moment of inertia about the longitudinal axis was negligible in comparison to that of the transverse axis. The quick release method assumed that muscle contraction was absent, that the point of release was clean and noise-free and that all joints were frictionless.

2.3 Medical Imaging Technology

Recent improvements in medical imaging technology has led to an increase in studies using these instruments to measure human BSPs. Studies using CT imaging, MRI and gamma-mass scanning have indicated that greater accuracy in measuring the BSPs of living humans is possible. Zatsiorsky and Seluyanov (1983) investigated the possibility of measuring mass-inertial characteristics of human body segments using gamma-mass scanning. One hundred men were scanned and anthropometric measurements were taken from which 150 regression equations were developed for 10 body segments. In 1990, Zatsiorsky, Seluyanov and Chuganova used the gamma-scanner technique to develop geometric models and

regression equations from 100 male and 15 female subjects. The two prediction methods were compared and the results showed that errors from the regression equations were 1.5 times larger than those from the geometric.

Computed tomography (CT) has also been investigated for its potential in measuring BSPs. Huang (1983) used CT to compare BSPs from a pig specimen with a 3 year old female cadaver, finding that the animal specimens did not provide adequate representation of children. Pearsall, Reid and Livingston (1996) have also used CT to determine BSPs of the human trunk and found differences in centre of mass and moment of inertia measurements between subjects. Differences were also found when results were compared with previous studies.

MRI has been examined by Martin, et al. (1989) using fixed baboon cadaver specimens. Segment volume, density, mass, centre of mass location and moment of inertia about a transverse axis were all calculated using MRI and compared to standard experimental techniques. Percent differences between the two yielded differences of 6.3%, 0.0%, 6.7%, -2.4% and 4.4% for volume, density, mass, centre of mass location and moment of inertia, respectively. While the values for centre of mass and moment of inertia showed a high degree of accuracy, the procedure involved in obtaining these results was very time consuming and expensive. This method therefore proved to be impractical for providing personalized BSP information as well as for developing BSP predictor models.

2.4 Mathematical Modeling

Several investigators have developed mathematical models and/or regression equations to help predict human BSPs. As previously indicated, regression equations have been developed by Drillis and Contini (1966), Clauser, McConville and Young (1969), Chandler et al. (1975), Young, Chandler and Snow (1983), Clarys and Marfell-Jones (1986; 1994), Zatsiorsky and Seluyanov (1983; 1985) and Zatsiorsky, Seluyanov and Chugunova (1990). The equations developed by Clarys and Marfell-Jones (1986; 1994) were unable to predict within 5% of segment mass for all segments. Zatsiorsky and Seluyanov (1983; 1985) were unable to predict BSPs with multiple regression equations within 24% of any parameter. Geometric representations of body segments as right circular cylinders were reported to be 50% more accurate than the regression equations. Furthermore, the anthropometric variables used in these models were biomechanical measurements rather than surface measurements. As a result, the investigators presented coefficients in which surface measurements could be converted to biomechanical ones.

In 1964, Hanavan developed geometric models of human body segments (circular ellipsoid, elliptical cylinders, spheres and right circular frusta) using anthropometric measurements where centres of mass were predicted within 0.7 inches and moments of inertia within 10%. Hatze (1980) developed a mathematical model for determining segment parameter values which required the input of 242 anthropometric variables taken from the subject. The models were claimed to predict with a maximum error of 5%.

predict with a maximum error of 5%.

Hinrichs (1985) used data from Chandler et al. (1975) to develop linear regression equations for moments of inertia of body segments based on anthropometric measurements. The accuracies of these equations were questionable, however, because of assumptions discussed previously and because the linearity of the predictive equations may not have been representative of the actual composition and nature of human body segments (Morlock and Yeadon, 1986). Morlock and Yeadon (1986) developed regression equations based on Chandler et al. (1975), but constructed them for the thigh segment only. These equations were of a nonlinear nature constructed to show that linear relationships did not produce accurate predictors when relating anthropometric measurements and moments of inertia. In a following study, Yeadon and Morlock (1989) constructed both linear and nonlinear regression equations from the data published by Chandler et al. (1975). The nonlinear equations consisted of three to four components depending on the segment under study. The standard error estimates had average values of 21% for the linear predictors and 13% for the nonlinear ones.

Winter (1990) used data from Dempster (1955) (adapted from three sources), constructing tables to predict segment mass from whole body mass, segment length from whole body height and centre of mass and radius of gyration from segment length. These predictions assumed perfect symmetry between body segments, however and were subject to the limitations of the cadaver studies discussed

previously.

While many studies have provided equations or models for BSP prediction, the accuracies of these predictors have been dependent upon the measurement technique used as well as the type of subjects used for data collection. In many of these studies, prediction errors were high and those equations producing better estimates were based on males only. As a result, these predictors may be less accurate if applied to women or to individuals of different age, activity level or race. The more accurate cadaver research also lacks external validity and the imaging techniques of living subjects are too onerous to contribute significantly to BSP estimations in biomechanical analyses of human movement. As a result, most studies today use the tables reported by Winter (1990) which are constrained by the limitations of the studies used for the estimates. A method that allows the accuracy of cadaver dissections and the external validity of the large population living subject studies is therefore needed.

3.0 METHODS

3.1 Principle of DPX

DPX has typically been used to measure bone density and has provided this information at a low cost with low radiation doses (1/10 of chest x-ray) to the patient. DPX operates on the premise that a photon emitted from a beam will interact with body tissues and either be absorbed or scattered. One of three occurrences are possible when a photon interacts with an atom: photoelectric absorption, Compton scattering or coherent scattering (Webber, 1995).

Photoelectric absorption occurs when a photon interacts with an inner shell electron of an atom. This electron becomes ejected from the atom and the photon disappears. The vacancy of this inner shell electron is then filled with an outer shell electron and an x-ray is emitted. When living bodies are scanned with DPX, the photons interact with atoms that have a low atomic number such as carbon, oxygen, hydrogen, nitrogen, calcium and phosphorus. Since these atoms are of low atomic number, the x-rays emitted are low energy (Webber, 1995).

Compton scattering occurs when a photon interacts with a loosely bound or free electron of an atom. This theory, developed by Arthur Compton, was sparked by the observation that when x-rays were scattered from a solid body, the scattered x-rays had lower frequencies than those of the incident rays. Thus, when a photon collides with an electron, a portion of the photon's energy is transferred to the

electron, and the direction of the photon is changed (Halliday and Resnick, 1968). Coherent scattering occurs when a photon interacts with an outer-shell electron of an atom and is scattered. The electron remains in place and the direction of the photon is changed (Webber, 1995).

The probability of one of these three interactions to occur may be represented by their respective atomic cross-sections; σ_{photo}, σ_{Com}, σ_{coh}. Each atomic cross-section varies depending on the energy of the interacting photon and depending on the composition of the material it interacts with (Webber, 1995). If atomic cross-sections were converted to represent the bulk properties of the object, the equation would proceed as follows:

$$\mu_{photo} = \sigma_{photo}(N_o/A) \quad (1)$$

"where N_o/A is Avagadro's number (atom·mole^{-1}) divided by the atomic mass (g·mole^{-1}) and μ is the partial attenuation coefficient for the photoelectric effect in the object (cm^2·g^{-1})" (Webber, 1995; 59). Similar equations could be written for μ_{Com} and μ_{coh}. Each of these 3 interactions occur independently, therefore the sum of each of these partial coefficients yields a total mass attenuation coefficient, μ, which represents the probability of a photon interacting with the object (Webber, 1995).

The Hologic QDR-1000 delivers x-rays through a collimated beam to the subject and the tissue in the path of the beam is measured on the other side by a detector. The photons are delivered at two significantly different energies (140 keV and 70 keV) (Hologic QDR-1000 Operators Manual, 1989). When a beam emits a

photon with a certain intensity (I_o) onto an object, the resulting attenuated intensity (I) measured by the detector is related to the original intensity by:

$$I = I_o e^{-\mu m} \quad (2)$$

where *m* is the mass of the material in the path of the beam ($g \cdot cm^{-2}$). This equation assumes that regardless of how the photon interacts with an object (through absorption or scattering), the photon is removed from the beam and is not detected. Therefore, given I_o, I and μ, the mass of the object may be calculated. (Webber, 1995).

The use of a single value of μ assumes that only one type of material is present in the object and that all photons have the same energy. To take into account the various types of materials within living bodies, the equation is adapted using two attenuation coefficients:

$$I = I_o e^{-(\mu 1 m 1 + \mu 2 m 2)} \quad (3)$$

This equation leaves two masses left unknown which may be determined if the measurement is conducted at two different photon intensities. As such, the mass of one component can be eliminated to find the mass of the other. Calculating the mass of a component using DPX therefore proceeds as follows:

$$m_1 = \frac{\ln(I_{o,L}/I_L) - R_{ST}\ln(I_{o,H}/I_H)}{(\mu_{1,L} - R_{ST}\mu_{1,H})} \quad (4)$$

where $I_{o,L}$ is the incident low intensity photon, $I_{o,H}$ is the incident high intensity photon, I_L is the remaining low intensity photon, I_H is the remaining high intensity photon, R_{ST} is given by $\mu_{2,L}/\mu_{2,H}$ and is dependent on the composition of soft tissue

(Webber, 1995).

If component 1 represents bone tissue and component 2 represents soft tissue, then this equation allows the separate computation of bone and soft tissue mass within an object. The measured intensities (μ_1 and μ_2) can be determined through calibration. Calibration is done using a phantom constructed of known materials which approximate the attenuation coefficients of bone, soft tissue and air at each photon energy (Webber, 1995).

3.2 Technical Use of the Hologic QDR 1000

The Hologic QDR 1000 functions by scanning objects in a serpentine manner. The software allows the user to choose the type of scan to be performed, ranging from regional scans of the hip, spine and forearm to whole body scans. For a whole body scan, the patient is placed on the bed and the DPX begins to scan, from head to toe, in a serpentine (X-Y) manner. Figure 1 displays the apparatus when a human scan is being performed. The photons are emitted from a collimated beam beneath the subject and are detected by the scanner arm located above the subject, directly in line with the beam. A calibration wheel, which is composed of various x-ray absorbing materials, rests between the x-ray source and the subject, providing an automatic internal reference system (Hologic QDR-1000 Operators Manual, 1989).

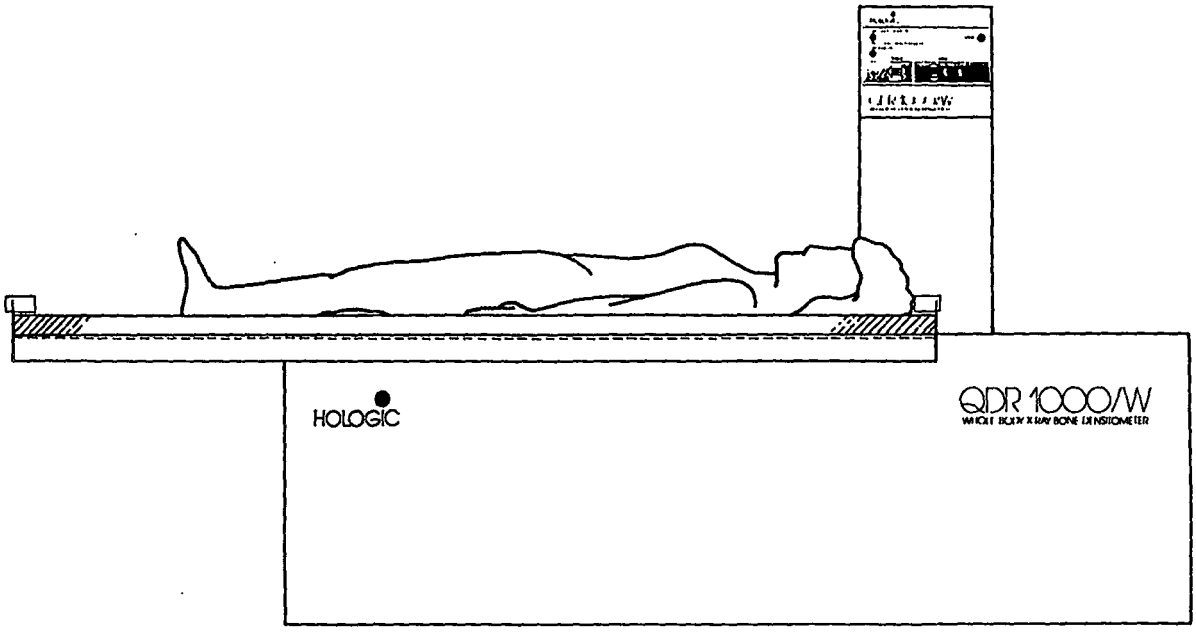

Figure 1: Apparatus of a Human Scan with the Hologic QDR-1000

3.3 Mass Measurement Using DPX

The Hologic QDR-1000 emits x-rays at two significantly different energies (70 KeV and 140 KeV). During a scan, the higher energy photons are more likely to interact with both calcium (present in bone) and carbon (present in soft tissue) while the lower energy photons mostly interact with calcium (Webber, 1995). Since the higher energy photons interact with all atoms with relative equality, these intensity values were thought to be reflective of body mass. A computer program (DXA, Durkin and Dowling, 1998) was therefore written to extract these numbers from the raw data file produced during a scan and write them to an ascii file for later use. Figure 2 shows a plot of these numbers arranged in a three dimensional format to produce a *'MASSMAP'* of a human male.

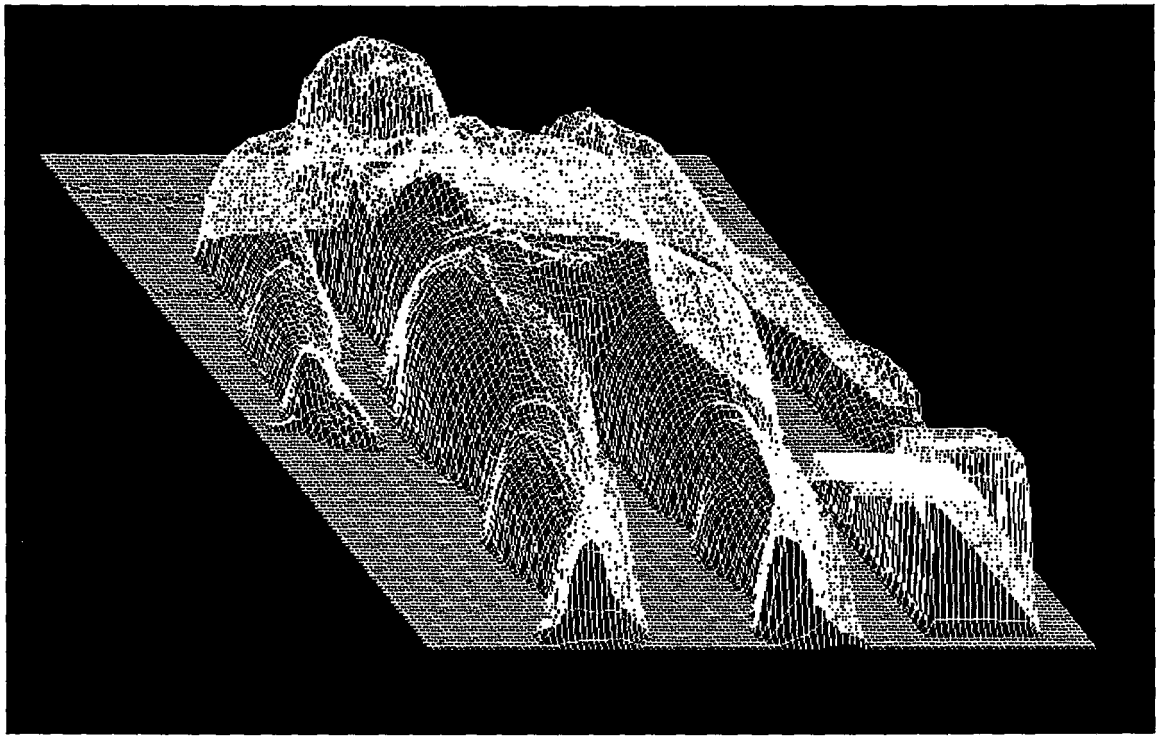

Figure 2: *MASSMAP* of a Human Male

3.3.1 DPX Mass Constant

The numbers from the raw data file were proportional to, but not equal to mass, therefore a mass constant needed to be calculated. To determine the mass constant, two objects of known mass (a plastic cylinder and soft cover book) were scanned (Hologic QDR 1000/W). The masses of these objects were found by weighing on a force plate (AMTI). Mass information from the cylinder scan was then extracted from the raw data file and written to an ascii file. These numbers were summed and the value divided by the force plate mass. The quotient represented the mass constant for the DPX values.

The mass constant was validated by summing the mass values for the book, multiplying the sum by the mass constant and comparing this value to the book mass measured using the force plate. A percent difference between the two values was calculated using the following formula:

$$\text{Percent Difference} = [\,(\text{DPX} - \text{Criterion}) / \text{Criterion}] \cdot 100\% \qquad (5)$$

(Martin et al., 1989).

3.3.2 DPX Length and Width Constants

As was previously mentioned, the Hologic QDR 1000/W scanned objects in a serpentine (X-Y) manner. The default sampling frequency for a whole body scan was to collect data over 146 lines with 112 samples per line. The length and width of each DPX element was measured by plotting the DPX values from the cylinder scan. Figures 3 and 4 represent plots of the data (Figure 4 is an enlargement of Figure 3). Each point along the x-axis represented a scanned element and the y-axis represented the amount of mass contained within that element.

The length and diameter of the cylinder and length and width of the book were measured using a measuring tape accurate to the nearest 0.5 mm. The DPX values of the cylinder scan were then plotted (Mathpack, 1990) and the total number of peaks in the plot were calculated. The measured length of the cylinder was divided by the number of peaks to arrive at a length constant. The length constant was then validated by plotting the values of the book in the same manner, multiplying the number of peaks by the length constant and comparing this value

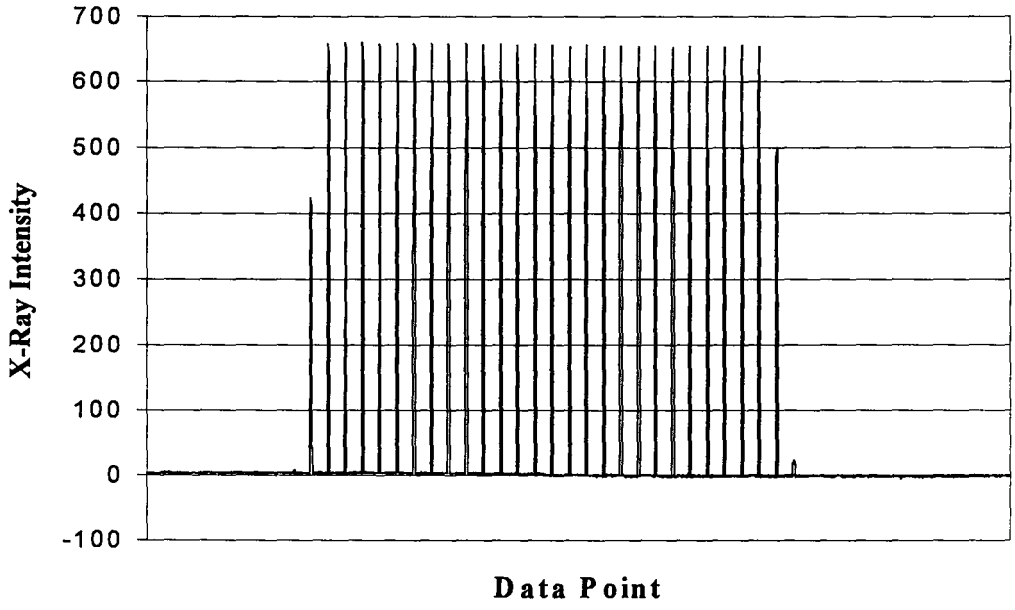

Figure 3: Plot of DPX X-Ray Intensity Values from Cylinder Scan

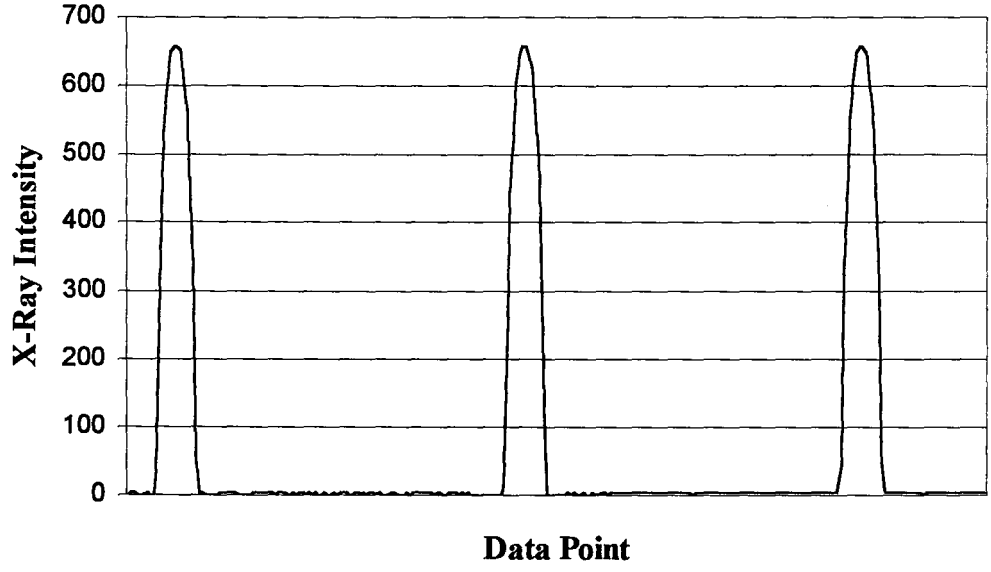

Figure 4: Enlarged Plot of DPX X-Ray Intensity Values from Cylinder Scan

to the measured length of the book. The comparison was done by calculating the percent difference between the measured and DPX values for the book.

The width constant was determined in a similar manner to the length constant. The diameter of the cylinder was measured and the data from the cylinder scan plotted (Mathpack, 1990). The plot was enlarged (see Figure 4) and the width of each peak was measured. The mean of these widths was calculated and divided by the measured diameter of the cylinder. To validate this constant, the mean width of the peaks from the book plot was multiplied by the width constant and a percent difference was calculated between the DPX value and the measured width of the book.

3.4 BSP Calculations

To compute BSP information from a DPX scan, subroutines were created within the "DXA" program (Durkin and Dowling, 1998) to enable the segmentation of a scan image. The program included an imaging subroutine, a cursor subroutine and a BSP calculation subroutine.

The Hologic QDR-1000/W produced two files from a scan, a raw data file and a patient file. The patient file contained, among other information, graphical information from the scan. The graphical information consisted of a series of gray scale values ranging from 0 to 255 which were proportional to density. The resolution of the graphical information was 730 by 336 elements, 15 times the resolution of the raw data. A subroutine was written using this graphical information

to produce an image of the scan on the computer screen. Figure 5 shows an example of a scan image produced by the "DXA" program (Durkin and Dowling, 1998).

Since this image was created to enable the digital sectioning of segments from a scanned subject, a subroutine was also written in which a cursor could be moved around the screen to enable digitization of the image. The cursor was set to advance in units proportional to the image data, 730 by 336 units, with cursor coordinates being displayed in the top right hand corner of the screen.

A BSP calculation subroutine allowed the user to select coordinates based on cursor location for i) the selection of an area containing a segment and ii) digitization of proximal and distal joint centres. Once these coordinates were selected by the user, the program proceeded to calculate BSP information on the segment.

Four body segment parameters were calculated from the DPX information; segment mass, length, centre of mass location along a transverse axis and moment of inertia about the centre of mass. Mass was calculated by summing the values contained within the perimeter defined by the digitized coordinates, producing the mass of the segment in kilograms. Segment length was calculated using the proximal and distal joint centre information from the digitization procedure. Pythagorean Theorem was used in conjunction with the length and width constants to arrive at a segment length in meters.

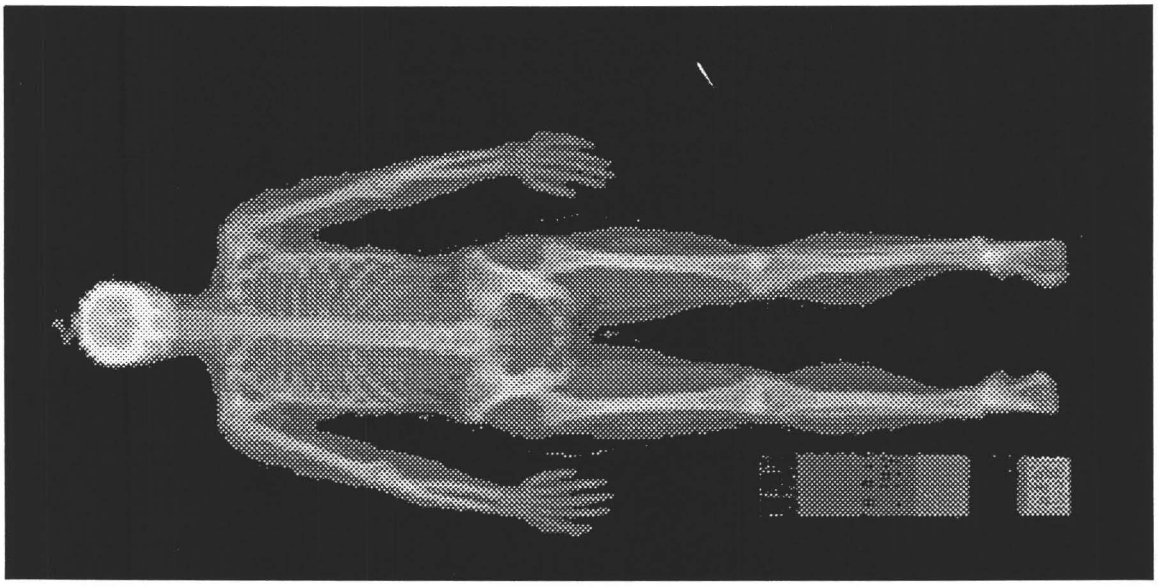

Figure 5: DPX Scan Image of a Human Female

Centre of mass along the transverse axis was calculated by first extracting the segment information within the perimeter defined by the digitization procedure. The centre of mass along the x-axis was determined using the following formula:

$$CM_x = \frac{\sum (x \cdot m)}{\sum m} \quad (6)$$

where *x* was the location of the mass element in the x-direction and *m* was the mass of the element. The centre of mass along the y-axis was determined in the same manner:

$$CM_y = \frac{\sum (y \cdot m)}{\sum m} \quad (7)$$

where *y* was the location of the mass element in the y-direction. The distance of the centre of mass from the proximal (CM_p) and distal (CM_d) ends of the segment were then calculated using the proximal and distal joint centre coordinates, the length

and width constants and Pythagorean Theorem to arrive at CM_p and CM_d distances in meters.

The moment of inertia about the centre of mass (I_{CG}) of the selected segment along its transverse axis was calculated using the following formula:

$$I_{CG} = \sum mr^2 \quad (8)$$

where *m* was the mass of each element in kg and *r* was the distance of each element from the centre of mass in meters.

3.5 Validation of BSP Calculations

Validation of the above calculations were performed in three ways. The first involved comparing DPX whole body mass calculations of a living human subject to measured whole body mass. The second method involved calculating mass, centre of mass about a transverse axis, moment of inertia about the centre of mass and length of an homogeneous object using DPX and comparing these results to standard experimental measurements. The third method involved calculating the above listed BSPs from a biological specimen using DPX and comparing the values to standard experimental measurements.

Ten young active male subjects were selected from the student body at McMaster University to validate DPX measurements of whole body mass. Subjects underwent a whole body DPX scan (Hologic QDR 1000/W) followed by weighing on a scale accurate to 0.5 kg. The scan data from each of the subjects was processed using the "DXA" (Durkin and Dowling, 1998) software created for the

study. Whole body mass was calculated using the program and compared to the criterion (scale measured) body mass of each subject. A percent differerence between the measured and DPX values was calculated as well as a mean percent difference and standard deviation for the entire subject group.

The accuracy of BSP measurement using DPX was validated by comparing DPX calculations of an object of constant density to criterion BSP values. The plastic cylinder used for the determination of the mass, length and width constants was chosen for this purpose as it had already undergone a DPX scan (Hologic QDR 1000/W) and had been previously measured for mass, length and diameter.

Centre of mass of the cylinder along a transverse axis was measured by balancing the object on a knife-edge and measuring the distance from the proximal and distal ends. Because the object was a symmetrical geometric shape, the centre of mass was one-half the length of the object.

The I_{CG} along the transverse axis of the cylinder was measured using the formula for the I_{CG} of a cylinder about a transverse axis:

$$I_{CGg} = 1/12\ (m \cdot (3a^2 + l^2)) \qquad (9)$$

where *m* was the mass of the cylinder, *a* was the radius of the cylinder and *l* was the length (Beers and Johnston, 1993). The percent difference between the DPX and criterion BSP values for the cylinder was then calculated.

Further validation of DPX in providing accurate BSP information was done using a biological specimen. One embalmed cadaver segment was used for this purpose, the selection of which was chosen according to its ease in the testing

procedure. A leg segment was cut from the lower limb of a cadaver at the knee and ankle. Accuracy in segmentation was not crucial as the specimen was used specifically to validate the accuracy of DPX with biological tissue.

The mass of the specimen was measured on a force plate (AMTI) and the location of its centre of mass along a transverse axis was determined by balancing on a knife-edge. A ruler 1 mm in width was secured in a vice and the segment was positioned across the ruler edge such that it was exactly balanced. The location at which the leg was exactly balanced was measured both from the proximal and distal ends.

The moment of inertia about the centre of mass was measured using a pendulum method. The segment was tied at the distal end with a string and swung about an axis at a measured distance from the centre of mass. The maximum angle at which the cylinder was oscillated was less than 5° at all times so as not to compromise the validity of the calculations. The time over ten oscillations was measured and the mean time for one oscillation was used for the period of oscillation in seconds. The moment of inertia about this axis was calculated using the formula:

$$I_a = \frac{t^2 \cdot m \cdot g \cdot r}{4\pi^2} \qquad (10)$$

where *t* was the period of oscillation in seconds, *m* was the mass of the object in kg, *g* was the gravitational constant (9.81 $kg \cdot m \cdot s^{-1}$) and *r* was the distance from the axis of rotation to the centre of mass. The moment of inertia about the centre of mass

was then calculated using parallel axis theorem:

$$I_a = I_{CGp} + mr^2 \quad (11)$$

The segment was then placed on the DPX scan bed which was covered with a plastic sheet. The segment was scanned (Hologic QDR 1000/W) and the data processed using the "DXA" software (Durkin and Dowling, 1998). In this instance, the removal of the bias created by the plastic sheet was incorporated into the program. The location of the proximal and distal end-points were selected according to the locations from which the centre of mass was manually calculated. BSP information was then calculated and the DPX results compared with the experimental results by calculating the percent difference.

As was indicated earlier, the Hologic QDR 1000/W sampled data by scanning in a serpentine manner. The length and width constants demonstrated that the data was collected in units measuring 1.323 cm X 0.053 cm. To determine whether improved accuracy could be achieved with a higher scan resolution, an interpolation procedure was incorporated into the program. A cubic spline algorithm (adapted from Hewlett-Packard library) was applied to the mass data increasing the number of data points to fifteen times the raw data. The resolution was therefore increased to 0.026 cm X 0.018 cm. The cursor program was adapted to the new unit dimensions and the images of the cylinder and cadaver specimen were then re-digitized. The segment parameters were recalculated and compared to the criterion values by calculating the percent differences.

4.0 RESULTS

Table 1: Comparison of Criterion and DPX Calculations of Whole Body Mass (WBM)

Subject	Criterion WBM (kg)	DPX WBM (kg)	% Difference
1	85.5	85.8	-0.32%
2	80.3	81.4	-1.33
3	86.4	87.2	-0.87
4	80.2	82.4	-2.79
5	77.7	78.4	-0.93
6	69.7	69.4	+0.40
7	67.7	69.4	-2.54
8	71.0	69.8	+1.76
9	74.7	75.9	-1.61
10	73.3	73.3	-2.10
11	71.4	72.3	-1.25
Group Mean	****	****	**-1.05**
Group S.D.	****	****	**1.32**

The results from Table 1 show that DPX can measure whole body mass of human subjects with a high degree of accuracy as percent differences between measured and DPX mass calculations ranged from -2.79 to +1.76% with a group mean of -1.05% (± 1.32%).

Table 2: Comparison of Criterion and DPX Cylinder Parameter Results

Parameter	% Difference Raw DPX	% Difference Interpolated DPX
Mass (kg)	+3.24	-2.05
Length (m)	-5.26	-1.30
CM_p *(m)*	+1.22	-0.44
CM_d *(m)*	+15.84	-0.72
I_{CG} *(kg·m²)*	+1.83	-2.63

The results from Table 2 show that mass measurements using the original data resolution were very accurate, yielding a percent difference of 3.2% when compared with criterion measurements. DPX measurement of length and centre of mass using the original resolution were less accurate, however, as percent differences were -5.3% for length and 15.8% for Cm_d. I_{CG} measurement using the original DPX resolution showed accurate results with a percent difference of 1.83.

The accuracy of the mass measurements using the interpolation procedure improved from 3.24 to -2.05 percent difference. Length and centre of mass calculations also greatly improved with percent differences decreasing to less than 2% for the three values. I_{CG} accuracy decreased only slightly with the percent difference increasing from +1.83% to-2.63%.

The results shown in Table 3 indicate that DPX was able to accurately measure segment mass, length and centre of mass location of a human biological specimen. The raw DPX results, when compared to the criterion results, revealed a high degree of accuracy in mass measurement at less than 2% difference. The

Table 3: Comparison of Criterion and DPX Segment Parameter Results

Parameter	% Difference Raw DPX	% Difference Interpolated DPX
Mass (kg)	+1.23	+3.20
Length (m)	-2.05	+1.28
CM_p *(m)*	-4.10	+2.73
CM_d *(m)*	+5.80	+0.97
I_{CG} $(kg \cdot m^2)$	+9.91	+8.19

centre of mass results also show a relatively high degree of accuracy, although the accuracy was less than that obtained for mass. The results showed a rather large percent difference in the I_{CG} measurements.

When examining the interpolated DPX results, accuracy in the mass measurements decreased such that mass was overestimated by 3.2% compared with 1.23% from the raw data. Again the interpolation procedure greatly improved the accuracy of the centre of mass calculations, however. Centre of mass calculations improved from -4.10% to 2.73% for the proximal end and from 5.8% to 0.97% for the distal end. Accuracy in the measurement of segment length also increased as the percent difference improved from -2.05% to 1.28%. The percent difference for moment of inertia in the interpolation procedure was still rather large, however, decreasing only to 8.19% from 9.91%.

5.0 DISCUSSION

The results have shown that DPX can measure whole body mass of humans with a high degree of accuracy. DPX has also been shown to measure mass, length, centre of mass and I_{CG} of an inanimate object and a human biological specimen with great accuracy. The original resolution of the data provided accurate measurements of mass for both objects when compared to criterion measurements. An accurate calculation of I_{CG} for the cylinder was also found when compared to the criterion measurement which was obained using a geometric formula. Length and centre of mass measurements were highly prone to error using this resolution, however. Furthermore, I_{CG} measurement of the leg segment revealed large errors when compared with the criterion measurement which was obtained using a pendulum method.

Interpolation of the data to fifteen times the original resolution greatly improved length and centre of mass measurements for both objects and maintained a high level of accuracy for mass measurements. I_{CG} measurements of the cylinder also remained accurate, however, a comparison of the leg segment still produced rather large percent differences.

Comparing percent differences between the geometric and pendulum methods for the cylinder and leg segment indicated that the pendulum method for measuring I_{CG} may have contained some error. The pendulum method was not

performed in a calibrated system and may have been subject to measurement error. The geometric equation is known mathematically to be correct, however and therefore provided an accurate benchmark to compare DPX values with (Beer and Johnston, 1993). Since the geometric method matched closely with the DPX inertia value for the cylinder and all other parameters were measured by DPX with minimal error, this would indicate that DPX can also accurately measure I_{CG} of a biological specimen.

The centre of mass measurements resulted in slight differences in accuracy between the proximal and distal ends. For example, the differences in accuracy for the leg centre of mass location were 2.73% and 0.97% from the proximal and distal ends, respectively. Slight differences may have existed as a result of data resolution limitations but could be minimized by further increasing the resolution. The differences in accuracy between the proximal and distal centre of mass measurements of the leg segment were most likely due to differences in the selection of end point locations between the experimental measurements and the DPX digitization. Greatest care was taken to ensure the accurate location of the exact points from which the centre of mass was measured experimentally, however, discrepancies may still have resulted. When segmenting living humans, strict definitions of joint centre locations should be set to minimize variability in segment separation and thus minimize segmentation errors in the digitization process.

The interpolation procedure greatly increased the accuracy of length and centre of mass measurements. These improvements in accuracy could have

important effects when measuring BSPs of living humans. Although the interpolation procedure did not create large improvements in mass and inertial calculations and in some instances, accuracy even decreased somewhat, the effect of this procedure may be more important when digitizing whole body scans of living humans. Digitization of the cylinder or the cadaver segment did not require digital segmentation from other parts or tissue. When analyzing living beings, however, segments will need to be digitally separated from others. The interpolation procedure will provide greater accuracy when separating segments at joint centres and will therefore help to minimize potential over- or underestimations of segment boundaries. This will be important for mass and centre of mass calculations but may be even more important for moment of inertia calculations since inertia is more affected by mass at the outer regions of the segment.

While DPX has been shown to provide accurate BSP calculations of inanimate objects and biological specimens, many studies have been conducted to evaluate the effectiveness of a particular instrument in the measurement of body segment parameters. Martin et al. (1989) investigated MRI as a potential technique and found results to be highly accurate. This method posed minimal risk for subjects, however the processing time and expense rendered it impractical for providing personalized body segment parameter information. When comparing DPX results to those from Martin et al. (1989), the DPX results showed less error. Martin et al. (1989) found a 6.7% mean difference for mass, -2.4% for centre of mass from the proximal end and 4.4% for inertia compared with DPX cylinder values of -2.05%,

0.44% and -2.63% difference for mass, centre of mass and moment of inertia (geometric method), respectively. Results for mass and centre of mass from the biological specimen were also more accurate with 3.2% and 2.73% difference, respectively. DPX can therefore provide a quick and easy measurement of personalized BSPs with a high degree of accuracy. Furthermore, the resolution of the data can be increased or decreased to whatever the user wants through interpolation.

DPX as a measurement tool, combined with the custom "DXA" software (Durkin and Dowling, 1998) has many practical applications. In addition to providing personalized BSP information, DPX could be used to develop geometric models and/or regression equations to predict BSPs of different body segments for different populations. While predictive equations exist in the literature, the majority of the equations are based on males only and many are compromised by questionable assumptions and the selected subject base. Zatsiorsky and Seluyanov (1983; 1985) and Zatsiorsky, Seluyanov and Chugunova (1990) developed sets of predictive equations using gamma-mass scanning, a method similar to DPX. These equations were based on one hundred young men, however. With DPX, equations can be developed for different populations based on race, gender, age, activity level and so forth. Furthermore, population differences have not been examined, therefore DPX may provide a means for such an investigation.

6.0 CONCLUSION

The results have shown that DPX can accurately measure whole body mass of human subjects as well as mass, length, centre of mass about a transverse axis and I_{CG} of both homogeneous and biological specimens. The interpolation procedure greatly improved the accuracy of length and centre of mass measurements and may be modified to provide any data resolution the user wishes. Furthermore, the scanning procedure is rapid, taking less than fifteen minutes for a whole body scan. The procedure is safe, exposing the subject to minimal radiation doses of less than 1/10 of a chest x-ray and the software written to perform the calculations is easy to operate, provides accurate measurements, clear graphical resolution and rapid processing time. It is therefore evident that DPX can be a useful tool for providing subject specific BSP information and can provide a means for developing predictive equations for several different populations. DPX may therefore be considered the new gold standard for BSP measurement.

Future directions are therefore to i) create a database of different populations according to gender, age, race, etc. and compare the BSP characteristics between these populations and ii) develop geometric models and/or regression equations for each of these populations.

CHAPTER II

STUDY 2:
THE PREDICTION OF BODY SEGMENT PARAMETERS USING GEOMETRIC MODELLING AND DUAL PHOTON ABSORPTIOMETRY

1.0 INTRODUCTION

A review of literature in Study 1 showed that there is a limited availability of accurate BSP information or predictive equations for different subpopulations of humans. For instance, cadaver studies have been based on small sample sizes, most of which consisted of elderly males and living subjects studies have had large sample sizes but the methods used involved questionable assumptions. Studies using medical imaging technology have provided accurate results, however the methods used are too onerous to allow the practical acquisition of BSP information. Mathematical modelling has been used for the prediction of BSPs and while regression equations and geometrical modelling have both been used, the equations available often yield large errors and/or may only be applied to specific populations such as young active males.

A review of the literature also revealed limited comparison of BSP values between subpopulations of humans. Most studies involving the measurement or prediction of BSPs have examined only one subpopulation. Consequently, Jensen (1978; 1989) and Jensen and Fletcher (1994) have used photogrammetry to investigate the morphology of humans across the life span and have reported differences between genders and between age groups of humans. This supports the need for further investigation of BSP differences between different subpopulations of humans.

Dual photon absorptiometry (DPX) has been shown in Study I to be a safe, economical and accurate tool for providing measurements of whole body mass of humans as well as mass, centre of mass and moment of inertia of both biological specimens and homogeneous objects of low atomic weight. The results indicated that DPX may be a new gold standard for measuring body segment parameters (BSPs) and could be used to acquire personalized BSP information. DPX may also be used to create large databases of humans based on different subpopulations for the prediction of BSPs. While DPX has been shown to provide accurate measurements of BSPs, a researcher would require this rather large machine in order to measure their subjects. Furthermore, while the radiation doses are minimal, subjects would be exposed to radiation and therefore be at some risk. If large databases of humans could be constructed for different subpopulations based on age, gender, race, body type, etc., equations could be developed to predict BSPs for these groups. This would eliminate the need for researchers to scan each subject, process the files, section the segments and run the calculations. The researcher would only require the input of specific anthropometric variables to obtain estimations of BSPs such as segment mass, center of mass and moment of inertia.

Two methods of BSP prediction have been used in the past: i) regression equations which include both linear and nonlinear methods and ii) geometric models which involve the representation of body segments as simple geometric shapes. Both methods require the input of specific parameters, most often

anthropometric variables. These methods have been used by researchers with limited success, however a study by Zatsiorsky, Seluyanov and Chugunova (1990) has shown geometric models to be more accurate than regression equations for predicting BSPs. Zatsiorsky, Seluyanov and Chugunova (1990) used a gamma-scanner method to develop predictive equations from 100 young athletic men and 15 athletic young women. They developed regression equations and geometric models from their data and found that the geometric models were 1.5 times more accurate than the regression equations.

The use of geometric models for BSP prediction would be more advantageous than regression equations simply because these models could account for segment shape more so than a regression line could. Individual differences could therefore be accounted for and BSP predictions would be better. Geometric models also have an advantage in that only one model need be applied to all subpopulations of humans. This would be easier than having to apply a separate regression equation to each person based on their gender, age, body type, etc.

While many studies have provided equations or models for BSP prediction, the accuracies of these predictors have been dependent upon the measurement technique used as well as the type of subjects used for data collection. Furthermore, investigations of population differences in BSPs have been limited and the use of the predictors in the literature are cautioned for individuals not fitting

the description of the subjects from which the equations were developed. Nevertheless, most studies today use the tables reported by Winter (1990) which are constrained by the limitations of the studies used for the estimates.

Given the current situation of BSP measurement and prediction in biomechanics, the purposes of this study are as follows:

i) to investigate BSP differences between four human subpopulations using DPX

ii) to investigate a method for predicting body segment parameters using geometrical modelling

iii) to compare the accuracy of the geometric predictions with another currently used method (Winter, 1990)

It is hypothesized that there will be significant differences in BSPs between human subpopulations, supporting the need for a new method for predicting BSPs for different populations. It is also hypothesized that the geometrical models developed will provide more accurate BSP predictions for different populations than the method presented in Winter (1990).

2.0 METHODS

2.1 Subjects

Volunteers from four different subpopulations of humans were selected to participate in the study. The four subpopulations consisted of two gender categories (male, female) and two age groups (19-30 years, 55^{+} years). Racial characteristics were not specified for this study, therefore the participants were from various ethnic origins. Twenty-five volunteers were selected for each subpopulation according to specific body height and mass criteria. Twenty-five cells representing five percentiles for body height and five percentiles for whole body mass were created, the values for which were obtained from Demirjian (1980). Individuals who fit the age and gender criteria and fell into an empty cell for height and weight were chosen to participate. An example of height and mass percentile characteristics for females 19-30 years old is displayed in Table 4. Demirjian (1980) specified seven percentile groups (5^{th}, 10^{th}, 25^{th}, 75^{th}, 90^{th}, 95^{th}) for whole body height and mass, therefore the fifth and tenth percentile values were grouped for this study as were the ninetieth and ninety-fifth percentiles. The height and mass frequency distributions for each subject group are displayed in Appendix A.

2.2 Data Collection

Prior to testing, all subjects were informed of the purposes and procedures of

Table 4: Mean Height and Mass Percentile Values for Females Aged 19-30 Years (from Demirjian, 1980)

		Percentile for Height (cm)				
		5th - 10th	**25th**	**50th**	**75th**	**90th - 95th**
Percentile for Mass (kg)	**5th - 10th**	150.9 - 153 (cm) 42-46 (kg)	157.1 42-46	160.3 42-46	165.4 42-46	169.2-170.9 42-46
	25th	150.9 - 153 50.9	157.1 50.9	160.3 50.9	165.4 50.9	169.2-170.9 50.9
	50th	150.9 - 153 58.2	157.1 58.2	160.3 58.2	165.4 58.2	169.2-170.9 58.2
	75th	150.9 - 153 65.8	157.1 65.8	160.3 65.8	165.4 65.8	169.2-170.9 65.8
	90th - 95th	150.9 - 153 73.2-82.1	157.1 73.2-82.1	160.3 73.2-82.1	165.4 73.2-82.1	169.2-170.9 73.2-82.1

the study. The risks associated with each procedure were explained and each participant was asked to read and sign an information and consent form. Following this, each participant was required to undergo a fifteen minute whole body bone density scan (Hologic QDR 1000/W). Subjects were asked to change into a hospital gown prior to scanning, removing all jewelery and clothing except their undergarments. The subjects were instructed to lie supine on the scan bed with palms facing down and were instructed to remain still for the duration of the scan. Following the DPX scan, subjects were asked to change into shorts and a t-shirt after which a set of fifteen anthropometric measurements were taken. Anthropometric measurements of each subject were made on four body segments: the forearm, thigh, leg and head. A complete list and description of these

measurements is presented in Appendix B. All DPX and anthropometric measurements were made in the same testing session. Time of day was not specified for the testing procedure but usually occurred in the late afternoon due to availability of the DPX machine.

2.3 Data Processing

DPX scan files from each subject were processed using custom software to extract mass information, increase data resolution and create a bitmap image of the subject for segmentation (see Study 1, Figure 5). Following this, each image was sectioned based on specific segmentation guidelines. Six segments were measured for mass including the forearm, hand, thigh, leg, foot and head. Four segments were measured for centre of mass (CM), moment of inertia about the centre of gravity (I_{CG}) and length including the forearm, thigh, leg and head. The hand and foot segments required more specific scanning techniques to obtain these measurements and were therefore left for future study. The segment parameter values obtained from DPX were recorded for later use.

2.3.1 Segmentation Procedures

The scanning procedures selected were similar to those of Clauser, McConville and Young (1969). These methods were selected according to i) the location of joint centres, ii) the position of the subject during the DPX scan and iii) the reproducibility of the segmentation procedure. For instance, bony landmarks

were often used as a guideline to reduce the amount of variance in the segmentation procedure.

Sectioning of body segments was performed through joint centres. The forearm was segmented at the elbow by a line crossing the elbow crease through the lateral and medial epicondyles. The forearm was sectioned at the wrist by a line crossing just distal to the distal ulnar and radial styloids. The proximal joint centre at the elbow was defined as a point midway through the elbow along the segmentation line. The distal joint centre at the wrist was defined as a point midway through the wrist along the segmentation line. Figure 6 displays the sectioning of a forearm segment.

The thigh was sectioned at the hip through the neck of the greater trochanter. A straight line was drawn such that the thigh was sectioned just lateral to the anterior superior iliac spine and the ischial tuberosity. The thigh was sectioned at the knee by a line cutting between the femoral condyles and tibial plateau. The proximal joint centre at the hip was defined as a point midway through the neck of the femur along the line of segmentation. The distal joint centre at the knee was defined as a point along the line of segmentation midway through the knee joint. Figure 7 displays the sectioning of a thigh segment.

The leg was sectioned at the knee as was for the thigh. The leg was sectioned at the ankle by drawing a straight line just distal to the lateral and medial malleoli. The proximal joint centre was located at the knee as was for the distal joint centre of the thigh. The distal joint centre at the ankle was located at a point midway along

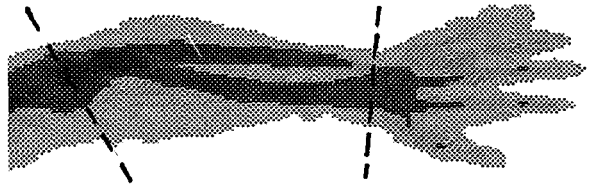

Figure 6: Section Lines of a Pronated Left Forearm Segment (Frontal View)

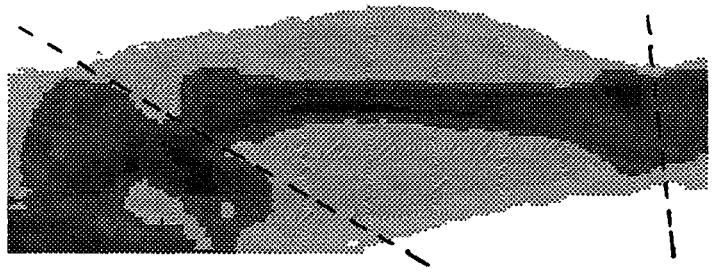

Figure 7: Section Lines of a Left Thigh Segment (Frontal View)

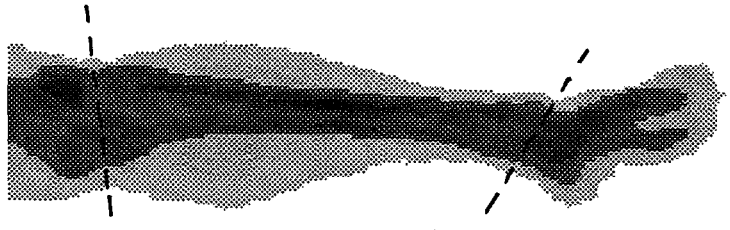

Figure 8: Section Lines of a Left Leg Segment (Frontal View)

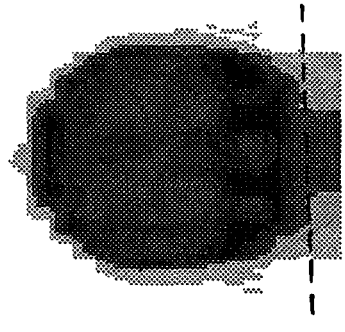

Figure 9: Section Lines of a Tilted Head Segment (Frontal View)

the segmentation line at the ankle. Figure 8 displays the sectioning of a leg segment.

The hands and feet were sectioned for mass measurements using the distal line of the forearm at the wrist and the distal line of the leg at the ankle, respectively.

The head was sectioned from the neck by drawing a straight line just distal to the lower ridge of the mandible and the occipital condyles. During scanning, subjects were instructed to tilt their head back as much as possible. This prevented the lower portion of the mandible to be placed over the neck and therefore allowed a more accurate sectioning of the head from the cervical vertebrae. Figure 9 displays the sectioning of a head segment.

2.4 Geometric Models

2.4.1 Forearm and Leg

The forearm and leg segments were modeled as two right circular frustrums positioned end-to-end. Because this model consisted of a combination of two geometric objects, formulas for the volume, centre of mass (CM) and moment of inertia about the centre of gravity (I_{CG}) of a right circular frustrum (Hanavan, 1966) were combined using the rules for composite bodies (Beer and Johnston, 1990) to arrive at the respective segment parameters for a forearm or leg. A diagram and the resulting equations are presented in Appendix C.

2.4.2 Thigh

The model for the thigh segment was composed of a right circular cylinder cut on an oblique plane positioned on top of a right circular frustrum. The mass, CM and I_{CG} of this object were calculated by combining formulas for the individual components and adding them together using the rules for composite bodies. A diagram and the resulting equations are presented in Appendix C.

2.4.3 Head

The model for the head segment consisted of an ellipsoid with one semi-major axis and two equal semi-minor axes. The mass, CM and I_{CG} of the object were calculated using the respective formulas for an ellipsoid (Beer and Johnston, 1990). A diagram and the resulting equations are presented in Appendix C.

2.5 Statistical Analysis

The sample sizes chosen for each group were originally twenty-five per group. This resulted in a total of fifty forearm, hand, thigh, leg and foot segments each per group and a total of twenty-five head segments per group. During the final analysis, however, segments from some subjects had to be excluded. Segments were excluded from the analysis for reasons such as subjects moving during the scan or the presence of joint replacements. As a result, the ANOVA's performed to investigate population differences were calculated using unequal sample sizes. This problem was also considered for the post-hoc analyses and the appropriate

test was selected (Tukey HSD for unequal N).

2.5.1 Population Differences

Differences between the four subpopulations were investigated for up to six body segments and for four body segment parameters. Population differences in segment mass differences were examined for six body segments including the forearm, hand, thigh, leg , foot and head. Population differences in segment centre of mass and I_{CG} were examined for four body segments including the forearm, thigh, leg and head. For the analysis, DPX mass values from each subpopulation group were represented as a percentage of whole body mass and centre of mass (CM) and radii of gyration (K) values were represented as a percentage of segment length. A 2X2 ANOVA with gender and age as factors was performed ($\propto = 0.05$) for each segment and each body segment parameter to determine the differences. If statistically significant differences were found, a Tukey HSD post-hoc analysis was then performed ($\propto = 0.05$) to determine which means were significantly different from each other. ω^2 calculations were also made where significant effects were found to determine how much variance was accounted for by the effect under consideration.

2.5.2 Linear Regression Equations

Linear regression equations were developed using the mass, CM and K values for each segment determined by DPX, allowing the prediction of mass from whole

body mass and centre of mass and radius of gyration from segment length. The coefficient of determination was then calculated for each regression line as well as the standard error of estimate. Population specific linear regression equations were calculated for each subject group and general linear regression equations were generated using the entire subject database.

2.5.3 Geometric Models

The accuracies of the geometric models in predicting BSPs were measured by calculating the standard error of estimate between the predicted BSP values and the DPX measurements for each subpopulation. Four segments (forearm, thigh, leg and head) were compared for three BSP parameters (Mass, CM, K), resulting in twelve standard error of estimate values per group.

2.5.4 Predictions Using Winter (1990)

Accuracy of the BSP predictions from Winter (1990) were measured by calculating the standard error of estimate between the predicted BSP values and the DPX measurements for each subpopulation. Five segments were analyzed for mass (forearm, hand, thigh, leg and foot), three for centre of mass and three for radius of gyration (forearm, thigh and leg), resulting in eleven standard error of estimate values. Head segment parameter predictions using Winter (1990) were excluded from the analysis since the segmentation methods between this study and Winter (1990) differed. The head segment in Winter (1990) included the neck

whereas this study did not.

2.5.5 Comparison of Predictive Equations

Predictive equations were compared with each other by comparing percent errors from the DPX mean as calculated from standard error of estimate values. Differences between the two linear regression equations and Winter (1990) were also compared visually by plotting the three predictors together. This helped to visualize when the predictors produced similar values and when they departed from each other. The population specific linear regression lines were plotted with standard error of estimate bars. These plots appear in Appendix D.

2.6 Reliability Measures

2.6.1 Segmentation Reliability

To ensure that the segmentation process was reliable, five subjects were randomly chosen from the subject database. One of six segments was randomly chosen from each of these subjects, including the left and right forearm, thigh and leg segment. These segments were redigitized and the body segment parameters compared with the original digitized values. A two factor repeated measures ANOVA was performed ($\propto$ = 0.05) to compare the differences. The first factor represented the digitization time with two levels (Time 1 and Time 2). The second factor represented the measured body segment parameter and had four levels (Mass, CM, I_{CG}, Length). The intra-class correlation coefficient was then calculated

to give a measure of the reliability of the procedure.

3.0 RESULTS

3.1 Population Differences

Table 5 shows the results from the analyses of variance of population differences. F-ratios, degrees of freedom, p-levels and the amount of variance accounted for by gender and age (ω^2) are presented for six segments (forearm, hand, thigh, leg, foot and head) and three body segment parameters (mass, centre of mass (CM) and radius of gyration (K)).

The analyses of population differences in forearm mass, centre of mass and radius of gyration showed main effects for both gender and age. A post-hoc analysis of forearm mass results (Tukey HSD, $p < .05$) revealed statistically significant differences between all groups except between females aged 19-30 years and 55^+ years. A post-hoc analysis of forearm centre of mass results (Tukey HSD, $p < .05$) showed statistically significant differences between males aged 19-30 years and all other groups. A post-hoc analysis of forearm radius of gyration results (Tukey HSD, $p < .05$) showed males aged 19-30 years to be statistically significantly different from both males aged 55^+ years and females aged 19-30 years. The analysis for hand mass differences revealed no main effects for either gender or age.

The analyses of thigh mass, centre of mass and radius of gyration (Tukey HSD, $p < .05$) revealed statistically significant differences

Table 5: Population Difference Results from Two-Factor Analysis of Variance (α=0.05)

SEGMENT	PARAMETER	FACTOR	F	df	p	ω^2	
Forearm	Mass (% WBM)	G	120	1, 177	<.001	37.6%	*
		A	17.1	1,177	<.001	5.20%	*
	CM (%SL)	G	6.37	1,177	<.05	2.80%	*
		A	6.98	1,177	<.01	3.10%	*
	K (%SL)	G	6.01	1,177	<.05	2.50%	*
		A	13.7	1,177	<.001	6.40%	*
Hand	Mass (%WBM)	G	3.15	1,154	<.08	-	
		A	<1.0	1,154	<.50	-	
Thigh	Mass (% WBM)	G	60.9	1,187	<.001	21.4%	*
		A	30.6	1,187	<.001	10.6%	*
	CM (%SL)	G	27.7	1,187	<.001	9.60%	*
		A	62.1	1,187	<.001	22.0%	*
	K (%SL)	G	36.9	1,187	<.001	10.2%	*
		A	125	1,187	<.05	35.0%	*
Leg	Mass (% WBM)	G	73.6	1,195	<.001	22.4%	*
		A	49.9	1,195	<.001	15.1%	*
	CM (%SL)	G	2.87	1,195	<1.0	-	
		A	9.12	1,195	<.01	3.90%	*
	K (%SL)	G	0.33	1,195	<1.0	-	
		A	20.4	1,195	<.001	8.90%	*
Foot	Mass (%WBM)	G	13.3	1,182	<.01	6.10%	*
		A	4.7	1,182	<.05	2.00%	*
Head	Mass (% WBM)	G	15.6	1,91	<.001	11.6%	*
		A	16.7	1,91	<.001	12.5%	*
	CM (%SL)	G	11.8	1,91	<.001	10.0%	*
		A	2.08	1,91	<.20	-	
	K (%SL)	Gender	<1.0	1,91	<1.0	-	
		Age	10.6	1,91	<.01	9.3%	*

(G = gender, A = age, df = degrees of freedom, * = statistically significant)

between all groups except between males aged 19-30 years and both female groups. A post-hoc analysis of thigh centre of mass results (Tukey HSD, $p < .05$) showed statistically significant differences between all groups except between males aged 55^+ years and females aged 19-30 years. A post-hoc analysis of thigh radius of gyration results (Tukey HSD, $p < .05$) showed statistically significant differences between all groups.

The analysis for leg mass differences revealed main effects for both gender and age. A post-hoc analysis (Tukey HSD, $p < .05$) revealed statistically significant differences between all groups except between males aged 19-30 years and females aged 55^+ years. The analyses of leg centre of mass and radius of gyration differences showed main effects for age only. A post-hoc analysis of leg centre of mass results (Tukey HSD, $p < .05$) showed statistically significant differences between females aged 55^+ years and 19-30 years as well as between females aged 55^+ years and males aged 19-30 years . A post-hoc analysis of leg radius of gyration results (Tukey HSD, $p < .05$) showed statistically significant differences between all groups except males aged 19-30 years were not significantly different from males aged 55^+ years or from females aged 19-30 years.

The analyses for foot mass differences revealed main effects for both gender and age. A post-hoc analysis (Tukey HSD, $p < .05$) showed that females aged 55^+ years were significantly different from both male populations.

The analysis for head mass differences revealed main effects for both gender and age. A post-hoc analysis (Tukey HSD, $p < .05$) revealed that females

19-30 years differed significantly from all other groups. The analysis of head centre of mass differences showed a main effect for gender only. A post-hoc analysis (Tukey HSD, $p < .05$) showed females 19-30 years to be significantly different from both male populations. Finally, the analysis of head radius of gyration differences showed a main effect for age only. A post-hoc analysis (Tukey HSD, $p < .05$) showed a statistically significant difference between both male populations.

3.2 Linear Regression Equations

Tables 6 through 8 display the linear regression equations developed from the raw DPX values, along with the respective coefficients of determination (r^2). Table 6 presents regression equations for the prediction of segment mass from whole body mass (kg) for six body segments (forearm, hand, thigh, leg, foot and head). Table 7 displays regression equations for the prediction of segment centre of mass (CM) from segment length (m) and Table 8 displays equations for the prediction of segment radius of gyration (K) from segment length (m), both for four body segments (forearm, thigh, leg and head). Population specific linear regression equations are listed for the four subpopulations studied and general linear regression equations are listed based on pooled data from the four subpopulations.

The coefficients of determination for both population specific and general linear regression equations revealed excellent predictive abilities for some segments and limited predictive abilities for others. The performance often varied

Table 6: Linear Regression Equations for Segment Mass Prediction

Segment	Population	Regression Equation	R^2
Forearm	Males (19-30)	0.017 (WBM) + 0.08	0.85
	Females (19-30)	0.020 (WBM) - 0.25	0.89
	Males (55+)	0.015 (WBM) + 0.11	0.86
	Females (55+)	0.014 (WBM) + 0.03	0.80
	General	0.019 (WBM) - 0.18	0.89
Hand	Males (19-30)	0.004 (WBM) + 0.15	0.64
	Females (19-30)	0.004 (WBM) + 0.10	0.71
	Males (55+)	0.004 (WBM) + 0.19	0.58
	Females (55+)	0.003 (WBM) + 0.20	0.47
	General	0.005 (WBM) + 0.05	0.79
Thigh	Males (19-30)	0.147 (WBM) - 1.47	0.91
	Females (19-30)	0.188 (WBM) - 2.81	0.97
	Males (55+)	0.144 (WBM) - 2.05	0.94
	Females (55+)	0.147 (WBM) - 1.07	0.89
	General	0.117 (WBM) + 0.74	0.89
Leg	Males (19-30)	0.041 (WBM) + 0.09	0.76
	Females (19-30)	0.044 (WBM) + 0.29	0.86
	Males (55+)	0.027 (WBM) + 0.98	0.81
	Females (55+)	0.038 (WBM) + 0.34	0.77
	General	0.028 (WBM) + 1.01	0.78
Foot	Males (19-30)	0.009 (WBM) + 0.30	0.69
	Females (19-30)	0.007 (WBM) + 0.30	0.66
	Males (55+)	0.006 (WBM) + 0.56	0.59
	Females (55+)	0.003 (WBM) + 0.51	0.45
	General	0.010 (WBM) + 0.16	0.79
Head	Males (19-30)	0.025 (WBM) + 2.86	0.60
	Females (19-30)	0.013 (WBM) + 3.42	0.30
	Males (55+)	0.022 (WBM) + 3.05	0.55
	Females (55+)	0.016 (WBM) + 2.98	0.52
	General	0.027 (WBM) + 2.57	0.70

(Whole body mass (WBM) measured in kilograms)

Table 7: Linear Regression Equations for Segment Centre of Mass Prediction

Segment	Population	Regression Equation	R^2
Forearm	Males (19-30)	0.37 (SL) + 0.012	0.89
	Females (19-30)	0.39 (SL) + 0.008	0.92
	Males (55+)	0.33 (SL) + 0.023	0.75
	Females (55+)	0.35 (SL) + 0.017	0.90
	General	0.37 (SL) + 0.013	0.93
Thigh	Males (19-30)	0.39 (SL) + 0.006	0.86
	Females (19-30)	0.45 (SL) - 0.026	0.8
	Males (55+)	0.50 (SL) - 0.051	0.65
	Females (55+)	0.50 (SL) - 0.055	0.58
	General	0.50 (SL) - 0.050	0.78
Leg	Males (19-30)	0.41 (SL) + 0.001	0.94
	Females (19-30)	0.42 (SL) - 0.004	0.96
	Males (55+)	0.38 (SL) + 0.010	0.91
	Females (55+)	0.41 (SL) - 0.002	0.94
	General	0.41 (SL) - 0.002	0.95
Head	Males (19-30)	0.58 (SL) - 0.004	0.91
	Females (19-30)	0.42 (SL) + 0.023	0.70
	Males (55+)	0.62 (SL) - 0.011	0.79
	Females (55+)	0.49 (SL) + 0.011	0.82
	General	0.57 (SL) - 0.004	0.84

(Segment length (SL) measured in meters)

Table 8: Linear Regression Equations for Segment Radius of Gyration Prediction

Segment	Population	Regression Equation	R^2
Forearm	Males (19-30)	0.32 (SL) - 0.012	0.91
	Females (19-30)	0.26 (SL) + 0.004	0.97
	Males (55+)	0.22 (SL) + 0.016	0.78
	Females (55+)	0.24 (SL) + 0.011	0.94
	General	0.26 (SL) + 0.005	0.94
Thigh	Males (19-30)	0.31 (SL) + 0.001	0.85
	Females (19-30)	0.22 (SL) + 0.042	0.79
	Males (55+)	0.23 (SL) + 0.046	0.47
	Females (55+)	0.19 (SL) + 0.061	0.49
	General	0.22 (SL) + 0.045	0.61
Leg	Males (19-30)	0.27 (SL) + 0.002	0.98
	Females (19-30)	0.27 (SL) + 0.001	0.98
	Males (55+)	0.27 (SL) + 0.002	0.97
	Females (55+)	0.29 (SL) - 0.002	0.96
	General	0.28 (SL) + 0.001	0.98
Head	Males (19-30)	0.14 (SL) + 0.032	0.77
	Females (19-30)	0.19 (SL) + 0.021	0.84
	Males (55+)	0.16 (SL) + 0.028	0.78
	Females (55+)	0.15 (SL) + 0.028	0.78
	General	0.17 (SL) + 0.025	0.80

(Segment length (SL) measured in meters)

depending on the segment, the population under study and the segment parameter being predicted. Population specific predictors were able to estimate segment mass within 3% of the actual DPX values at best and at worst 71%. Predictions of segment mass were best overall for the thigh segment and worst for the head segment. Population specific predictors were able to estimate segment centre of mass within 5% of actual DPX values at best and at worst 31% Predictions of centre of mass were best overall for the leg and worst for the thigh segment. Finally, population specific predictors of radius of gyration were at best 4% within actual DPX values and at worst 88%. Predictions were best overall for the leg segment and worst for the thigh segment. The general linear regression equations were unable to estimate within 11% of raw DPX values for segment mass and 5% for centre of mass. Predictions of radius of gyration were at best 2% and at worst 39% within actual DPX values.

3.3 Comparison of Predictive Equations

The results of the four BSP predictive equations are presented in Tables 9 through 11. These tables present the percent errors of segment mass, centre of mass and radius of gyration predictions from the population specific linear regression equations, the general linear regression equations, the geometric models and the predictions from Winter (1990). The percent errors are calculated from the standard error of estimate values. Descriptive statistics for the DPX values

Table 9: Comparison of Segment Mass Predictors: Percent Errors from DPX Mean as Calculated from Standard Error of Estimates

Segment	Population	DPX Values			Population Specific Linear Regression	General Linear Regression	Geometric Model	Winter's Predictor
		n	Mean (kg)	S.D. (kg)	S_{EST} (% of Mean)	S_{EST} (% of Mean)	S_{EST} (% of Mean)	S_{EST} (% of Mean)
Forearm	Males (19-30)	90	1.29	0.21	8.9%	13.0%	9.9%	14.0%
	Females (19-30)	100	0.87	0.15	8.3%	8.1%	7.4%	10.4%
	Males (55+)	82	1.34	0.22	8.4%	9.0%	11.2%	9.2%
	Females (55+)	90	0.90	0.18	11.8%	16.4%	9.0%	15.9%
Hand	Males (19-30)	80	0.43	0.07	12.3%	12.7%	-	14.1%
	Females (19-30)	96	0.34	0.04	8.9%	10.1%	-	9.8%
	Males (55+)	76	0.51	0.08	13.7%	15.3%	-	15.3%
	Females (55+)	64	0.36	0.06	14.6%	17.3%	-	17.9%
Thigh	Males (19-30)	50	9.18	1.69	7.8%	8.5%	10.0%	23.5%
	Females (19-30)	100	7.92	1.36	4.2%	9.9%	7.0%	29.9%
	Males (55+)	84	9.87	2.06	7.3%	10.3%	19.8%	18.8%
	Females (55+)	98	8.20	1.71	9.7%	10.4%	10.5%	26.2%
Leg	Males (19-30)	100	3.06	0.56	11.9%	12.7%	18.3%	15.7%
	Females (19-30)	100	2.78	0.36	6.6%	9.8%	11.9%	8.1%
	Males (55+)	98	3.23	0.43	8.0%	8.8%	27.8%	22.5%
	Females (55+)	100	2.71	0.50	11.9%	12.7%	22.6%	14.8%
Foot	Males (19-30)	92	0.96	0.14	10.9%	12.1%	-	16.3%
	Females (19-30)	100	0.72	0.08	8.2%	9.6%	-	18.9%
	Males (55+)	80	1.07	0.15	11.2%	13.5%	-	20.5%
	Females (55+)	100	0.73	0.08	10.0%	17.2%	-	31.0%
Head	Males (19-30)	48	4.71	0.44	7.6%	8.5%	12.9%	-
	Females (19-30)	50	4.16	0.31	7.3%	7.8%	12.3%	-
	Males (55+)	44	4.85	0.48	8.5%	8.7%	6.2%	-
	Females (55+)	48	3.99	0.32	7.1%	10.5%	8.2%	-

Table 10: Comparison of Segment Centre of Mass Predictors: Percent Errors from DPX Mean as Calculated from Standard Error of Estimates

Segment	Population	DPX Values			Population Specific Linear Regression	General Linear Regression	Geometric Model	Winter's Predictor
		n	Mean (m)	S.D. (m)	S_{EST} (% of Mean)	S_{EST} (% of Mean)	S_{EST} (% of Mean)	S_{EST} (% of Mean)
Forearm	Males (19-30)	90	0.110	0.007	2.8%	2.8%	4.9%	5.0%
	Females (19-30)	100	0.100	0.005	2.1%	2.1%	4.7%	3.1%
	Males (55+)	82	0.110	0.006	3.6%	3.7%	5.4%	4.4%
	Females (55+)	90	0.098	0.006	2.6%	2.6%	6.8%	3.3%
Thigh	Males (19-30)	100	0.177	0.012	3.5%	5.9%	10.2%	7.6%
	Females (19-30)	100	0.157	0.013	5.0%	5.5%	17.3%	12.8%
	Males (55+)	84	0.168	0.016	7.9%	8.3%	18.4%	16.5%
	Females (55+)	98	0.146	0.014	7.5%	9.0%	27.8%	21.4%
Leg	Males (19-30)	100	0.159	0.011	2.5%	2.6%	9.7%	6.2%
	Females (19-30)	100	0.150	0.010	1.9%	2.0%	8.7%	6.1%
	Males (55+)	98	0.160	0.010	2.6%	2.6%	11.8%	6.8%
	Females (55+)	100	0.146	0.008	2.0%	2.2%	10.8%	7.5%
Head	Males (19-30)	48	0.108	0.009	3.3%	3.6%	14.9%	-
	Females (19-30)	50	0.100	0.006	4.6%	5.5%	8.6%	-
	Males (55+)	44	0.107	0.008	4.6%	4.9%	11.7%	-
	Females (55+)	48	0.099	0.006	3.5%	3.6%	15.2%	-

Table 11: Comparison of Segment Radius of Gyration Predictors: Percent Errors from DPX Mean as Calculated from Standard Error of Estimates

Segment	Population	DPX Values			Population Specific Linear Regression	General Linear Regression	Geometric Model	Winter's Predictor
		n	Mean (m)	S.D. (m)	S_{EST} (% of Mean)	S_{EST} (% of Mean)	S_{EST} (% of Mean)	S_{EST} (% of Mean)
Forearm	Males (19-30)	90	0.074	0.006	3.1%	3.5%	5.7%	9.5%
	Females (19-30)	100	0.067	0.003	1.2%	1.3%	4.3%	7.9%
	Males (55+)	82	0.074	0.004	3.2%	3.4%	5.3%	8.1%
	Females (55+)	90	0.066	0.004	1.8%	1.8%	6.2%	6.8%
Thigh	Males (19-30)	100	0.135	0.010	3.9%	6.0%	15.0%	6.0%
	Females (19-30)	100	0.129	0.006	3.0%	4.6%	29.0%	3.7%
	Males (55+)	84	0.146	0.009	5.5%	6.3%	12.8%	6.1%
	Females (55+)	98	0.140	0.007	4.7%	6.6%	19.4%	8.6%
Leg	Males (19-30)	100	0.107	0.007	1.3%	1.3%	4.5%	7.6%
	Females (19-30)	100	0.101	0.006	1.3%	1.4%	4.5%	4.8%
	Males (55+)	98	0.109	0.009	1.6%	1.7%	6.3%	8.2%
	Females (55+)	100	0.101	0.007	1.5%	1.6%	6.6%	11.9%
Head	Males (19-30)	48	0.058	0.002	2.8%	2.9%	9.5%	-
	Females (19-30)	50	0.056	0.002	2.3%	2.7%	8.0%	-
	Males (55+)	44	0.059	0.002	2.2%	3.4%	11.7%	-
	Females (55+)	48	0.055	0.002	2.4%	2.5%	8.7%	-

and the results from the four predictive equations are presented in Appendix E.

The results showed on average that the linear regression equations provided the best BSP estimations. The performance of the predictors from Winter (1990) and the geometric models depended on the segment under study. Since the linear regression equations and the predictions from Winter (1990) all estimated segment mass from whole body mass and centre of mass or radius of gyration from segment length, these values were arranged in a graph to help visualize their differences (See Appendix D). The predictions from the population specific and general linear regression lines were often similar, however estimations using Winter (1990) were sometimes over- or underestimated. Furthermore, estimation using Winter (1990) often resulted in an increase or decrease in error as a function of whole body mass or segment length. For instance, Figure 10 shows how Winter (1990) provided predictions of forearm centre of mass that were similar to the linear regression predictions at shorter segment lengths. As segment length increased, however, estimations of centre of mass were increasingly overestimated for males aged 55^{+} years.

3.3.1 Forearm

The results of forearm parameter predictions revealed that the linear regression equations provided the best estimates. The specific linear regression equations provided better estimates than the general equations, however the

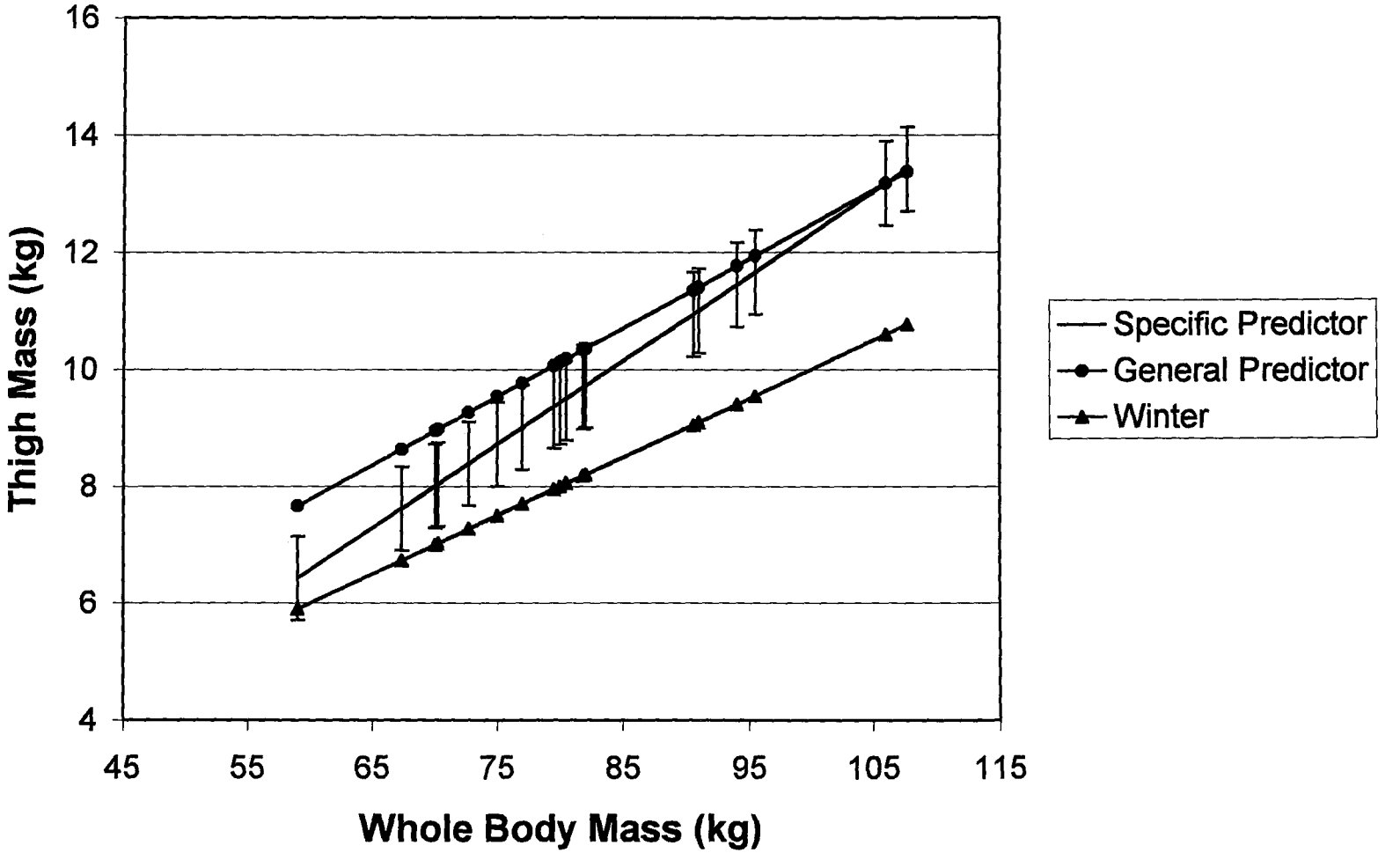

Figure 10: Comparison of Thigh Mass Predictors (Males 55^{+} Years)
(Specific Predictor ± S.E.)

difference between the two was most often minimal.

Comparison of the standard error of estimate values for each forearm mass predictor revealed that the population specific linear regression equation predicted best overall for each subpopulation. The population specific predictors predicted best for young females, within 8.3% of mean DPX values and worst for older females, estimating within 11.8% of mean DPX values. The geometric model was found to predict forearm mass better than Winter (1990) for all groups except older males and provided the best estimations for the older female group, predicting within 9.0% of the mean DPX value.

Standard error of estimates for forearm centre of mass predictors revealed that the linear regression equations provided the best estimates, followed by Winter (1990) and lastly the geometric models. The specific linear regression equations were able to estimate forearm centre of mass best for young females within 2.1% of mean DPX values. Winter (1990) predicted better than the geometric model for all groups except younger males, predicting within 5% of mean DPX values. The geometric models were found to predict within 5.5% of mean DPX values for all groups except older females where the prediction was within 6.8%.

Standard error of estimates for forearm radius of gyration predictors revealed again that the linear regression equations provided the best estimates with specific predictors estimating best again for young females within 1.2% of mean DPX values. The geometric models also provided good estimates and were substantially more accurate than Winter (1990), predicting best for young females within 4.3%

of mean DPX values. Winter (1990) was able to predict best for older females within 6.8% of mean DPX values and worst for young males within 9.5%.

3.3.2 Hand

Standard error of estimates for each hand mass predictor revealed rather poor estimates. The specific linear regression equations predicted best but were not able to predict within 8.9% of DPX means, predicting best for young females and worst for older females. Winter (1990) was unable to predict within 9.8% of DPX means, also predicting best for young females.

3.3.3 Thigh

Standard error of estimates for thigh mass predictors revealed again that linear regression equations provided the best estimates. The specific linear regression equation predicted best for young females within 4.2% of the DPX mean and predicted worst for older females, predicting within 9.7% of the DPX mean. The geometric model provided less accuracy, predicting within 7% for young females and 19.8% for older males. Winter (1990) provided the worst predictions, however, predicting within 18.8% of the DPX mean for older males and 29.9% for young females.

Standard error of estimates for thigh centre of mass predictors revealed linear regression equations to provide the best estimates, followed by Winter (1990) and last the geometric models. The specific linear regression equations were able

to predict best for younger males where centre of mass was estimated within 3.5% of the DPX mean and predicted worst for older males within 7.9%. Winter (1990) predicted best for young males, estimating within 7.6% of the DPX mean and worst for older females, estimating within 21.4% of DPX. The geometric models predicted best for young males, estimating within 10.2% and worst for older females, estimating within 28% of the DPX mean.

Standard error of estimates for thigh radius of gyration predictors showed linear regression equations to provide the best estimates, followed by Winter (1990) and last the geometric models. The specific linear regression equations were able to predict within 3.0% of mean DPX values, whereas the maximum error of the geometric model was 29.0%. The maximum error using Winter (1990) was 8.6% for older males.

3.3.4 Leg

Standard error of estimates for leg mass predictors showed that the population specific linear regression equations to provide the best estimates, predicting within only 6.6% of DPX means for young females. The geometric models provided the worst estimates predicting within 11.9% of DPX means for young females while Winter (1990) was able to predict only within 8.1%%, again for young females.

Standard error of estimates for leg centre of mass predictors showed population specific linear predictors to provide the best estimates, predicting within

1.9% of DPX means. The geometric model predicted worst, however, estimating only within 8.7% of the DPX mean whereas Winter (1990) was able to predict only within 6.1% of the DPX mean.

Standard error of estimates for leg radius of gyration predictors showed once again that the population specific linear regression equations provided the best estimates, predicting within 1.3% of DPX means for young females and within 1.6% for older males. Winter (1990) provided the worst predictions, estimating within 4.8% of DPX means for young females and 11.9% for older females. The geometric model was able to predict at best within 4.5% of the DPX mean for young females and at worst 6.6% for older females.

3.3.5 Foot

Standard error of estimates for foot mass showed the specific linear predictors to provide better estimates than Winter (1990). Specific linear regression equations were able to predict at best within only 8.2% of foot mass for young females while Winter (1990) predicted best within 16.3% for young males.

3.3.6 Head

Standard error of estimates for head mass revealed that linear predictors provided the best estimates, predicting better for the younger populations than the older ones. The specific linear regression equations were able to predict within 7.1% of DPX means for older females while the geometric models were able to

predict at best within 6.2% of DPX means for older males. The geometric models predicted better for the older populations than for the younger ones.

Standard error of estimates for head centre of mass revealed that the specific linear regression equations could estimate within 3.3% of head centre of mass for young males whereas geometric models could estimate only within 8.6% for young females.

Standard error of estimates for head radius of gyration showed linear regression equations to estimate at best within 2.2% of DPX means for older males while geometric models were able to predict at best within 8.0% of DPX means for young females.

3.4 Reliability Measures

Table 12: Raw Results of Segmentation Reliability Analysis

Subject	Segment	Mass (kg)		CM (m)		K (m)		Length (m)	
		Time 1	Time 2	Time 1	Time 2	Time 1	Time 2	Time 1	Time 2
1	Thigh	9.25	9.31	0.16	0.17	0.160	0.165	0.408	0.413
2	Thigh	7.94	7.93	0.20	0.19	0.790	0.183	0.479	0.476
3	Forearm	1.35	1.29	0.11	0.15	0.007	0.006	0.261	0.250
4	Leg	3.41	3.39	0.16	0.16	0.041	0.040	0.396	0.396
5	Forearm	0.71	0.72	0.10	0.10	0.003	0.003	0.235	0.236

Table 12 displays the raw results of the segmentation reliability analysis. The analysis of segmentation reliability revealed no main effects for segmentation time

$F(1, 4) = 1.006$, $p < .40$. The variance created by repeat digitizations was therefore not significant. The calculation of the intra-class correlation coefficient revealed a correlation of 0.99997. This indicated that the error due to repeat digitizations was not significant in comparison to the error due to variability in subjects

4.0 DISCUSSION

4.1 Population Differences

The results showed statistically significant differences between the DPX values from the four subpopulations studied. These differences were found for all segment parameters and all body segments except hand mass. The differences between sample groups depended on the segment analyzed as well as on the parameter measured. As a result, we may then reject the null hypothesis that there is no difference between BSPs of the four subpopulations studied.

Although the sample means between groups proved to be significantly different, ω^2 calculations showed little variance accounted for by gender and age. For instance, differences in thigh radii of gyration revealed the most variance due to gender and age combined which amounted to only 45.2%. Much of the existing variance may have been due to large segmental differences between individuals within the same group who were of similar size. For example, individuals with the same whole body mass did not necessarily have the same thigh mass and individuals with the same thigh length did not necessarily have the same radius of gyration. This supports the need for a model that is robust enough to account for differences between populations as well as individual differences within groups. The best way to account for such differences would be to use a model that accounts for shape as well as size. Geometric models would seem to provide this flexibility, given that an appropriate shape is chosen to represent the segment under study.

Subjects were selected for this study based on specific whole body height and mass criteria. This was done so as to ensure the inclusion of a wide variety of body types within the sample groups. The results showed that the height and mass percentile frequencies (See Appendix A) were similar for all subject groups except for males aged 55^{+} years. The availability of subjects who fit the criteria for the lower percentiles (as determined from Demirjian, 1980) was limited and time restrictions prevented a more even selection of subjects. As a result, the height and mass characteristics of this population were shifted towards the higher percentiles. While this may have affected the external applicability of the linear regression equations for this group, the effects were most likely minimal as the height and mass characteristics of the older males were very similar to those of the younger male group. Furthermore, compared to past studies, the characteristics of the older male group is much more representative of the actual population.

One hundred subjects were selected to participate in this study which resulted in a total of two hundred forearm, hand, thigh, leg and foot segments. The use of both right and left limbs from each subject in the analysis of variance violated the assumption that the individual scores were independent of each other. Since both limbs from each subject were included in the analysis, a repeated measures analysis of variance should have been conducted in place of the between measures analysis. This violation of independence had minimal effects on the results, however since it only created a more conservative analysis. For example, a comparison of two limbs from the same subject would show less of a difference than

a comparison from two different individuals. Therefore, if a repeated measures analysis were conducted, a greater difference between subpopulations may have been found. Given this, significant differences in hand mass between the subpopulations may also have been found.

4.2 Linear Regression Equations

The linear regression equations provided the most accurate predictions of body segment parameters in comparison to the geometric models and the predictions using Winter (1990). The population specific equations performed better than the general predictors and should be used over the general predictors, especially given that the differences between the subpopulations were statistically significant. The performance of these regression equations depended on the segment under study, the subpopulation examined and the body segment parameter that was being predicted. The errors in the predictions for each subpopulation were most likely a result of individual differences within groups as individuals with similar whole body mass or segment length often had different segment masses or centres of mass/radii of gyration.

4.3 Comparison of Predictive Equations

The results showed that the population specific linear regression equations provided better estimations of body segment parameters than the general predictors and were most often more accurate than the predictions from the

geometric models and from Winter (1990). While the linear regression equations provided the best BSP estimates, they did not always provide these estimates with an acceptable level of accuracy. The equations were developed using one predictor, estimating mass from whole body mass and centre of mass or radius of gyration from segment length. Perhaps if a multiple regression approach were used, including several anthropometric variables rather than just one predictor, more accurate estimations could have been achieved. A multiple regression approach using variables such as segment length, segment girth at the proximal and distal ends and whole body mass may provide more accurate estimations of segment mass, centres of mass and moments of inertia as these variables would help take into account the shape of the segment.

The use of only one predictor in the linear regression equations, such as whole body mass or segment length, also assumed that an individual has symmetry between contralateral limbs. The use of several variables to account for segment shape would account for asymmetrical differences and therefore provide more accurate BSP predictions.

Since the linear regression equations performed better than the geometric models, the null hypothesis stands true that the geometric models tested do not provide the best estimates of BSPs. An interesting finding, however, is that these results were opposite to those of Zatsiorsky, Seluyanov and Chugunova (1990). They found geometric models to estimate BSPs with 50% less error than regression equations. A similar trend was expected in this study but may not have emerged for

several reasons. First, predictions of thigh segment parameters using the selected geometric model may have been affected by certain anthropometric measurements. While the utmost care was taken to ensure accurate measurements, difficulty in finding some landmarks at the hip on more overweight subjects was encountered. Excess tissue around the pelvic region sometimes made the anterior superior iliac spine landmark difficult to detect. This may have affected outer thigh length measurements and possibly affected thigh segment parameter predictions.

Second, unexpected problems were also encountered upon sectioning the thigh segments of some subjects. The segmentation procedure at the hip provided consistency by using bony landmarks as a guide but as Figure 11 shows, the sectioning of more obese subjects sometimes resulted in the inclusion of tissue from the lower torso. Furthermore, sectioning of a more narrow pelvis sometimes resulted the exclusion of tissue from the inner thigh. While this may have balanced out in the mass calculations, centre of mass and radius of gyration measurements may have been affected. A possible solution to this may be to select an absolute angle at which to section the hip as was done by Zatsiorsky and Seluyanov (1983). In any case, a segmentation method must be devised so as to keep inner thigh mass in the segmentation area and exclude any upper torso mass that may interfere. This method must be reliable and must be consistent with the shape of the geometric model being applied to the segment.

The segmentation procedures selected for this study were similar to those of Clauser, McConville and Young (1969) and of Chandler et al. (1975). The

(a)

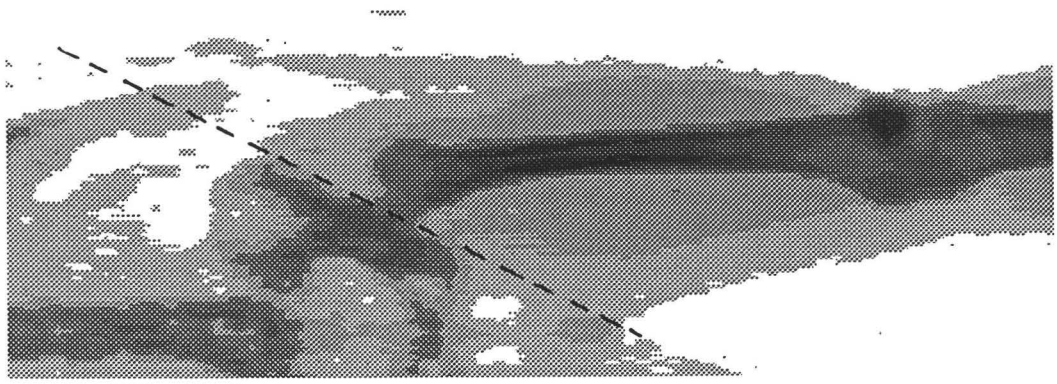

(b)

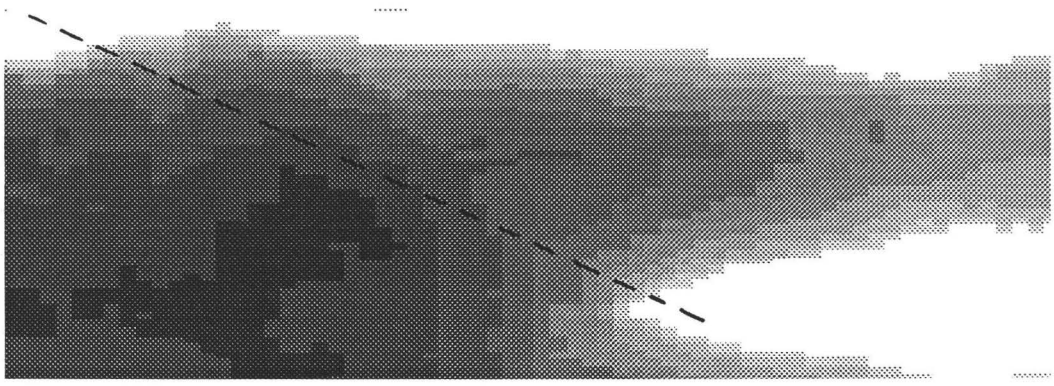

Figure 11: Example of a Problematic Hip Segmentation (a) Density Image (b) Mass Image

segmentation methods chosen were governed by several factors. First, the biomechanical analysis of movement involves the representation of body segments as rigid links connected together by hinge joints. Rotation about these joints is assumed to occur about a fixed joint centre. The segmentation methods used in this study therefore attempted to section body segments through joint centres. Second, the segmentation methods were governed by the position of the subjects during the

scan and were restricted by the resolution of the scan image. In order to minimize variability in the segmentation procedure, bony landmarks were often used as a guide.

The discrepancies between the geometric models and the DPX results may have been partially caused by the segmentation methods used. The anthropometric measurements taken for the geometric models were made using palpable bony landmarks that may not have exactly corresponded with the segmentation methods through joint centres. Care was taken to ensure the closest match between the two.

The position of the subjects during the scan may also have contributed to the error from the geometric models. The subjects were scanned in the supine position which would result in the redistribution of mass towards the table, especially for subjects with more body fat. This may have caused a slight discrepancy between the geometric model predictions and the measurements using DPX since anthropometric measurements for the geometric models were taken while the subjects were standing in the upright position. Furthermore, subjects were scanned with palms facing down on the table. Anthropometric measurements were taken with subjects' palms facing forward. This discrepancy may have affected the comparisons somewhat, however the amount of error was deemed to be minimal since the shape of the forearm barely changes from the pronated to the supinated position in the frontal plane.

The position of the head segment during the scan may have affected the performance of the geometric models. During the scan, subjects were instructed to

tilt their head back as far as possible so that complete segmentation of the head segment from the neck would be possible. This resulted in calculations of the centre of mass and radius of gyration about an axis that was not a principle one. This position was necessary, however to ensure that the head and neck segments did not overlap. It was therefore necessary to assume that the results about this non-principle axis were similar to those about the principle anteroposterior axis.

The reliability of anthropometric measurements was also considered as a possible factor that may have influenced geometric model accuracy. A study by Challis (1997) investigated the effects of inter- and intra-operator precision on geometric estimations of body segment parameters. The results yielded little difference between the inter- and intra-operator precisions. Furthermore, the effects of the existing measurement differences did not have a significant effect on BSP estimates using the geometric models. As a result, the effect of anthropometric measurement precision on geometric model accuracy was assumed to be minimal in this study.

The geometric shapes chosen to represent body segments may have affected BSP prediction performance. Since the models predicted well for only the leg and head radii of gyration, the shapes selected to represent the segments may not have been appropriate. Some segments may actually be better represented as volumes adapted from elliptical cylinders or stadium solids. Furthermore, the head may be better represented as an ellipsoid with a semi-major axis and two different semi-minor axes instead of two identical semi-minor axes. Differences in the performance

of geometric models between this study and Zatsiorsky, Seluyanov and Chugunova (1990) may be due to the methods used. Zatsiorsky, Seluyanov and Chugunova (1990) used constants with their models to correct for differences between the geometric shape and the shape of the actual segment. Furthermore, the models used by Zatsiorsky, Seluyanov and Chugunova (1990) were warned to be less accurate for males and females outside the age range of 19-28 years and with body fat percentages outside the ranges of 8-15% for men and 12-20% for women. Our models were tested for different subpopulations of humans with different body types.

A limitation of the geometric models, as well as all the models presented in this study, is the assumption that each segment has a constant density. Human body segments do not have a constant density but density varies along the length of a segment. While this assumption may have an affect on model predictions, it is necessary if one is to obtain segment masses from volume measurements. The alternative is to measure densities of segments in slices using an imaging procedure such as computed tomography or MRI and apply these density values to the model. This would severely complicate the procedure, however, increasing the measurement time, the number of anthropometric measurements needed and the chance of error. Modifying the geometric models to take into account body fat by including skinfold measurements could improve estimations. Future investigations using DPX could also look at trends in segment density for different body segments and different subpopulations, or even for different body types.

Another limitation of the geometric models is that density values were obtained from cadaver data (Winter, 1990). These values were used assuming that cadaver tissue retains similar properties to living tissue and that all the subjects examined had similar segment densities. As we know, some individuals have more body fat than others which may affect the bulk density of a segment. This may therefore have had an effect on the geometric model estimations. A method for measuring segment density using DPX may be investigated. A study by Chilibeck et al. (1994) investigated the reproducibility of DPX measurements of mass and density. They found errors for whole body bone mineral content, bone mineral density, lean tissue mass and fat mass to be 1.6%, 1.1%, 1.4% and 1.8% respectively. This suggested that DPX measurements were accurate enough to detect small changes (2%) in these four measurements. Given the reliability of DPX in measuring density, perhaps segment density values from DPX could be compared between populations and could be used in the geometric models to provide more accurate estimations of body segment parameters.

The use of DPX for providing BSP measurements of humans also has some limitations. DPX provides mass measurements based on an area and does not provide volume information. When a subject is scanned, information is obtained in one plane only and therefore centre of mass and moment of inertia information is provided about one axis only. For most segments, the differences between parameter values in the frontal plane and the sagittal plane may be minimal. Information in the transverse plane is significantly different, however and is not

possible to measure directly using DPX. For one, positioning of the subject in an upright position is not possible due to the structure of the machine (See Study 1, Figure 1). Also, the x-ray beam penetrates all tissues in its path. Since volume information is not given, separation of overlapping segments would not be possible. If measurements of a segment in both the frontal and sagittal planes could be obtained using DPX, however, information in the transverse plane could easily be calculated.

Problems may also be encountered if one wishes to obtain parameter information on some segments that have significantly different characteristics between the frontal and sagittal planes. For example, if one were to use DPX to measure BSPs of a human trunk, obtaining frontal plane values directly would be possible, sagittal plane values would be tricky and transverse plane values would be impossible. In the sagittal plane, the x-ray beam would pass through the shoulder before hitting the upper torso and would then pass through the other shoulder before reaching the detector. Separation of these overlapping masses would therefore be difficult if not impossible. These problems must be further investigated as it is a limitation to the method presented. DPX can provide extremely accurate predictions given optimal conditions, therefore an investigation into minimizing these restrictions is worth pursuing.

4.4 Reliability Measures

The analysis of segmentation reliability revealed that the segmentation

methods used were highly reproducible. The intraclass correlation coefficient was extremely high, although this value may have been exaggerated since a combination of different body segments (forearm, thigh and leg) were included in the analysis. With different segments being compared in the analysis, the variability due to subject was exaggerated and the variability due to the segmentation procedure was minimized. This resulted in a very high correlation coefficient. A more accurate measure of segmentation reliability would be to calculate a separate coefficient for each body segment. The segments should be digitized repeatedly and the variances calculated to yield a true measure of the reliability of the procedure for each segment. This was not done in this study due to time constraints and therefore should be conducted in the future.

5.0 CONCLUSION

Studies have shown that segment parameter errors may have a significant influence on the internal kinetic calculations of a movement (Krabbe, Farkas and Baumann, 1997; Pearsall and Costigan, 1998). As a result, a reliable and accurate method for measuring body segment parameters is greatly needed. Past studies have attempted to provide better BSP predictions, however the findings have been limited. Study 1 has shown dual photon absorptiometry (DPX) to provide accurate BSP estimations at safe, fast and economical rates, providing new possibilities for personalized BSP measurements as well as the development of predictive equations.

One of the purposes of this study was to examine population differences in three segment inertial properties. Four human subpopulations were compared for segment masses, centres of mass about a transverse axis and moments of inertia about the centre of mass. The results showed significant differences in body segment parameters between the four populations and also showed large differences within each group for individuals of similar size. This supported the need for a BSP prediction method that could account for differences between groups as well as large individual differences within groups. Geometric models were thought to provide the required flexibility for such predictions.

The second purpose of this study was therefore to develop geometric models for the prediction of BSPs. These geometric models were compared with a

prediction method in Winter (1990), a popular BSP source in the literature and were also compared with linear regression equations constructed from the DPX measurements. The results showed that population specific linear regression equations were able to predict body segment parameters with the greatest accuracy. The geometric models did not perform as well as was expected, however and could not be considered as an acceptable method for BSP prediction. BSP estimations from Winter (1990) were also very poor. As a result, caution should used if one wishes to use Winter (1990) as a BSP source for certain populations.

The present study was a preliminary attempt to estimate body segment parameters from geometric modelling using DPX. Adjustments to the geometric models, such as using volumes adapted from elliptical cylinders or stadium solids, may provide more accurate predictions. Furthermore, segmentation and measurement procedures of the thigh must be improved in order to obtain more accurate estimates. The population specific regression equations developed in this study should therefore be used to predict BSPs for individuals who have similar age and gender characteristics as the subjects in this experiment. While the use of Winter (1990) has been the method of choice, these predictors neglect important differences between populations and may introduce large errors in BSP predictions and therefore in kinetic calculations.

In this study, only six segments were measured for mass and four segments for centre of mass and radius of gyration. Investigation into the measurement of other body segments needs to be done in the future if we wish to fully understand

the inertial characteristics of the human body. Furthermore, the acquisition of BSPs in the sagittal plane using DPX needs to be investigated. DPX can provide safe and accurate measurements of mass characteristics and therefore should be tested for its full potential.

This study has provided useful information concerning the differences between populations and has helped emphasize the importance of accurate BSP predictors. The linear regression equations developed from this study can be used to provide reasonably accurate estimates of body segment parameters for the subpopulations studied. Further investigations into expanding the uses of DPX, increasing the number of segments under study, broadening the subject database and improving geometric models will hopefully lead us closer to more accurate BSP measurements. This will ultimately help to decrease the errors in kinetic calculations, providing us with a better understanding of human movement.

REFERENCES

Beer, F.P. and Johnston, E.R., Jr. (1990). Vector mechanics for engineers: statics. (2nd SI Metric Ed.). Singapore: McGraw-Hill Book Co.

Braune, W. and Fischer, O. (1889). The center of gravity of the human body as related to the german infantryman. Leipzig. (ATI 138 452. Available from National Technical Information Services.)

Capozzo, A. and Berme, N. (1990). Subject specific segment inertial parameter determination - a survey of current methods. In Capozzo, A and Berme, N. (Eds.) Biomechanics of Human Movement: Applications in Rehabilitation, Sports and Ergonomics (pp. 179-185). Worthington, OH: Bertec Corp.

Challis, J.H. (1997). Precision of human body segment inertial parameters. Proceedings of the Twenty-First Annual Meeting of the American Society of Biomechanics. Clemson Univerisity, South Carolina.

Chandler, R.F., Clauser, J.T., McConville, H.M., Reynolds, H.M. and Young, J.W. (1975). Investigation of inertial properties of the human body. AMRL-TR-74-137, Aerospace Medical Research Laboratory, Wright-Patterson Air Force Base: Ohio.

Chilibeck, P., Calder, A., Sale, D.G. and Webber, C. (1994). Reproducibility of dual-energy x-ray absorptiometry. Canadian Association of Radiologists Journal, 45(4): 297-302.

Clarys, J.P. and Marfell-Jones, M.J. (1986). Anatomical segmentation in humans and the prediction of segmental masses from intra-segmental anthropometry. Human Biology, 58(5): 771-787.

Clarys, J.P. and Marfell-Jones, M.J. (1994). Soft tissue segmentation of the body and fractionation of the upper and lower limbs. Ergonomics, 37(1): 217-229.

Clauser, C.E., McConville, J.V. and Young, J.W. (1969). Weight, Volume and Centre of Mass of Segments of the Human Body. AMRL-TR-69-70, Aerospace Medical Research Laboratory, Aerospace Medical Division, Air Force Systems Command, Wright-Patterson Air Force Base: Ohio.

Demirjian, A. (1980). Nutrition Canada anthropometry report: height, weight and body dimensions (pp. 28, 43). Ottawa: Health and Welfare Canada.

Dempster, W.T. (1955). Space requirements for the seated operator. WADC Technical Report 55-159, Aero Medical Laboratory, Wright Air Development Centre, Air Research and Development Council, Wright-Patterson Air Force Base: Ohio.

Drillis, R. and Contini, R. (1966). Body segment parameters. TR-1166-03, New York: New York University, School of Engineering and Science.

Fukijawa, K. (1963). The centre of gravity in the parts of the human body. Okajimos Folia Anat. Jap., 39(3): 117-126.

Halliday, D., Resnick, R. (1968). Physics, part II (pp. 1184-1188). New York: John Wiley and Sons, Inc.

Hanavan, E.P. (1964). A mathematical model of the human body. AMRL-TR-64-102, Aerospace Medical Research Laboratories, Wright-Patterson Air Force Base: Ohio.

Harless, E. (1860). The static moments of the component masses of the human body. Trans. Of the Math-Phys., Royal Bavarian Acad. Of Sci., 8(1): 69-96. Unpublished English Translation FTD-TT-61-295, Wright-Patterson Air Force Base: Ohio.

Hatze, H. (1980). A mathematical model for the computational determination of parameter values of anthropomorphic segments. Journal of Biomechanics, 13: 833-843.

Hinrichs, R.N. (1985). Regression equations to predict segmental moments of inertia from anthropometric measurements: an extension of the data of chandler, et al. (1975). Journal of Biomechanics, 18(8): 621-624.

Hologic QDR-1000/W Operators Manual and User's Guide. (1989). Waltham, MA: Hologic, Inc.

Huang, H.K. (1983). Evaluation of cross-sectional geometry and mass density distributions of humans and laboratory animals using computerized tomography. Journal of Biomechanics, 16(10): 821-832.

Jensen, R.K. (1978). Estimation of the biomechanical properties of three body types using a photogrammetric method. Journal of Biomechanics, 11: 349-358.

Jensen, R.K. (1989). Changes in segment inertia proportions between 4 and 20 years. Journal of Biomechanics, 22(6/7): 529-536.

Jensen, R.K., Fletcher, P. (1994). Distribution of mass to the segments of elderly males and females. Journal of Biomechanics, 27(1): 89-96.

Krabbe, B., Farkas, R. and Baumann, W. (1997). Influence of inertia on intersegment moments of the lower extremity joints. Journal of Biomechanics, 30(5): 517-519.

Martin, P.E., Mungiole, M., Marzke, M.W. and Longhill, J.M. (1989). The use of magnetic resonance imaging for measuring segment inertial properties. Journal of Biomechanics, 22(4): 367-376.

Mori, M. and Yamamoto, T. (1959). Die Massenanteile der einzeinen Korperabschnitte der Japaner., Acta Anatomica 37(4): 385-388.

Morlock, M. and Yeadon, M.R. (1986). Regression equations for segmental inertia parameters. Human Locomotion IV, Proceedings of the North American Congress on Biomechanics: Montreal, pp. 231-234.

Pearsall, D.J., Costigan, P.A. (1998). The effect of segment parameter error on gait analysis results. Accepted for publication in Gait and Posture.

Pearsall, D.J., Reid, J.G., Livingston, L.A. (1996). Segmental inertial parameters of the human trunk as determined from computed tomography. Annals of Biomedical Engineering, 24: 198-210.

Peyton, A.J. (1986). Determination of the moment of inertia of limb segments by a simple method. Journal of Biomechanics, 19(5): 405-410.

Plagenhoef, S. (1983). Anatomical data for analyzing human motion. Research Quarterly for Exercise and Sport, 54(2): 169-178.

Webber, C.E. (1995). Dual Photon Transmission Measurements of Bone Mass and Body Composition During Growth. In: Blimkie, C.J.R. and Bar-Or, O. New Horizons in Pediatric Exercise Science. Champaign, IL: Human Kinetics Publishers, pp. 57-76.

Winter, D.A. (1990). Biomechanics and Motor Control of Human Movement, 2nd Ed. New York: John Wiley and Sons, Inc., pp. 51-64.

Yeadon, M.R. and Morlock, M. (1989). The appropriate use of regression equations for the estimation of segmental inertia parameters. Journal of Biomechanics, 22(6/7): 683-689.

Young, J.W., Chandler, R.F., Snow, C.C. (1983). Anthropometric and mass distribution characteristics of the adult female. FAA-AM-83-16, FAA Civil Aeromedical Institute Oklahoma.

Zatsiorsky, V. and Seluyanov, V. (1983). The mass and inertia characteristics of the main segments of the human body. In: Matsui, H., Kobayashi, K. (Eds.). Biomechanics VIII-B (pp. 1152-1159). Champaign, IL: Human Kinetics Publishers.

Zatsiorsky, V. and Seluyanov, V. (1985). Estimation of the mass and inertia characteristics of the human body by means of the best predictive regression equations. In: Winter, D.A., Norman, R.W., Wells, R.P. (Eds.) Biomechanics IX-B, Champaign, IL: Human Kinetics Publishers, 233-239.

Zatsiorsky, V., Seluyanov, V., Chugunova, L. (1990). Methods of determining mass-inertial characteristics of human body segments. In: Chernyi, G.G., Regirer, A. Contemporary Problems of Biomechanics (pp. 273-291). Moscow: Mir Publishers.

APPENDIX A

Height and Mass Characteristics of Subjects

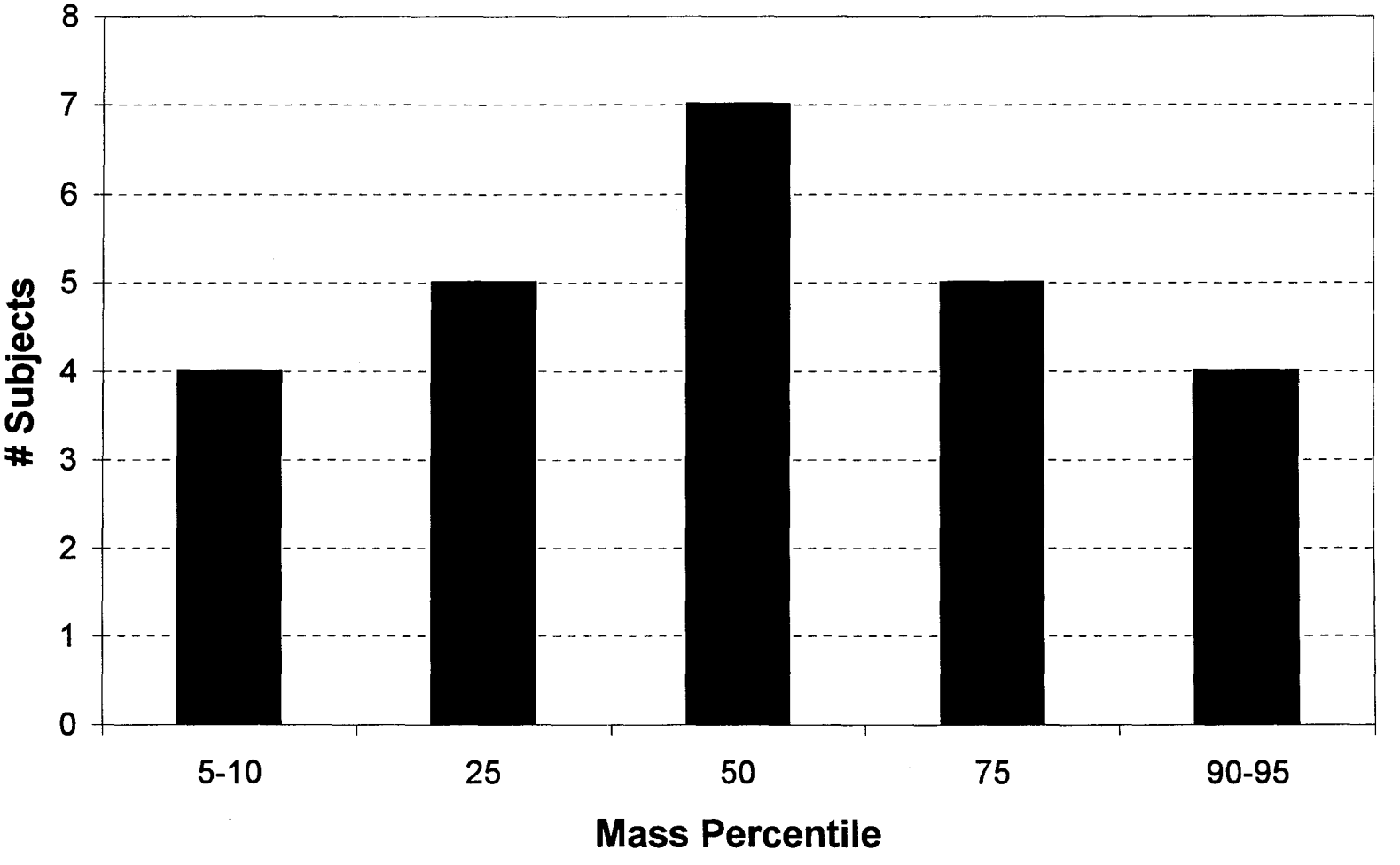

Figure A-1: Frequency Distribution of Mass Percentiles for Males 19-30

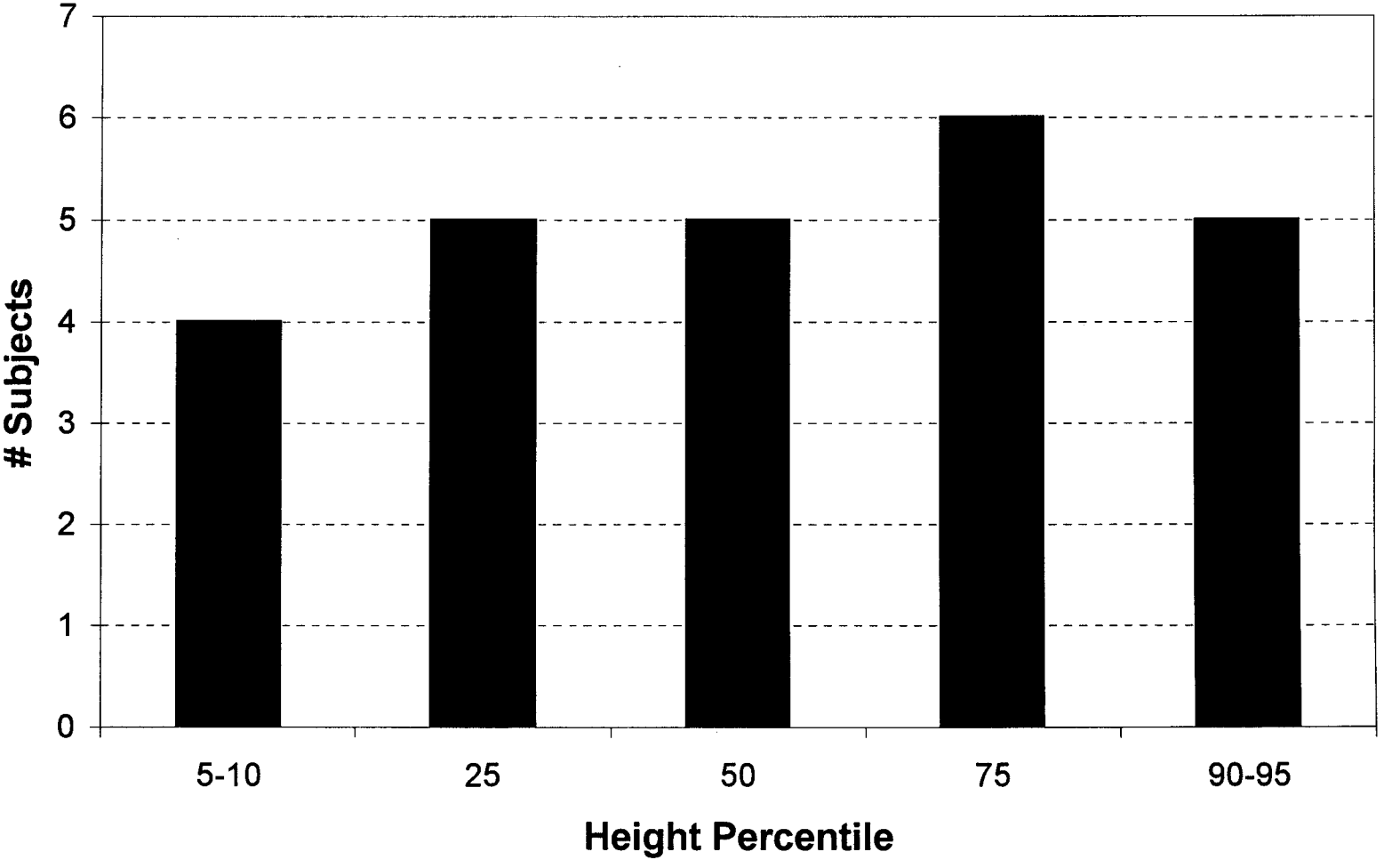

Figure A-2: Frequency Distribution of Height Percentiles for Males 19-30

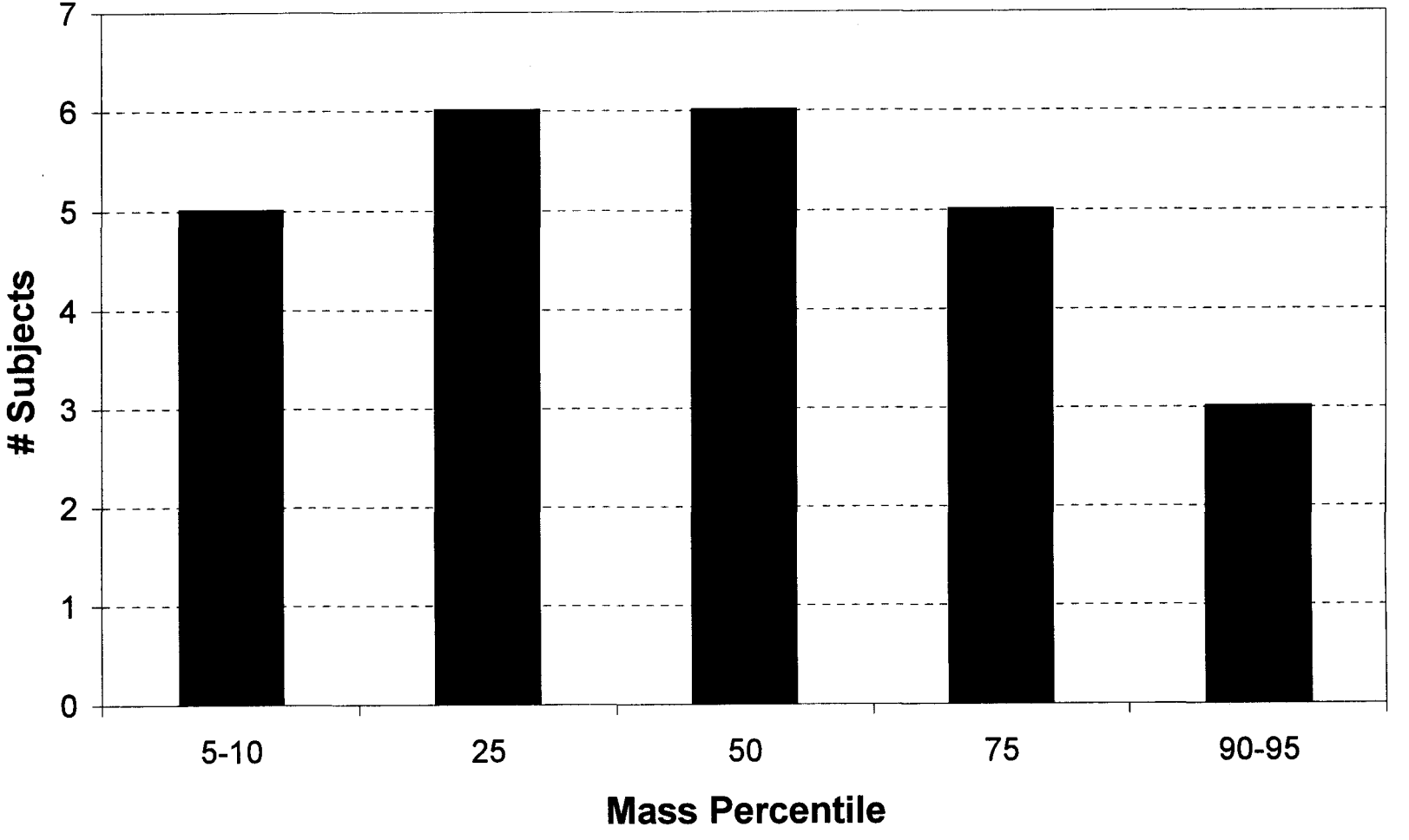

Figure A-3: Frequency Distribution of Mass Percentiles for Females 19-30

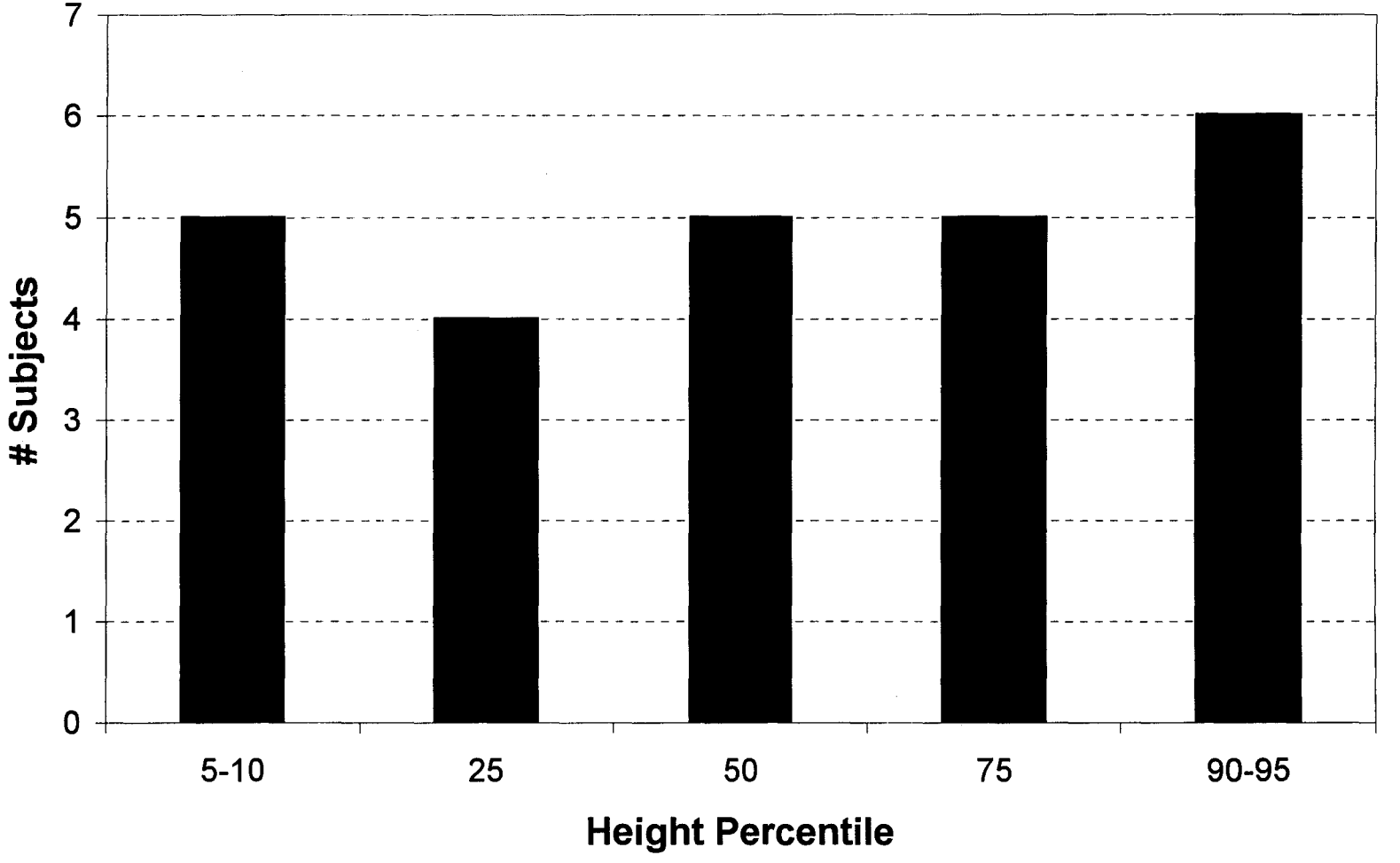

Figure A-4: Frequency Distribution of Height Percentiles for Females 19-30.

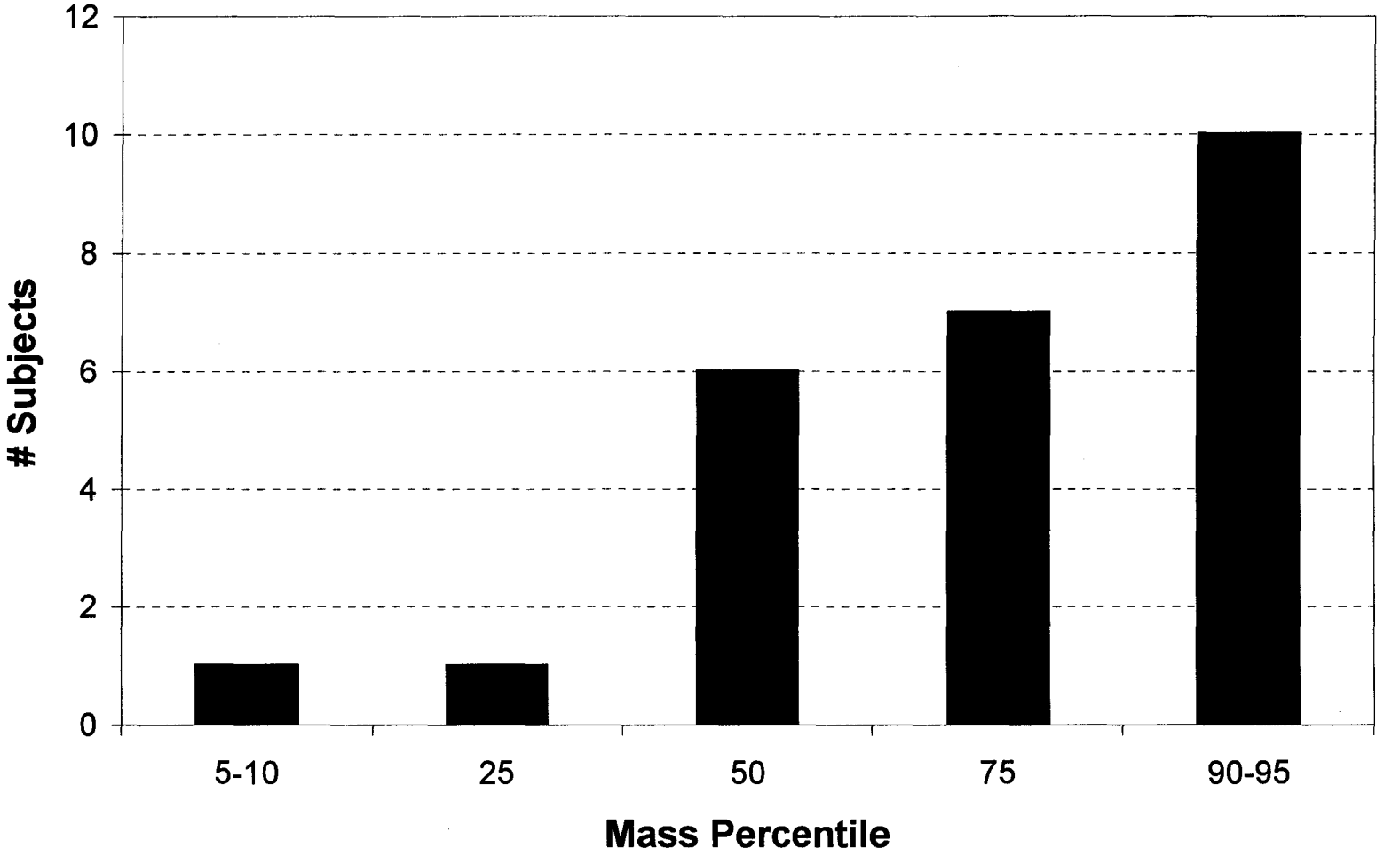

Figure A-5: Frequency Distribution of Mass Percentiles for Males 55^{+}

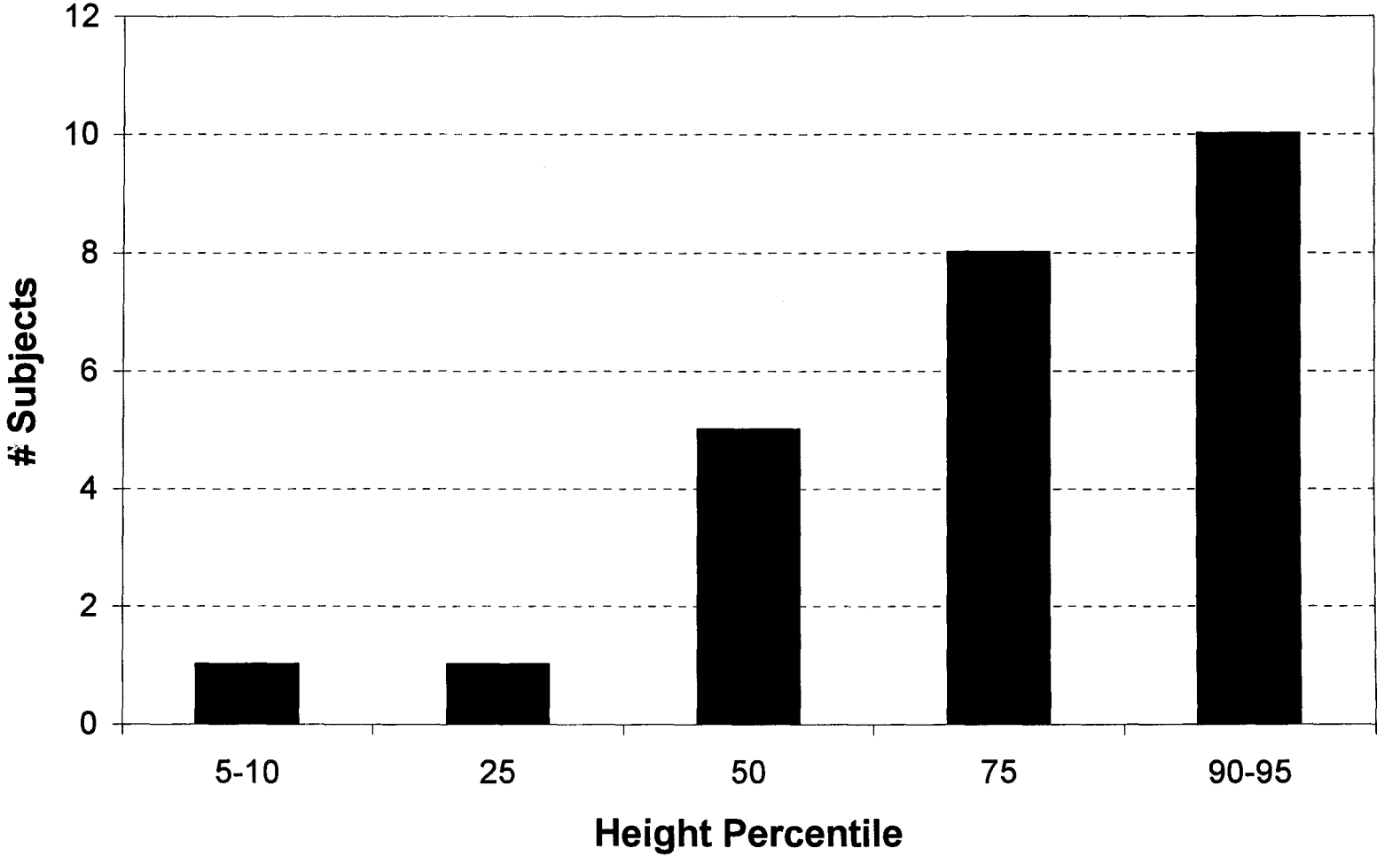

Figure A-6: Frequency Distribution of Height Percentiles for Males 55^{+}

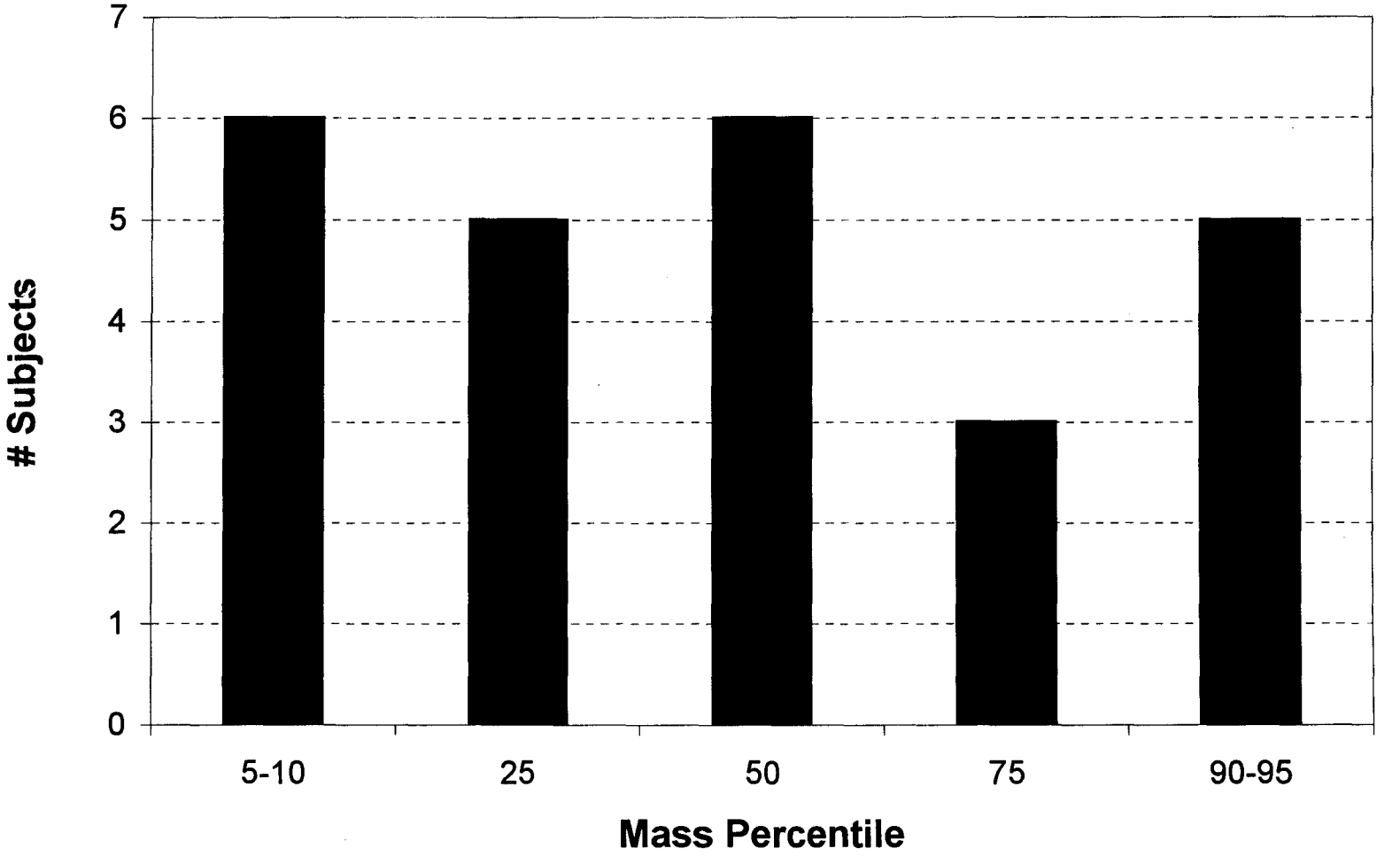

Figure A-7: Frequency Distribution of Mass Percentiles for Females 55^{+}

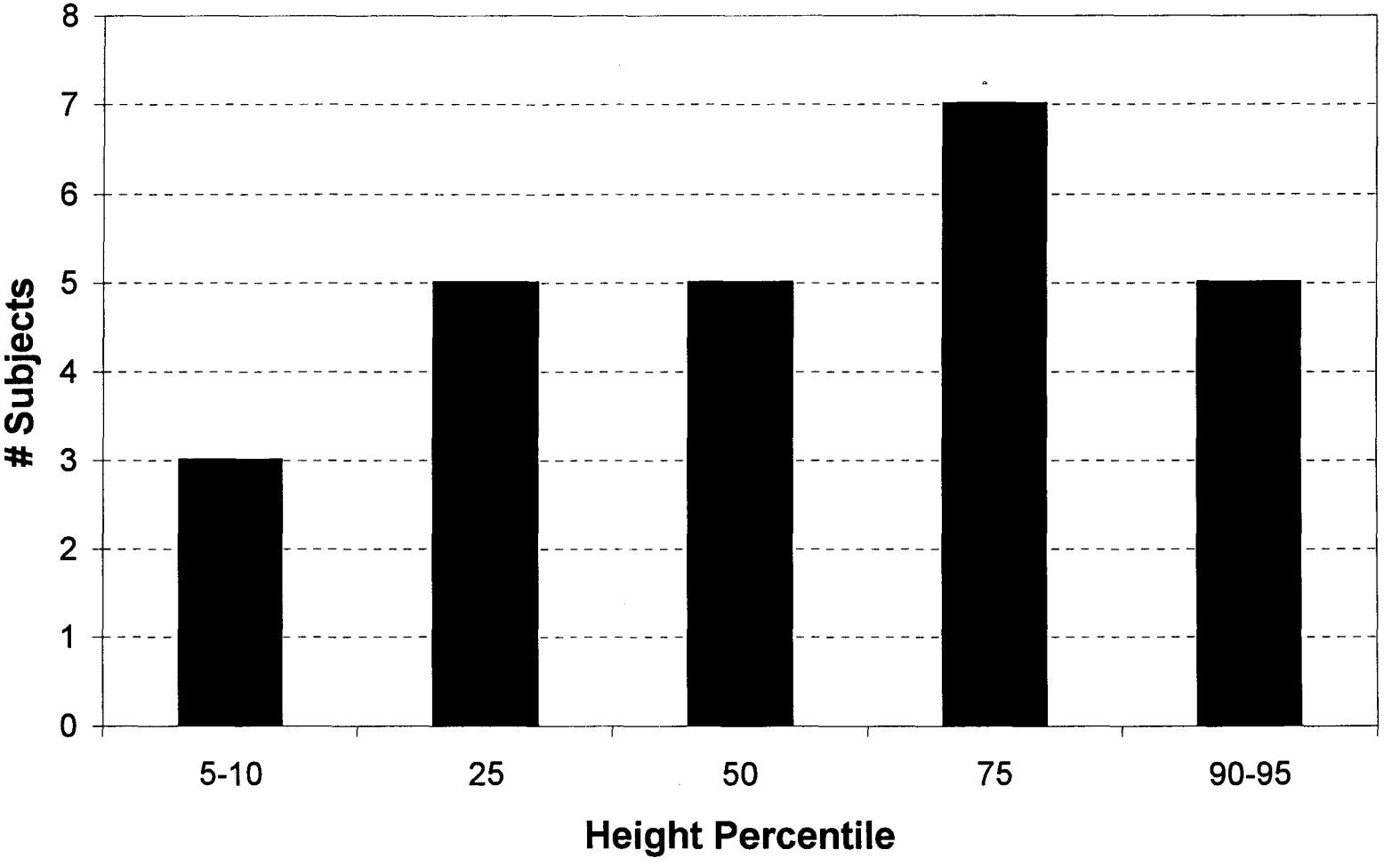

Figure A-8: Frequency Distribution of Height Percentiles for Females 55+

APPENDIX B

Description of Anthropometric Measurements

A) FOREARM MEASUREMENTS

Note: Subject is in anatomical position with elbows extended, palms facing forward

Elbow Circumference: Circumference over olecranon process and across the anterior crease of the elbow.

Wrist Circumference: Circumference over wrist crease just distal to ulnar and radial styloids.

Forearm Circumference: Largest circumference about forearm.

Proximal-to-Centre Forearm Length: Distance from lateral epicondyle to lateral location of largest forearm circumference.

Forearm Length: Distance from lateral epicondyle to the tip of the radial styloid.

B) THIGH MEASUREMENTS

Proximal Thigh Circumference: Horizontal circumference about thigh at medial proximal limit (pubic tubercle).

Inner Thigh Length: Distance between medial proximal limit (pubic tubercle) of thigh and medial joint line of the knee along tibial plateau.

Outer Thigh Length: Distance between greater trochanter and lateral joint line of the knee along the tibial plateau.

C) LEG MEASUREMENTS

Note: Subject is in standing position with feet pointed forward

Knee Circumference: Circumference about the knee along the joint line at the tibial plateau.

Ankle Circumference: Smallest circumference about distal end of leg, just distal to lateral and medial malleoli.

Leg Circumference: Largest circumference about leg.

Proximal-to-Centre Leg Circumference: Distance from the joint line of the knee at the lateral side of the tibial plateau to lateral location of largest leg circumference.

Leg Length: Distance from the joint line of the knee at the lateral side of the tibial plateau to the lowest point of the lateral malleolus.

HEAD MEASUREMENTS

Horizontal Head Circumference: Circumference about head at the level of the brow line.

Vertical Head Circumference: Circumference under chin just anterior to the neck and vertically about the top of the head.

APPENDIX C

Geometric Models

MODEL FOR FOREARM AND LEG

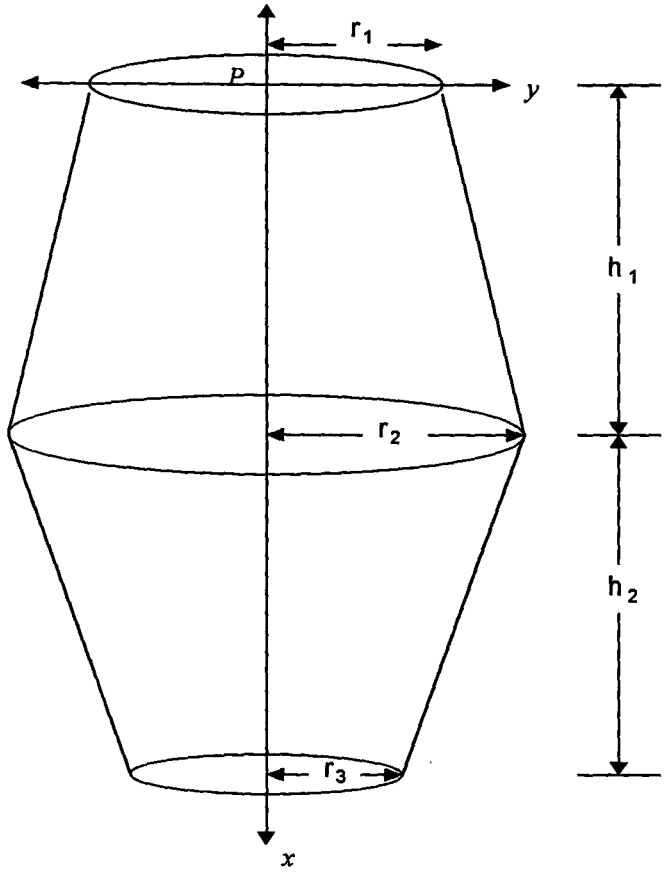

Where:

r_1 = Elbow Radius
or Knee Radius

r_2 = Forearm Radius
or Leg Radius

r_3 = Wrist Radius
or Ankle Radius

And:

h_1 = Proximal to Centre Length

$h_1 + h_2$ = Forearm Length or Leg Length

Figure C-1: Geometric Model of a Forearm or Leg Segment

Forearm and Leg Mass:

$$V_{Segment} = V_1 + V_2 = \frac{\Pi h_1}{3}(r_1^2 + r_1 r_2 + r_2^2) + \frac{\Pi h_2}{3}(r_2^2 + r_2 r_3 + r_3^2) \quad (1)$$

$$M_{Segment} = M_1 + M_2 = \rho(V_1 + V_2) = \rho V_{Segment} \quad (2)$$

Forearm and Leg Centre of Mass Location:

$$XX = \frac{x_1 V_1 + x_2 V_2}{V_{Segment}} \quad (3)$$

where:

$$x_1 = h_1 - [(\frac{h_1}{4})(\frac{r_2^2 + 2(r_1 r_2) + 3(r_1^2)}{r_1^2 + r_1 r_2 + r_2^2})] \quad (4) \qquad x_2 = h_1 + [(\frac{h_2}{4})(\frac{r_2^2 + 2(r_2 r_3) + 3(r_3^2)}{r_2^2 + r_2 r_3 + r_3^2})] \quad (5)$$

Forearm and Leg I_{CG}:

To arrive at the I_{CG} of the composite body, the I_{CG} of each component was calculated (Hanavan, 1966). Following this, parallel axis theorem was used to determine the moment of inertia of each component about the proximal end of the object at point *P* (I_P). These moments were summed to determine the moment of inertia of the entire object about point *P*. Parallel axis theorem was then used to determine the I_{CG} of the object. The resulting equations were as follows:

$$I_{XX_1} = (\rho V_1)[AA_1(\frac{V_1}{h_1}) + BB(h_1^2)] \quad (6) \qquad I_{XX_2} = (\rho V_2)[AA_2(\frac{V_2}{h_2}) + BB(h_2^2)] \quad (7)$$

where:

$$AA = (\frac{9}{20\pi})(\frac{1+\mu+\mu^2+\mu^3+\mu^4}{\vartheta^2}) \quad (8) \qquad B = (\frac{3}{80})(\frac{1+4\mu+10\mu^2+4\mu^3+\mu}{\vartheta^2}) \quad (9)$$

and:

$$\mu_1 = \frac{r_1}{r_2} \quad (10) \qquad \mu_2 = \frac{r_3}{r_2} \quad (11) \qquad \vartheta = 1+\mu+\mu^2 \quad (12)$$

therefore:

$$I_{P_1} = I_{XX_1} + M_1 x_1^2 \quad (13) \qquad I_{P_2} = I_{XX_2} + M_2 x_1^2 \quad (14)$$

$$I_P = I_{P_1} + I_{P_2} \quad (15)$$

$$I_{XX} = I_P - (M_{Segment} XX^2) \quad (16)$$

MODEL FOR THE THIGH SEGMENT

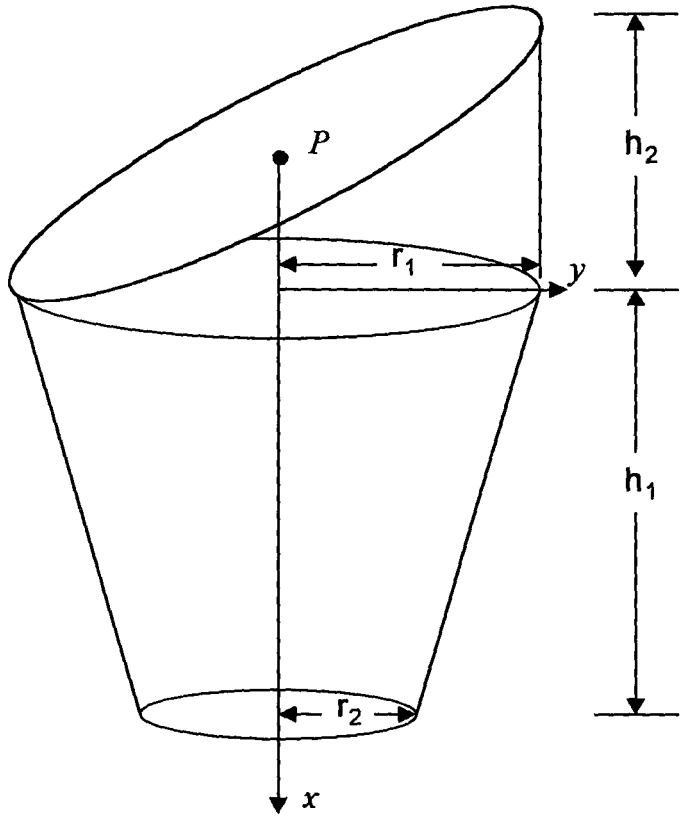

Where:

r_1 = Proximal Thigh Radius

r_2 = Knee Radius

h_1 = Inner Thigh Length

$h_1 + h_2$ = Outer Thigh Length

Figure C-2: Geometric Model of a Thigh Segment

Thigh Mass:

$$V_{Thigh} = V_1 + V_2 = \frac{\pi r_1^2 h_2}{2} + r_1^2 + r_1 r_2 + r_2^2 \quad (17)$$

$$M_{Thigh} = M_1 + M_2 = \rho(V_1 + V_2) = \rho V_{Thigh} \quad (18)$$

Thigh Centre of Mass:

$$XX = \frac{x_1 V_1 + x_2 V_2}{V_{Thigh}} \quad (19) \qquad YY = \frac{y_1 V_1 + y_2 V_2}{V_{Thigh}} \quad (20)$$

where:

$$x_1 = \frac{3h_1}{16} \quad (21) \qquad x_2 = \frac{h_1}{2} + [(\frac{h_2}{4})(\frac{r_1^2 + 2(r_1 r_2) + 3(r_2^2)}{r_1^2 + r_1 r_2 + r_2^2})] \quad (22)$$

$$y_1 = \frac{3r_1}{4} \quad (23) \qquad y_2 = 0 \quad (24)$$

Thigh I_{CG}:

The I_{CG} of the thigh model was measured by first calculating the moment of inertia of each component about the proximal end at point *P*. The two inertia

values were then added together and parallel axis theorem was used to determine the I_{CG} of the entire object. The moment of inertia of the right circular frustrum was found as for the model of the forearm. The moment of inertia of the upper circular cylinder component was found through integration. The volume was integrated using rectangular slices with thickness *dy*. The moment of inertia of this volume was found by integrating over the entire length of the volume using parallel axis theorem. The resulting equations were as follows:

$$V_1 = \int_{-r}^{r} (2\sqrt{r_1^2 - y^2})(\frac{h_1}{2} + 2y)dy \tag{25}$$

and

$$\begin{aligned} I_{z_1} &= I_{z_1}{}' + M_{Thigh} r^2 \\ &= \int_{-r}^{r} [\frac{1}{12}(\frac{h_1}{2} + 2x)^2 + (y^2 + (\frac{h_1}{2} + 2y)^2][(2\sqrt{r_1^2 + y^2})(\frac{h_1}{2} + 2y)]dy \end{aligned} \tag{26}$$

where I_{Z2} is found by calculating the I_{CG} of the frustrum (equations 6, 8-13) and transforming it in the following manner:

$$I_{Z_2} = I_{CG} + (M_2)(x^2) \tag{27}$$

$$I_Z = I_{Z_1} + I_{Z_2} \tag{28}$$

$$I_{CG}=I_Z-(M_{Thigh})[(XX^2)(YY^2)] \quad (29)$$

MODEL FOR THE HEAD SEGMENT

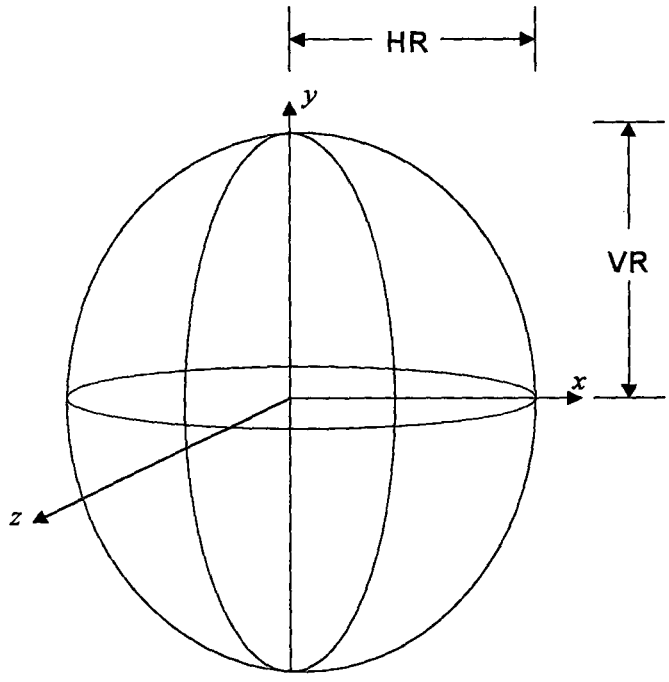

Where:

HR = Horizontal Head Radius

VR = Vertical Head Radius

and

the radius in the z-direction is equal to HR

Figure C-4: Geometric Model of a Head Segment

Head Mass:

$$V_{Head}=(\frac{4}{3}\pi)(VR)(HR) \quad \textbf{(30)}$$

$$Mass_{Head}=\rho V_{Head} \quad \textbf{(31)}$$

Head Centre of Mass:

Head centre of mass was equal to the vertical radius of the head.

Head I_{CG}:

$$I_{Z_{Head}}=(\frac{M_{Head}}{4})(VR^2+HR^2) \quad \textbf{(32)}$$

APPENDIX D

Sample Figures of BSP Predictor Comparisons

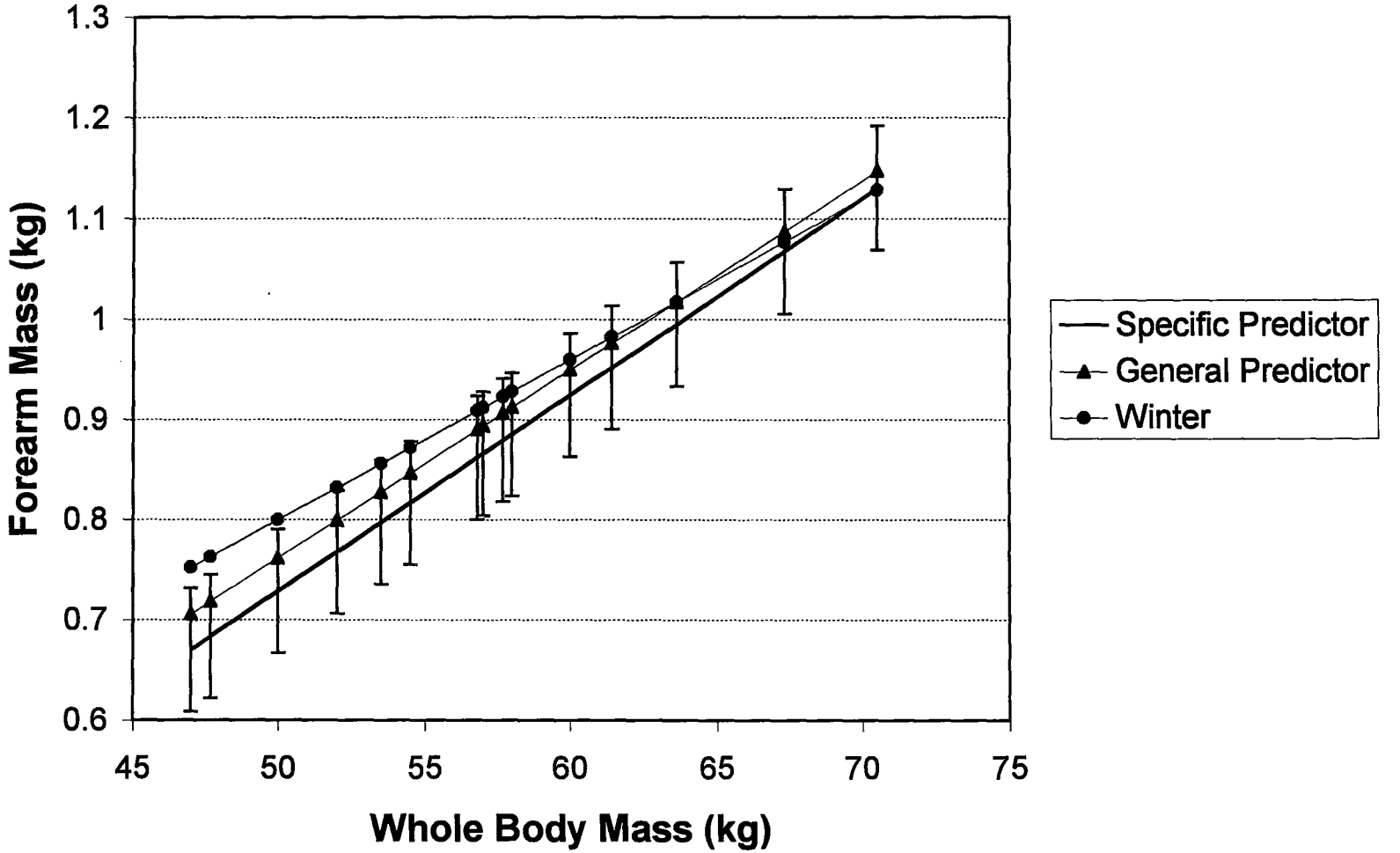

Figure D-1: Comparison of Forearm Mass Predictors (Females 19-30)
(Specific Predictor ± S.E.)

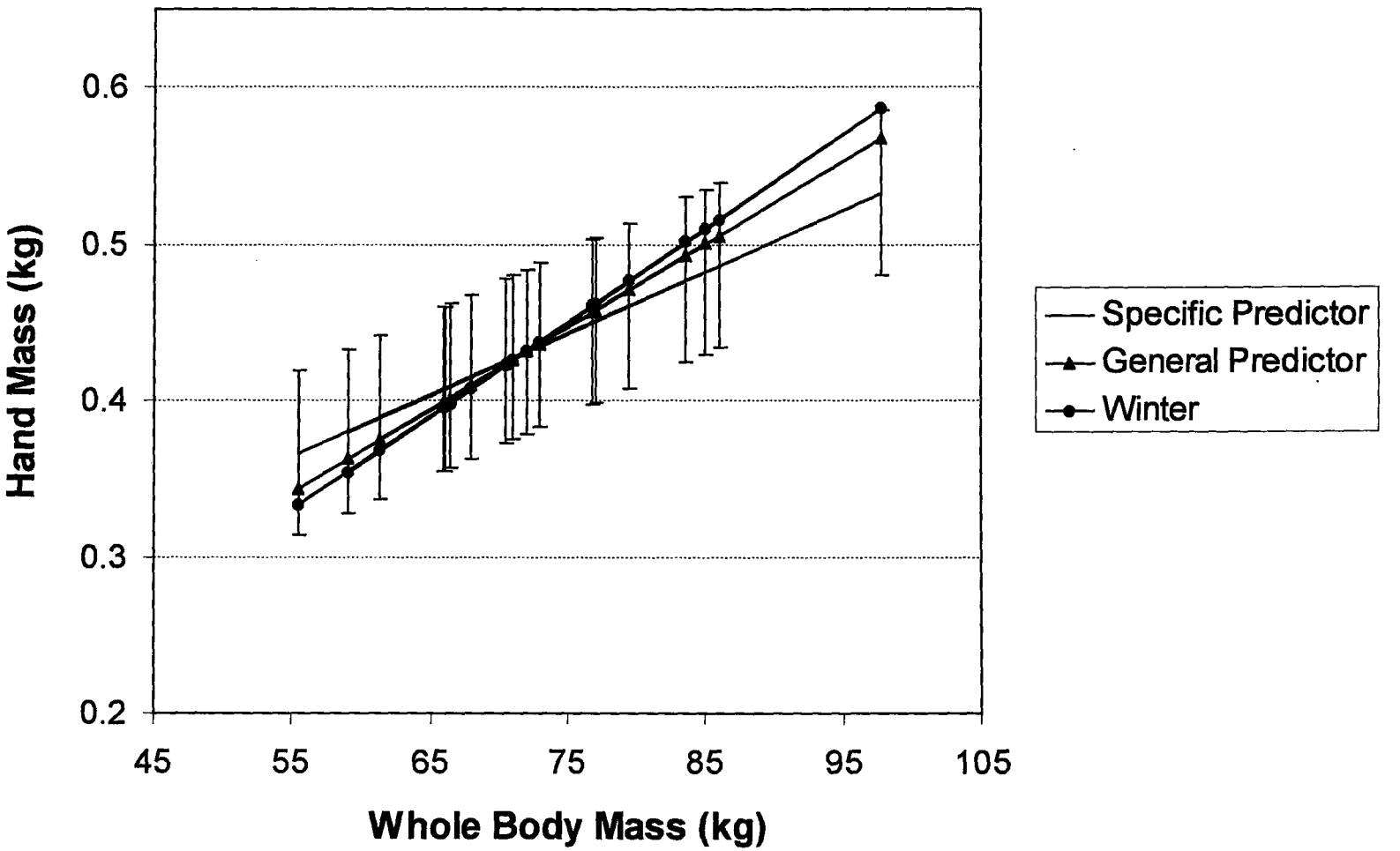

Figure D-2: Comparison of Hand Mass Predictors (Males 19-30)
(Specific Predictor ± S.E.)

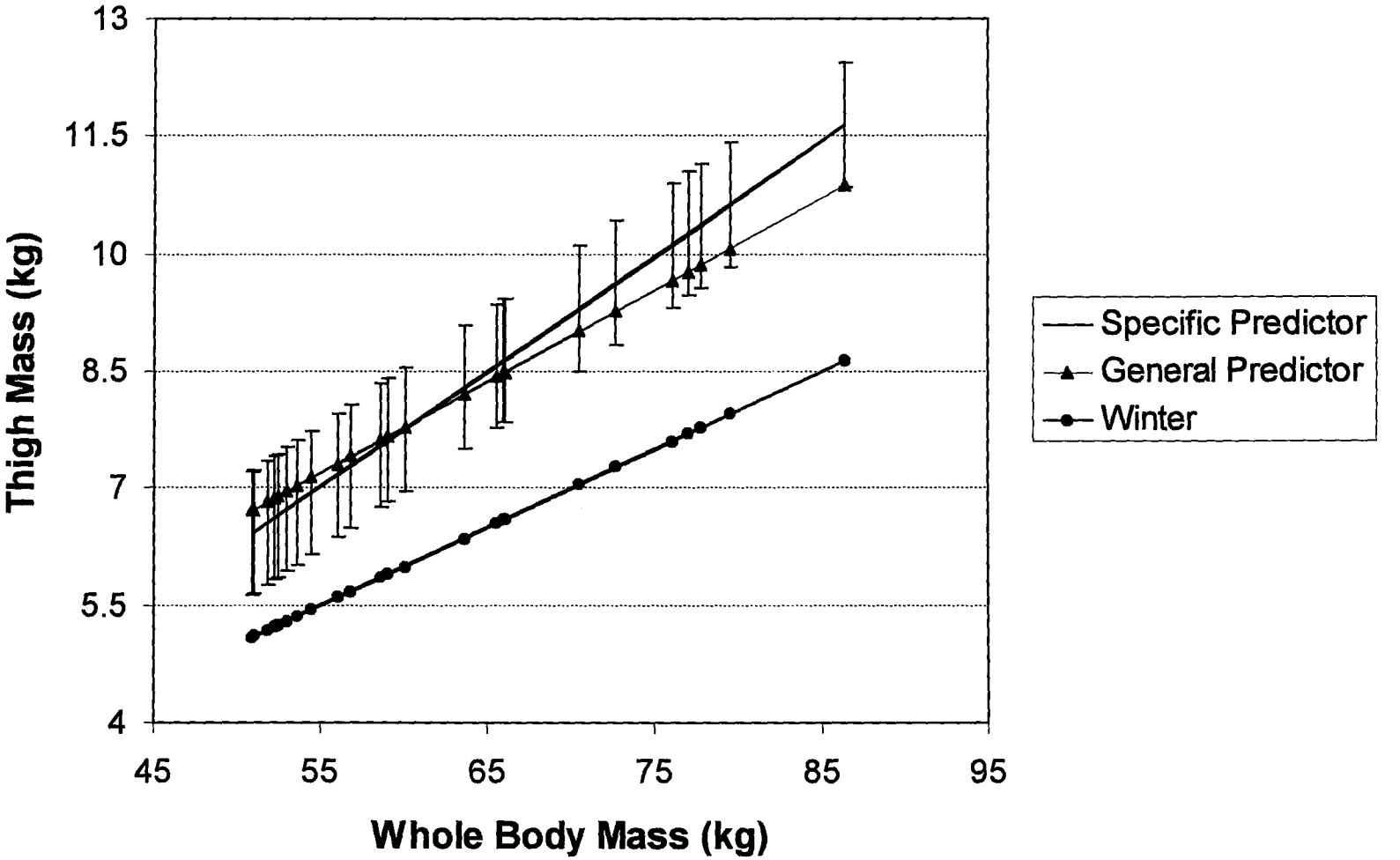

Figure D-3: Comparison of Thigh Mass Predictors (Females 55+)
(Specific Predictor ± S.E.)

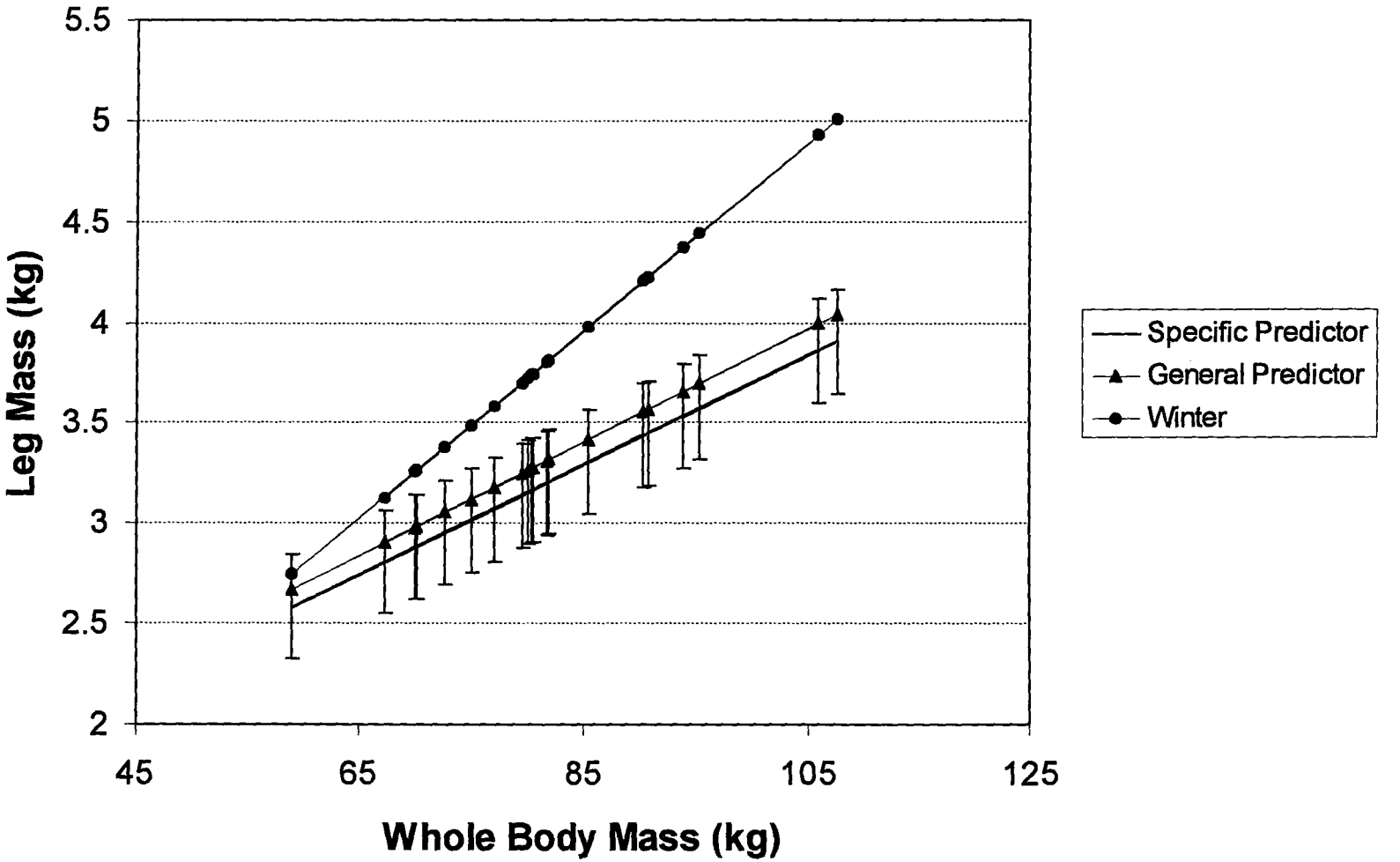

Figure D-4: Comparison of Leg Mass Predictors (Males 55+)
(Specific Predictor ± S.E.)

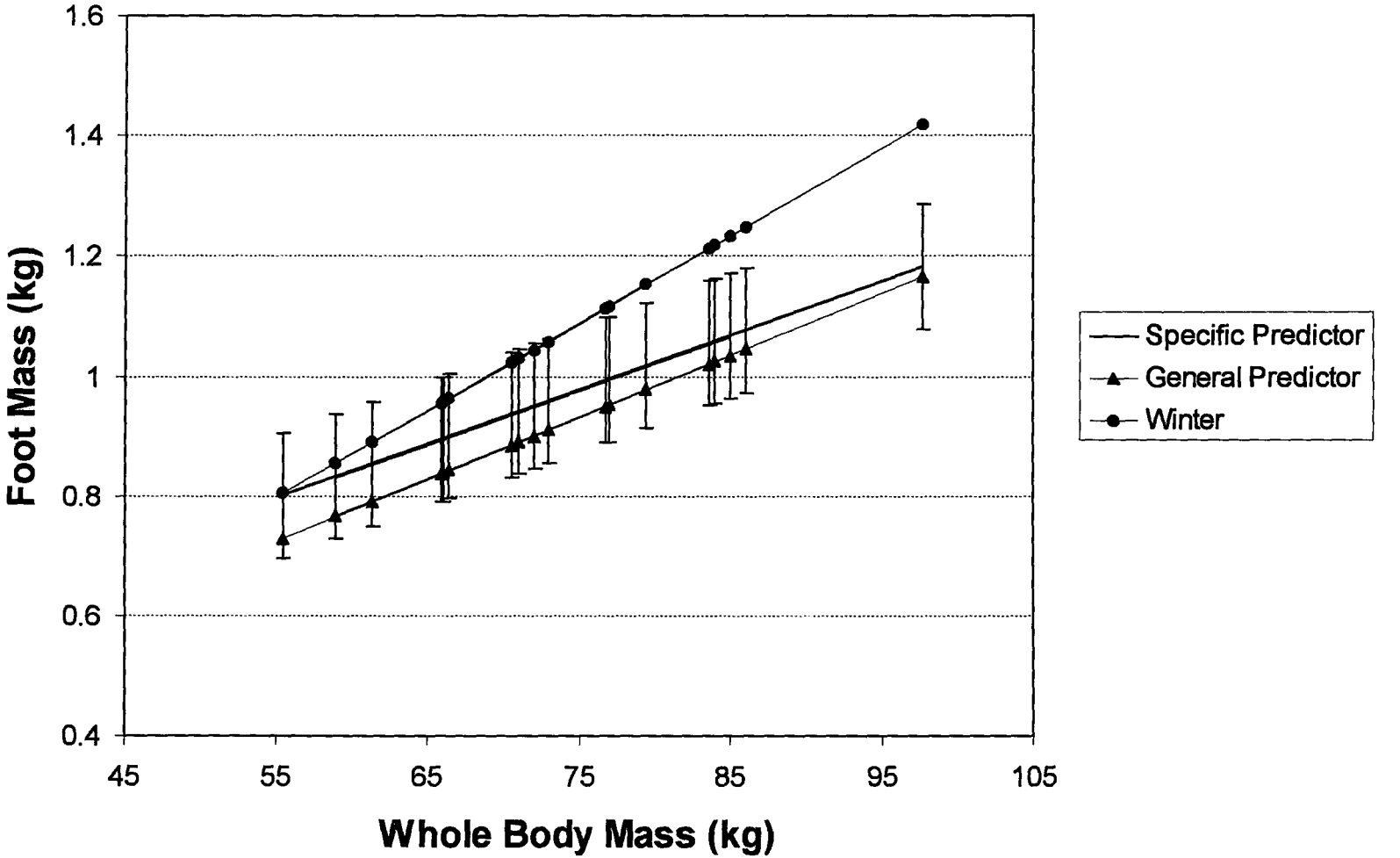

Figure D-5: Comparison of Foot Mass Predictors (Males 19-30)
(Specific Predictors ± S.E.)

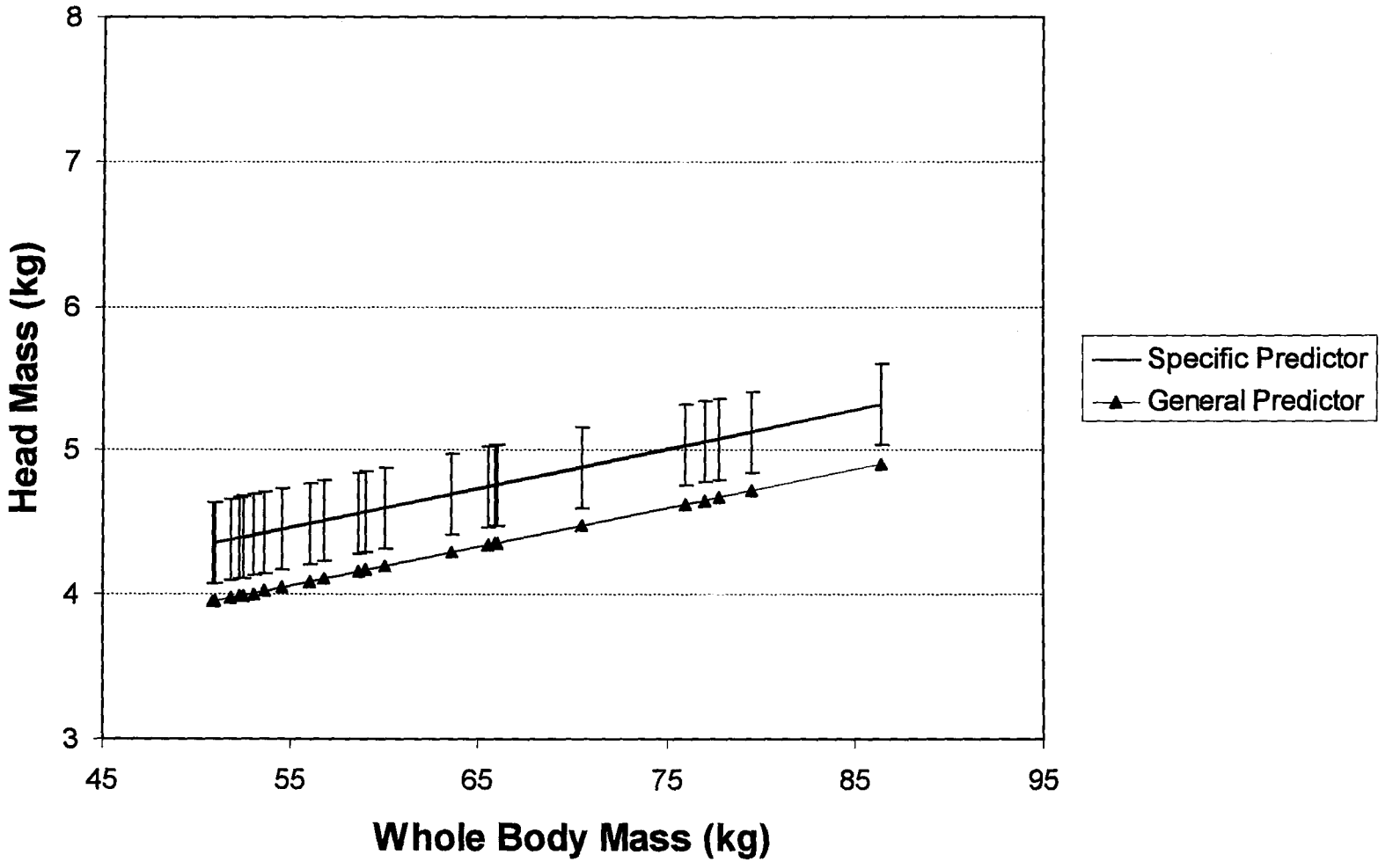

Figure D-6: Comparison of Head Mass Predictors (Females 55+ Years)
(Specific Predictor ± S.E.)

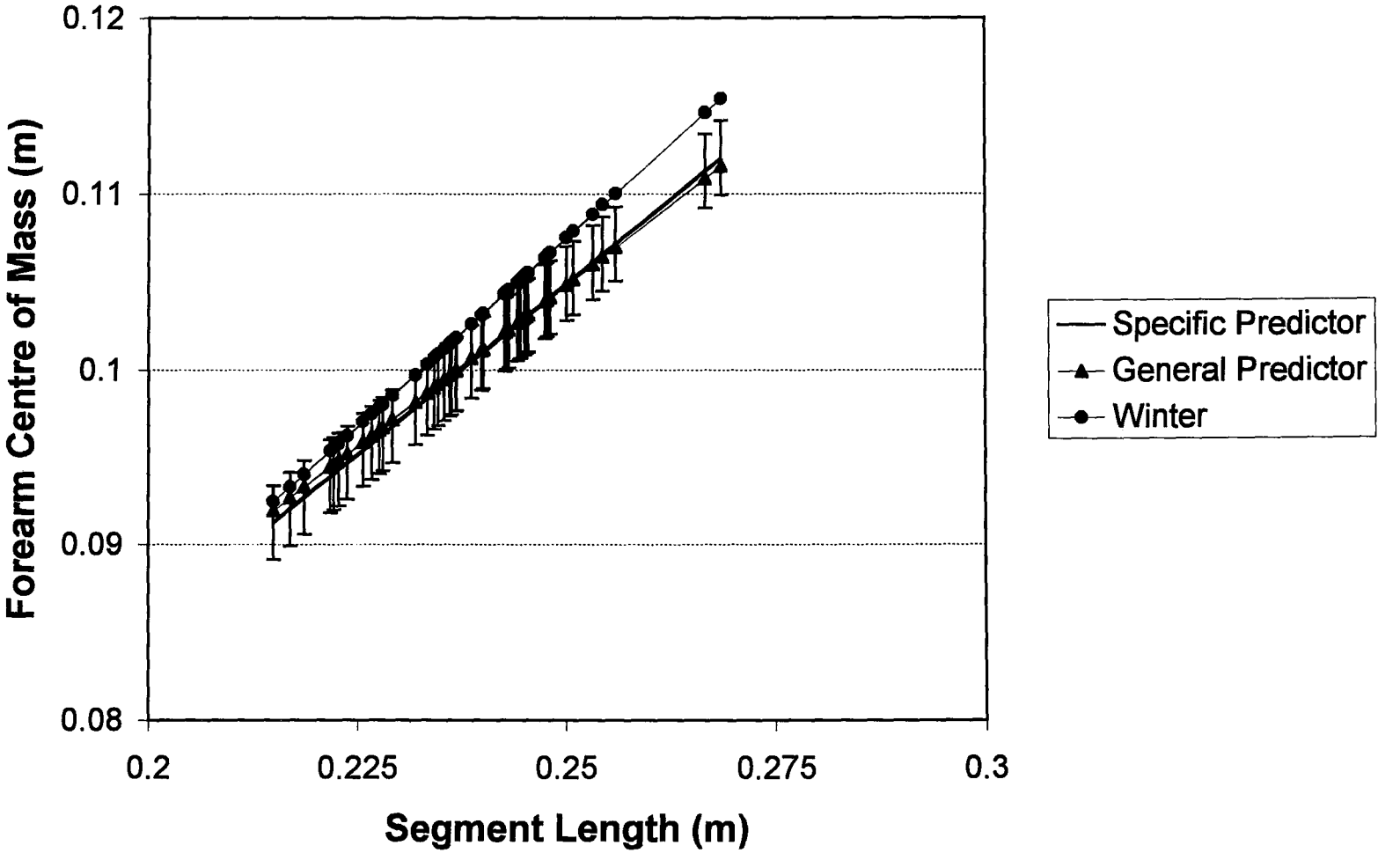

Figure D-7: Comparison of Forearm Centre of Mass Predictors (Females 19-30 Years) (Specific Predictor ± S.E.)

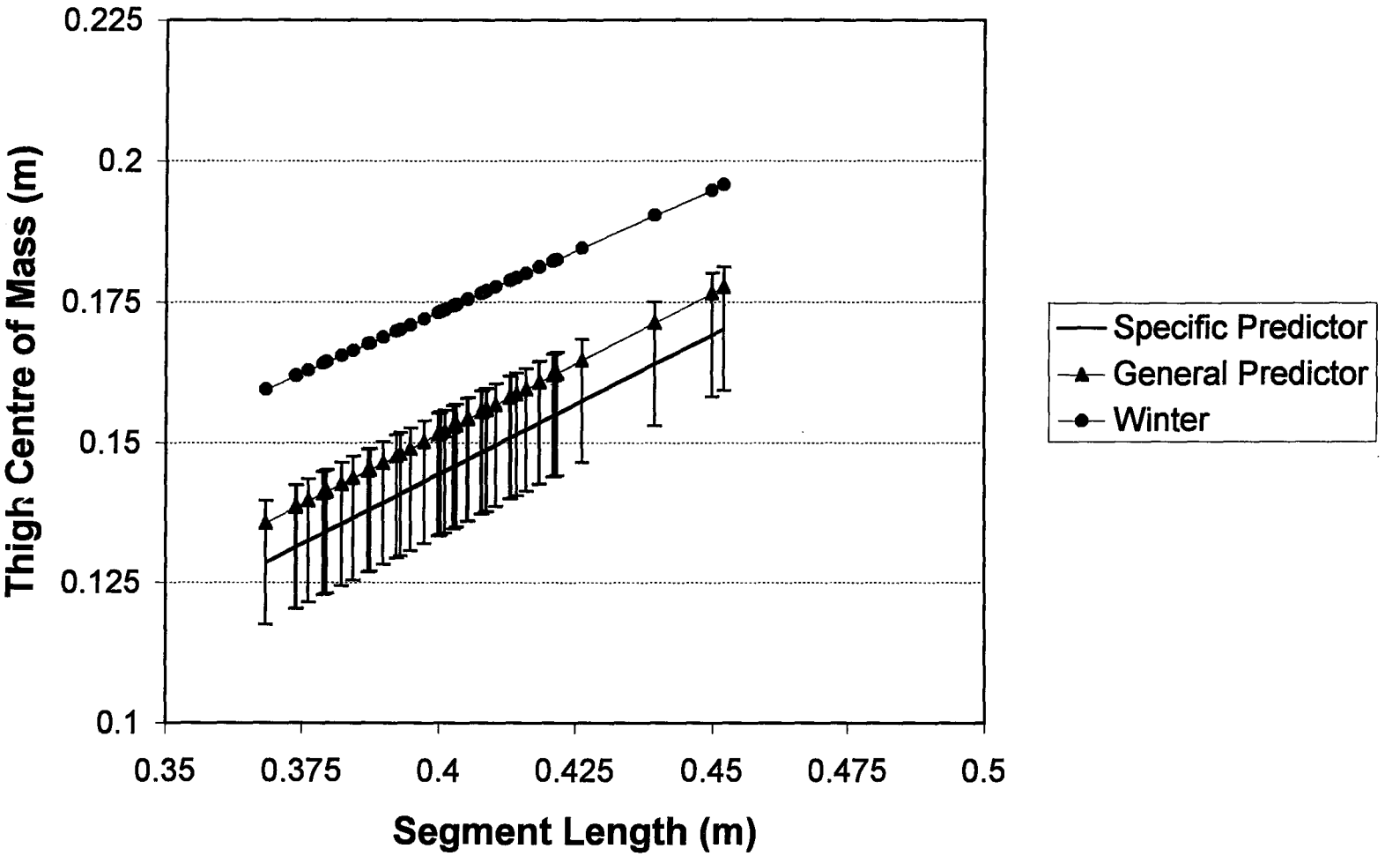

Figure D-8: Comparison of Thigh Centre of Mass Predictors (Females 55^{+} Years) (Specific Predictor ± S.E.)

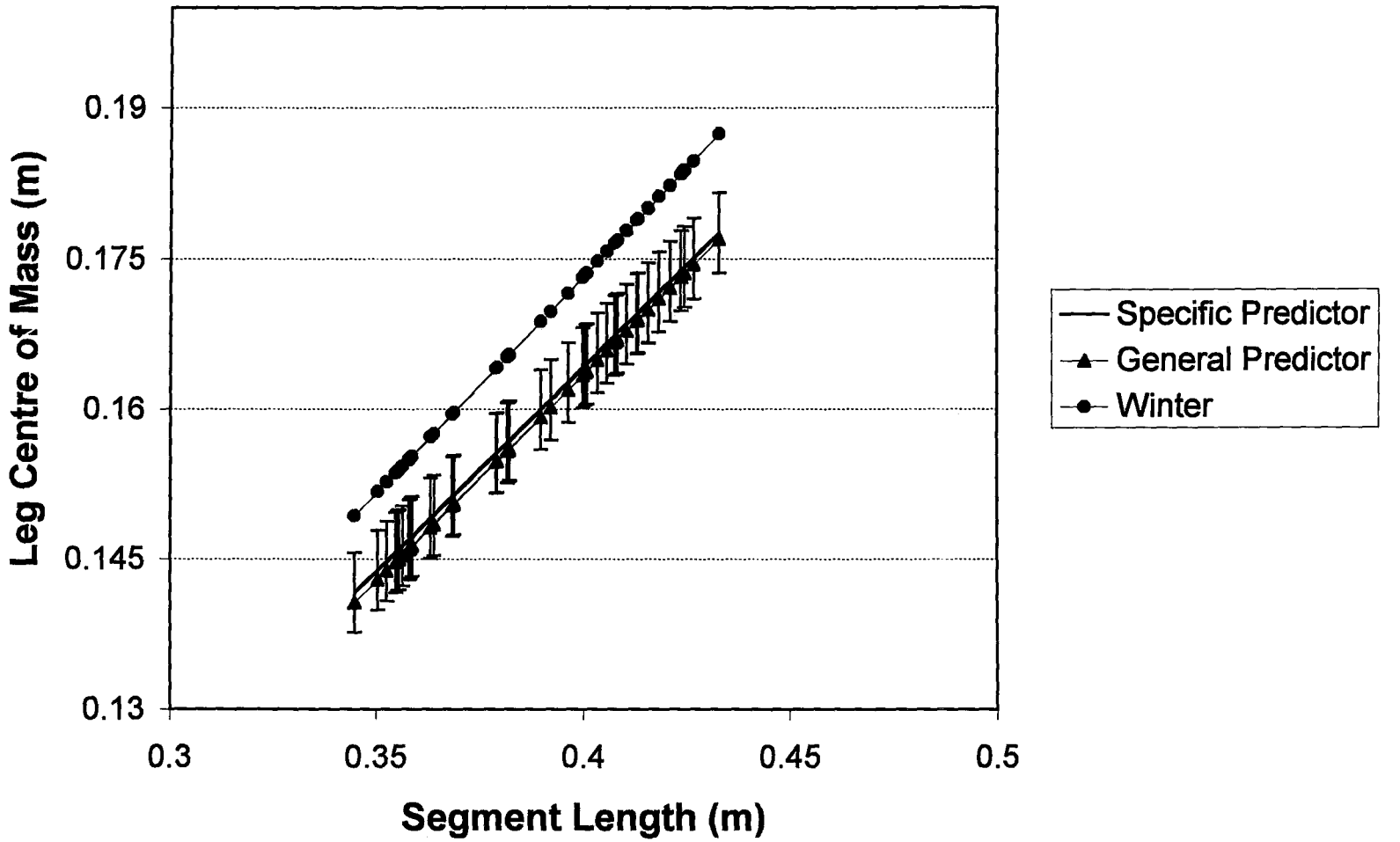

Figure D-9: Comparison of Leg Centre of Mass Predictors (Males 19-30 Years)
(Specific Predictor ± S.E.)

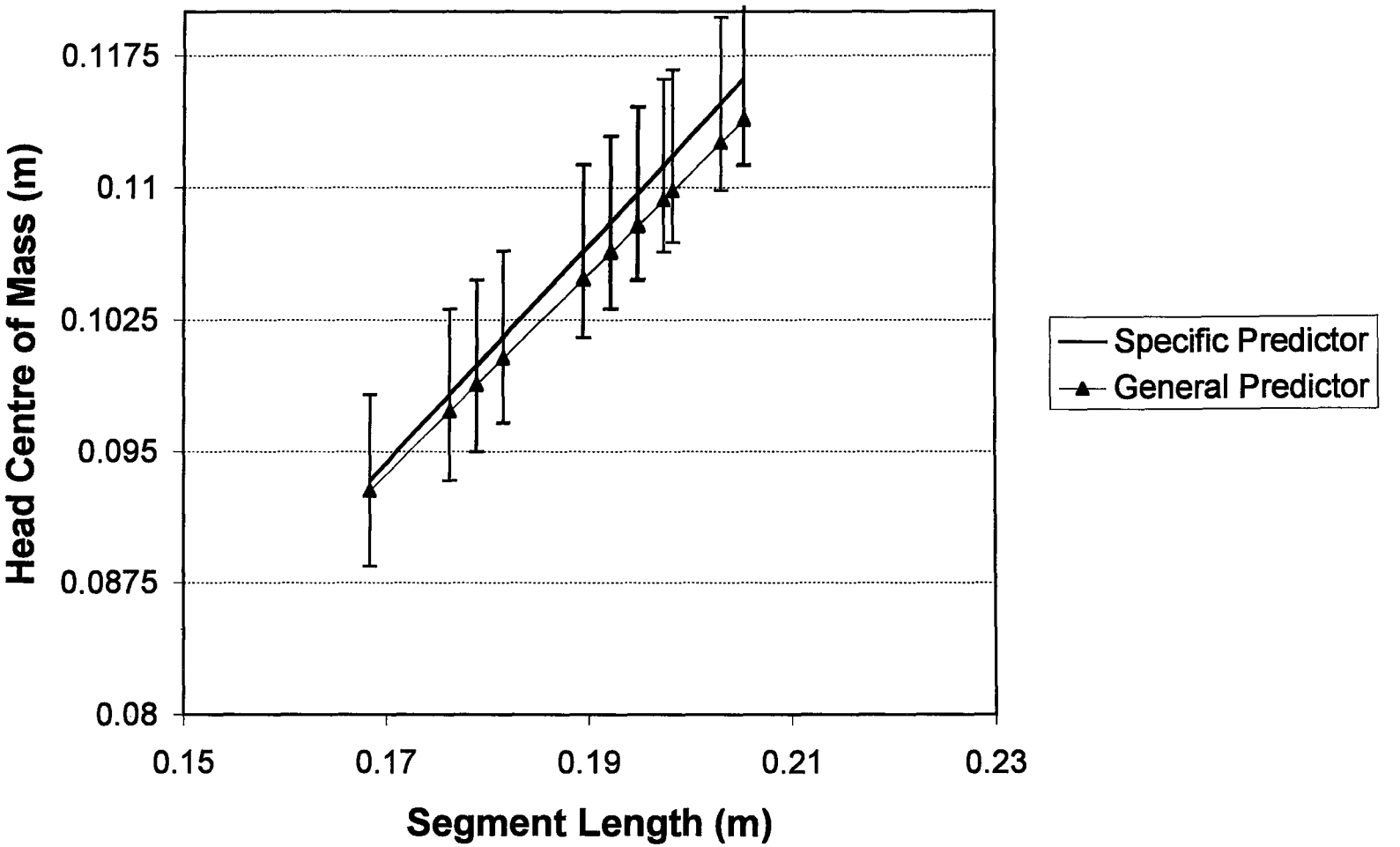

Figure D-10: Comparison of Head Centre of Mass Predictors (Males 55^{+} Years)
(Specific Predictors ± S.E.)

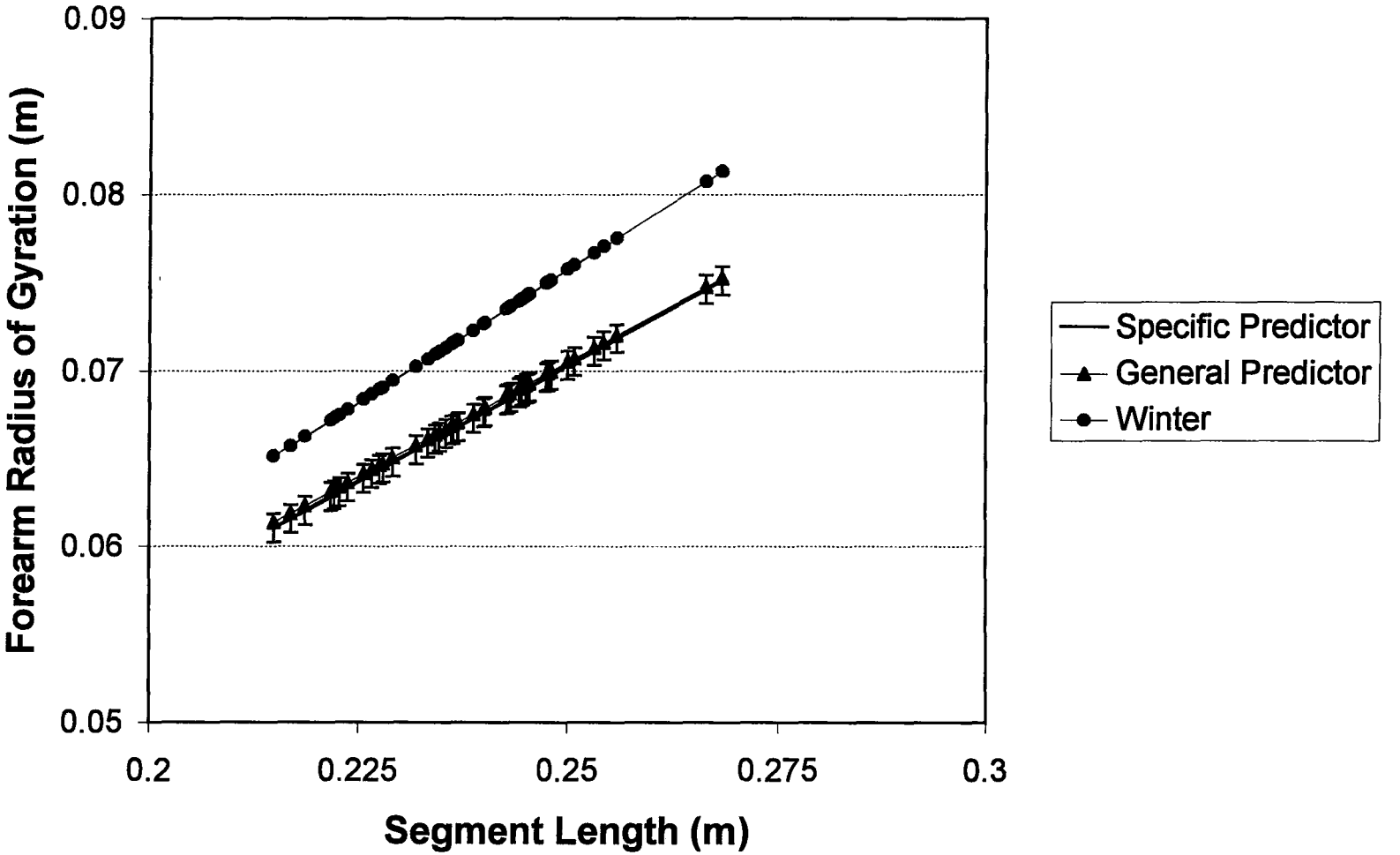

Figure D-11: Comparison of Forearm Radius of Gyration Predictors (Females 19-30 Years) (Specific Predictor ± S.E.)

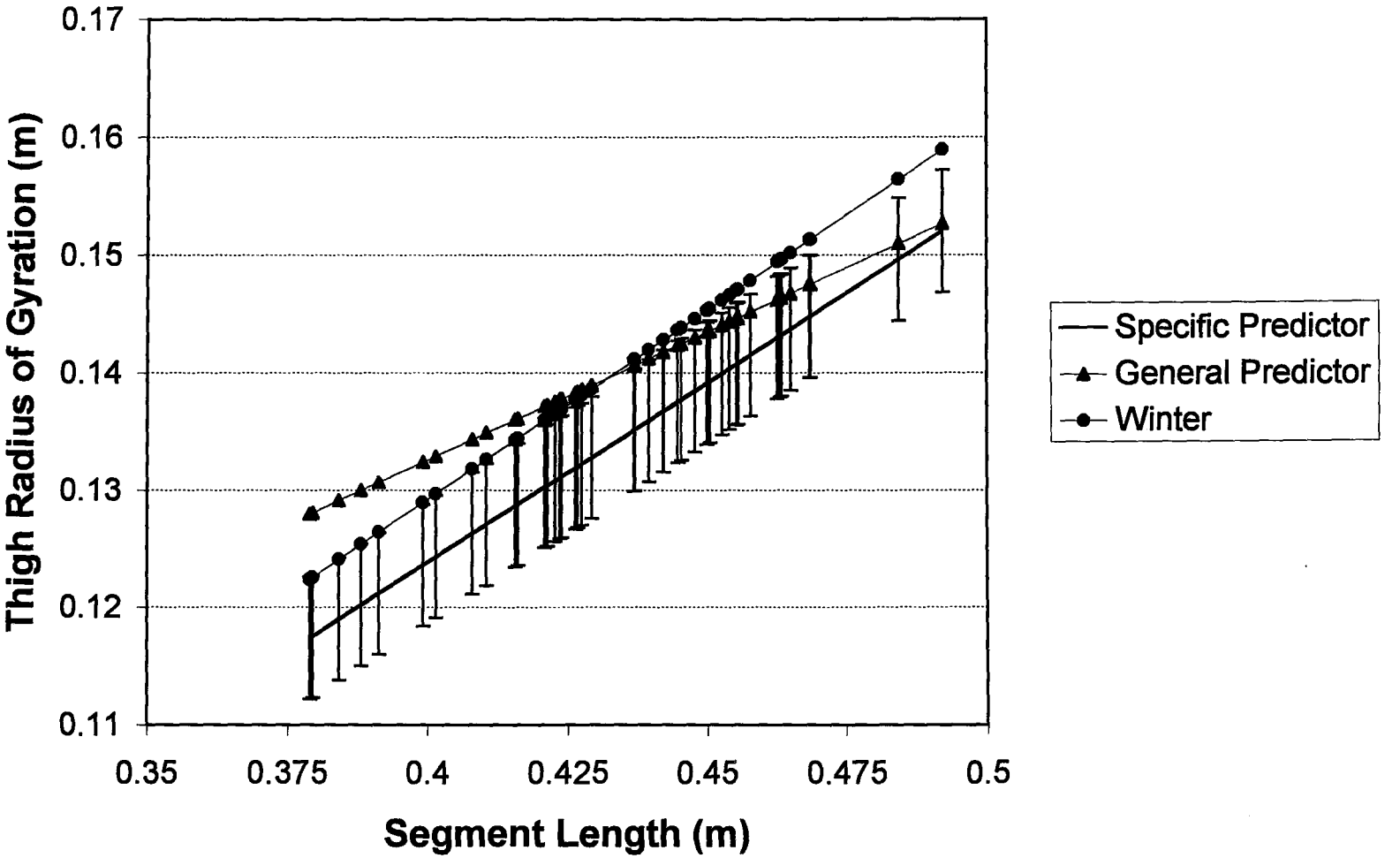

Figure D-12: Comparison of Thigh Radius of Gyration Predictors (Males 19-30 Years) (Specific Predictor ± S.E.)

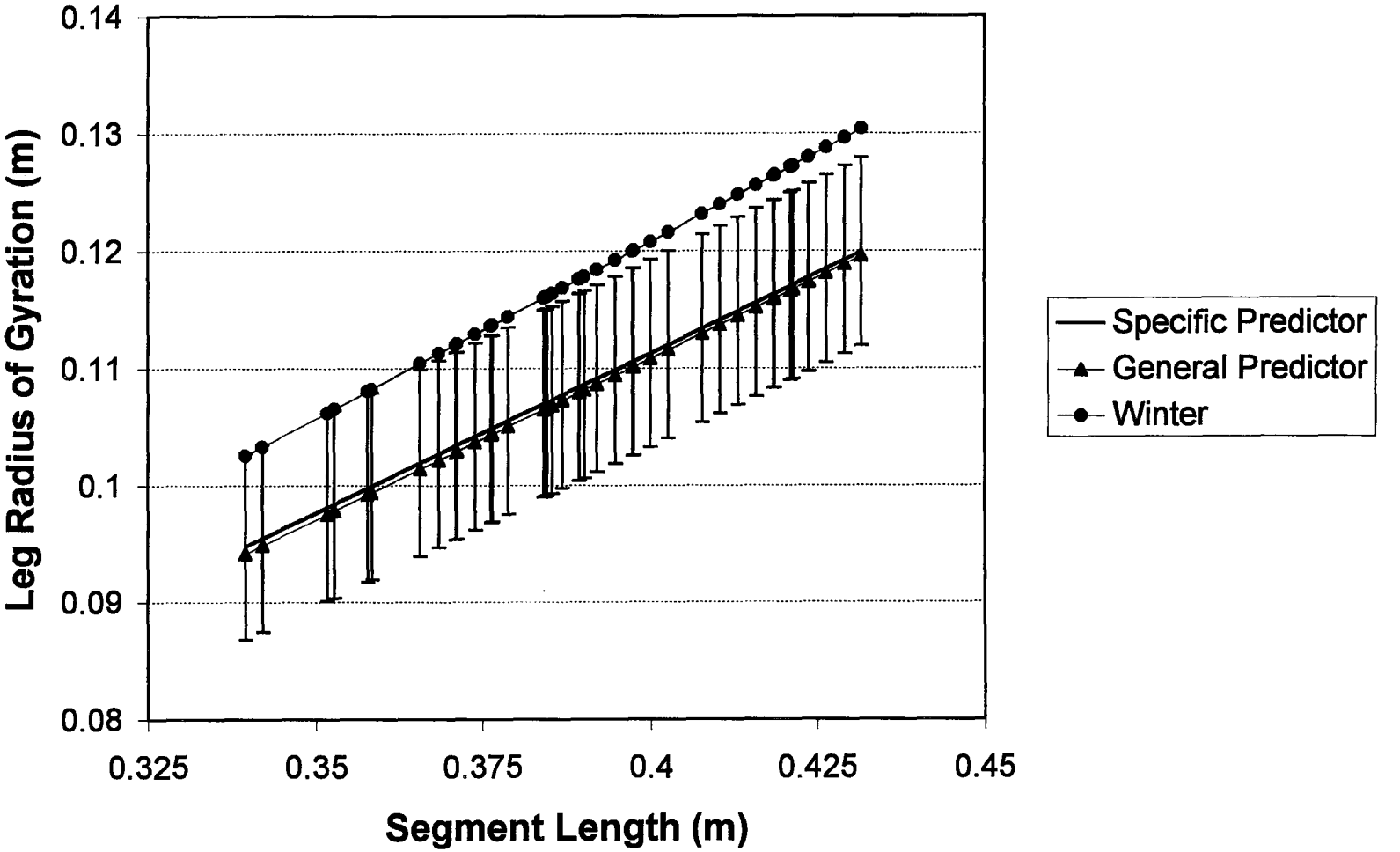

Figure D-13: Comparison of Leg Radius of Gyration Predictors (Males 55^{+} Years) (Specific Predictors ± S.E.)

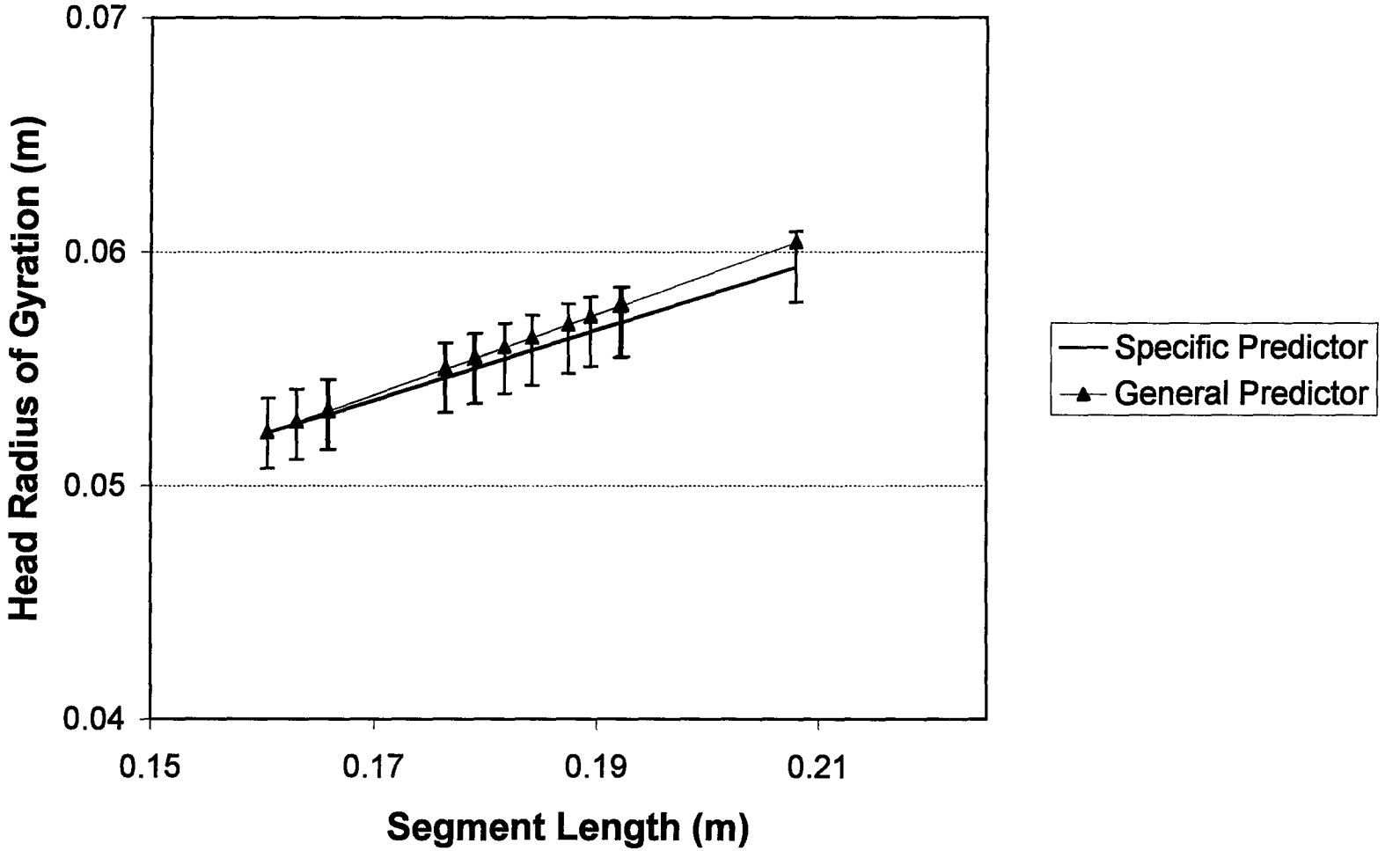

Figure D-14: Comparison of Head Radius of Gyration Predictors (Females 55^{+} Years)
(Specific Predictor ± S.E.)

APPENDIX E

Descriptive Statistics for DPX and BSP Prediction Values

Table E-1: Descriptive Statistics for Segment Mass Predictors

Segment	Population	n	DPX Values			Population Specific Linear Regression			General Linear Regression		
			Mean (kg)	S.D. (kg)	Range (kg)	Mean (kg)	S.D. (kg)	Range (kg)	Mean (kg)	S.D. (kg)	Range (kg)
Forearm	Males (19-30)	90	1.29	0.21	0.95-1.70	1.29	0.18	1.03-1.68	1.17	0.20	0.87-1.66
	Females (19-	100	0.87	0.15	0.66-1.32	0.87	0.14	0.67-1.30	0.89	0.13	0.71-1.15
	Males (55+)	82	1.34	0.22	0.66-1.44	1.34	0.19	1.01-1.75	1.34	0.23	0.93-1.85
	Females (55+)	90	0.90	0.18	0.99-1.89	0.90	0.14	0.75-1.24	0.99	0.19	0.78-1.45
Hand	Males (19-30)	80	0.43	0.07	0.25-0.55	0.43	0.04	0.37-0.53	0.43	0.06	0.34-0.57
	Females (19-	96	0.34	0.04	0.27-0.43	0.34	0.03	0.30-0.40	0.35	0.04	0.30-0.42
	Males (55+)	72	0.51	0.08	0.26-0.49	0.51	0.05	0.42-0.62	0.48	0.06	0.36-0.62
	Females (55+)	64	0.36	0.06	0.34-0.70	0.36	0.03	0.33-0.43	0.38	0.06	0.32-0.51
Thigh	Males (19-30)	100	9.17	1.69	6.70-13.64	9.18	1.54	6.69-12.90	9.23	1.23	7.25-12.20
	Females (19-	100	7.92	1.36	5.51-10.68	7.92	1.32	6.03-10.45	7.43	0.82	6.25-9.01
	Males (55+)	84	9.87	2.06	5.80-12.15	9.87	1.94	6.42-13.41	10.48	1.58	7.66-13.37
	Females (55+)	98	8.20	1.71	6.24-13.95	8.20	1.52	6.42-11.64	8.13	1.21	6.71-10.88
Leg	Males (19-30)	100	3.06	0.56	2.10-4.34	3.06	0.43	2.41-4.17	3.05	0.29	2.57-3.76
	Females (19-	100	2.78	0.36	2.14-3.57	2.78	0.31	2.34-3.36	2.61	0.20	2.33-2.99
	Males (55+)	98	3.23	0.43	1.94-4.33	3.23	0.35	2.58-3.91	3.34	0.36	2.67-4.04
	Females (55+)	100	2.71	0.50	2.41-4.02	2.71	0.39	2.26-3.60	2.78	0.29	2.44-3.44
Foot	Males (19-30)	92	0.96	0.14	0.71-1.20	0.96	0.10	0.80-1.18	0.91	0.11	0.73-1.17
	Females (19-	100	0.72	0.08	0.52-0.88	0.72	0.05	0.64-0.82	0.75	0.07	0.64-0.88
	Males (55+)	80	1.07	0.15	0.60-0.98	1.07	0.09	0.92-1.22	1.02	0.14	0.77-1.27
	Females (55+)	100	0.73	0.08	0.81-1.31	0.73	0.04	0.69-0.82	0.81	0.11	0.68-1.05
Head	Males (19-30)	48	4.71	0.44	3.97-6.62	4.71	0.26	4.27-5.34	4.55	0.28	4.07-5.22
	Females (19-	50	4.16	0.31	3.52-4.99	4.16	0.09	4.03-4.33	4.11	0.19	3.84-4.48
	Males (55+)	44	4.85	0.48	3.42-4.44	4.85	0.27	4.35-5.39	4.78	0.33	4.17-5.44
	Females (55+)	48	3.99	0.32	3.96-5.60	3.99	0.17	3.80-4.38	4.26	0.28	3.95-4.91

Table E-1: Continued

Segment	Population	n	Geometric Model			Winter's Model		
			Mean (kg)	S.D. (kg)	Range (kg)	Mean (kg)	S.D. (kg)	Range (kg)
Forearm	Males (19-30)	90	1.286	0.171	1.007-	1.146	0.171	0.888-
	Females (19-	100	0.872	0.142	0.647-	0.913	0.112	0.752-
	Males (55+)	82	1.374	0.211	0.988-	1.292	0.196	0.944-
	Females (55+)	90	0.947	0.156	0.724-	0.991	0.161	0.814-
Hand	Males (19-30)	80	-	-	-	0.433	0.066	0.333-
	Females (19-	96	-	-	-	0.341	0.043	0.282-
	Males (55+)	72	-	-	-	0.488	0.073	0.354-
	Females (55+)	64	-	-	-	0.374	0.063	0.305-
Thigh	Males (19-30)	100	8.580	1.345	6.64-11.77	7.250	1.022	5.55-9.77
	Females (19-	100	7.750	1.260	5.39-10.39	5.700	0.701	4.70-7.05
	Males (55+)	84	8.470	0.969	6.19-10.00	8.300	1.350	5.90-10.77
	Females (55+)	98	8.120	1.320	6.14-11.37	6.300	1.034	5.09-8.64
Leg	Males (19-30)	100	3.510	0.528	2.51-4.92	3.370	0.485	2.58-4.54
	Females (19-	100	3.030	0.443	2.23-3.93	2.650	0.326	2.19-3.28
	Males (55+)	98	4.030	0.516	2.92-4.84	3.850	0.598	2.74-5.01
	Females (55+)	100	3.280	0.559	2.37-4.65	2.920	0.481	2.37-4.02
Foot	Males (19-30)	92	-	-	-	1.055	0.157	0.805-
	Females (19-	100	-	-	-	0.827	0.102	0.682-
	Males (55+)	80	-	-	-	1.212	0.201	0.856-
	Females (55+)	100	-	-	-	0.910	0.150	0.738-
Head	Males (19-30)	48	4.280	0.491	3.37-5.33	-	-	-
	Females (19-	50	3.730	0.380	3.05-4.38	-	-	-
	Males (55+)	44	4.720	0.516	3.48-5.81	-	-	-
	Females (55+)	48	3.950	0.425	3.34-4.82	-	-	-

Table E-2: Descriptive Statistics for Segment Centre of Mass Predictors

Segment	Population	n	DPX Values			Population Specific Linear Regression			General Linear Regression		
			Mean (kg)	S.D. (kg)	Range (kg)	Mean (kg)	S.D. (kg)	Range (kg)	Mean (kg)	S.D. (kg)	Range (kg)
Forearm	Males (19-30)	90	0.110	0.007	0.094-0.123	0.110	0.006	0.094-0.120	0.111	0.006	0.095-0.121
	Females (19-	100	0.101	0.005	0.090-0.114	0.101	0.005	0.091-0.112	0.101	0.004	0.092-0.112
	Males (55+)	82	0.110	0.006	0.099-0.120	0.110	0.005	0.103-0.118	0.109	0.005	0.101-0.118
	Females (55+)	90	0.098	0.006	0.871-0.110	0.098	0.005	0.084-0.107	0.098	0.005	0.083-0.107
Thigh	Males (19-30)	100	0.177	0.012	0.155-0.205	0.177	0.010	0.154-0.199	0.170	0.013	0.141-0.177
	Females (19-	100	0.157	0.013	0.126-0.179	0.157	0.010	0.140-0.179	0.154	0.114	0.135-0.178
	Males (55+)	84	0.168	0.016	0.116-0.206	0.168	0.009	0.149-0.186	0.173	0.009	0.154-0.191
	Females (55+)	98	0.146	0.014	0.106-0.174	0.146	0.009	0.129-0.170	0.153	0.009	0.136-0.178
Leg	Males (19-30)	100	0.159	0.011	0.140-0.184	0.159	0.011	0.142-0.178	0.158	0.011	0.141-0.177
	Females (19-	100	0.150	0.010	0.126-0.163	0.150	0.009	0.128-0.165	0.150	0.009	0.128-0.164
	Males (55+)	98	0.160	0.010	0.140-0.182	0.160	0.009	0.140-0.175	0.160	0.010	0.139-0.177
	Females (55+)	100	0.147	0.008	0.129-0.161	0.147	0.008	0.129-0.160	0.148	0.008	0.130-0.161
Head	Males (19-30)	48	0.109	0.009	0.091-0.124	0.109	0.008	0.096-0.125	0.107	0.008	0.094-0.123
	Females (19-	50	0.100	0.006	0.088-0.111	0.100	0.004	0.092-0.108	0.103	0.006	0.091-0.114
	Males (55+)	44	0.107	0.008	0.088-0.117	0.107	0.006	0.093-0.116	0.106	0.006	0.093-0.114
	Females (55+)	48	0.099	0.006	0.086-0.116	0.099	0.005	0.090-0.113	0.009	0.006	0.082-0.115

Table E-2: Continued

Segment	Population	n	Geometric Model			Winter's Model		
			Mean (kg)	S.D. (kg)	Range (kg)	Mean (kg)	S.D. (kg)	Range (kg)
Forearm	Males (19-30)	90	0.111	0.007	0.097-0.1255	0.115	0.007	0.096-0.126
	Females (19-	100	0.103	0.005	0.092-0.1140	0.189	0.012	0.093-0.115
	Males (55+)	82	0.113	0.006	0.099-0.1235	0.168	0.011	0.103-0.123
	Females (55+)	90	0.103	0.005	0.093-0.1137	0.097	0.007	0.082-0.110
Thigh	Males (19-30)	100	0.193	0.017	0.153-0.225	0.103	0.005	0.164-0.213
	Females (19-	100	0.178	0.014	0.152-0.207	0.176	0.010	0.159-0.196
	Males (55+)	84	0.196	0.015	0.172-0.229	0.159	0.009	0.176-0.207
	Females (55+)	98	0.183	0.010	0.167-0.208	0.093	0.005	0.160-0.196
Leg	Males (19-30)	100	0.173	0.012	0.152-0.192	0.113	0.103	0.149-0.187
	Females (19-	100	0.162	0.009	0.139-0.177	0.191	0.176	0.136-0.173
	Males (55+)	98	0.177	0.010	0.156-0.198	0.169	0.147	0.147-0.187
	Females (55+)	100	0.161	0.009	0.142-0.177	0.093	0.005	0.139-0.171
Head	Males (19-30)	48	0.109	0.001	0.074-0.128	-	-	-
	Females (19-	50	0.103	0.007	0.090-0.118	-	-	-
	Males (55+)	44	0.118	0.008	0.101-0.133	-	-	-
	Females (55+)	48	0.108	0.007	0.094-0.118	-	-	-

Table E-3: Descriptive Statistics for Segment Radius of Gyration Predictors

Segment	Population	n	DPX Values			Population Specific Linear Regression			General Linear Regression		
			Mean (kg)	S.D. (kg)	Range (kg)	Mean (kg)	S.D. (kg)	Range (kg)	Mean (kg)	S.D. (kg)	Range (kg)
Forearm	Males (19-30)	90	0.074	0.006	0.063-0.096	0.074	0.005	0.061-0.083	0.075	0.004	0.064-0.082
	Females (19-	100	0.067	0.003	0.061-0.074	0.067	0.003	0.061-0.075	0.068	0.003	0.061-0.075
	Males (55+)	82	0.074	0.004	0.067-0.081	0.075	0.003	0.069-0.079	0.074	0.004	0.068-0.080
	Females	90	0.066	0.004	0.059-0.072	0.066	0.003	0.056-0.072	0.066	0.004	0.055-0.072
Thigh	Males (19-	100	0.135	0.010	0.115-0.163	0.135	0.008	0.117-0.152	0.141	0.006	0.128-0.137
	Females (19-	100	0.129	0.006	0.117-0.141	0.130	0.005	0.121-0.140	0.134	0.005	0.125-0.144
	Males (55+)	84	0.146	0.009	0.130-0.165	0.146	0.004	0.139-0.155	0.142	0.004	0.134-0.150
	Females	98	0.140	0.007	0.123-0.150	0.140	0.004	0.139-0.149	0.133	0.004	0.126-0.144
Leg	Males (19-	100	0.107	0.007	0.096-0.121	0.107	0.007	0.096-0.120	0.108	0.007	0.096-0.120
	Females (19-	100	0.101	0.006	0.087-0.111	0.101	0.006	0.086-0.110	0.102	0.006	0.087-0.111
	Males (55+)	98	0.109	0.009	0.095-0.121	0.109	0.006	0.095-0.120	0.100	0.005	0.089-0.109
	Females	100	0.101	0.007	0.089-0.114	0.101	0.005	0.089-0.110	0.108	0.007	0.094-0.120
Head	Males (19-	48	0.058	0.002	0.054-0.063	0.058	0.002	0.055-0.062	0.058	0.002	0.054-0.063
	Females (19-	50	0.056	0.002	0.052-0.060	0.056	0.002	0.052-0.060	0.057	0.002	0.053-0.060
	Males (55+)	44	0.059	0.002	0.054-0.062	0.059	0.002	0.055-0.061	0.058	0.001	0.054-0.060
	Females	48	0.055	0.002	0.051-0.058	0.055	0.002	0.052-0.059	0.056	0.002	0.052-0.060

Table E-3: Continued

Segment	Population	n	Geometric Model			Winter's Model		
			Mean (kg)	S.D. (kg)	Range (kg)	Mean (kg)	S.D. (kg)	Range (kg)
Forearm	Males (19-30)	90	0.075	0.005	0.065-0.084	0.088	0.005	0.068-0.089
	Females (19-	100	0.069	0.003	0.062-0.076	0.072	0.004	0.065-0.081
	Males (55+)	82	0.076	0.008	0.067-0.083	0.080	0.004	0.072-0.086
	Females (55+)	90	0.069	0.008	0.063-0.077	0.080	0.004	0.058-0.078
Thigh	Males (19-30)	100	0.153	0.009	0.132-0.170	0.141	0.009	0.122-0.159
	Females (19-	100	0.162	0.008	0.138-0.179	0.131	0.007	0.119-0.146
	Males (55+)	84	0.163	0.008	0.145-0.180	0.143	0.006	0.131-0.155
	Females (55+)	98	0.165	0.008	0.150-0.190	0.301	0.006	0.119-0.146
Leg	Males (19-30)	100	0.112	0.007	0.100-0.124	0.177	0.008	0.104-0.131
	Females (19-	100	0.104	0.006	0.092-0.114	0.111	0.007	0.095-0.121
	Males (55+)	98	0.114	0.006	0.102-0.128	0.118	0.007	0.103-0.130
	Females (55+)	100	0.104	0.005	0.094-0.115	0.109	0.006	0.097-0.119
Head	Males (19-30)	48	0.064	0.004	0.058-0.071	-	-	-
	Females (19-	50	0.061	0.003	0.056-0.065	-	-	-
	Males (55+)	44	0.067	0.003	0.059-0.074	-	-	-
	Females (55+)	48	0.063	0.003	0.057-0.067	-	-	-